Pressure Swing Absorption Device and Process for Separating CO_2 from Shifted Syngas and its Capture for Subsequent Storage

DOE- DE-09FE0001323

Final Scientific / Technical Report

Report Date: June 30, 2013

Investigators:
Kamalesh K. Sirkar
Xingming Jie
John Chau
Gordana Obuskovic

Point of Contact:
Kamalesh K. Sirkar
Otto H. York Department of Chemical, Biological and Pharmaceutical Engineering
Center for Membrane Technologies
New Jersey Institute of Technology
Newark, NJ 07102, USA
Phone: 973-596-8457
Facsimile: 973-642-7854
Email: sirkar@njit.edu

TITLE PAGE

REPORT TITLE:	Pressure Swing Absorption Device and Process for Separating CO_2 from Shifted Syngas and its Capture for Subsequent Storage
TYPE OF REPORT:	Final Scientific / Technical
REPORTING PERIOD START DATE:	October 1, 2009
REPORTING PERIOD END DATE:	March 31, 2013
PRINCIPAL AUTHOR(s):	Kamalesh K. Sirkar Xingming Jie John Chau Gordana Obuskovic
DATE REPORT WAS ISSUED:	June 30, 2013
DOE AWARD NUMBER:	DE-09FE0001323
ORGANIZATION:	New Jersey Institute of Technology Otto H. York Department of Chemical, Biological and Pharmaceutical Engineering, Center for Membrane Technologies Newark, NJ 07102

ABSTRACT

Using the ionic liquid (IL) 1-butyl-3-methylimidazolium dicyanamide ([bmim][DCA]) as the absorbent on the shell side of a membrane module containing either a porous hydrophobized ceramic tubule or porous hydrophobized polyether ether ketone (PEEK) hollow fiber membranes, studies for CO_2 removal from hot simulated pre-combustion shifted syngas were carried out by a novel pressure swing membrane absorption (PSMAB) process. Helium was used as a surrogate for H_2 in a simulated shifted syngas with CO_2 around 40% (dry gas basis). In this cyclic separation process, the membrane module was used to achieve non-dispersive gas absorption from a high-pressure feed gas (689-1724 kPag; 100-250 psig) at temperatures between 25-100^{0}C into a stationary absorbent liquid on the module shell side during a certain part of the cycle followed by among other cycle steps controlled desorption of the absorbed gases from the liquid in the rest of the cycle. Two product streams were obtained, one He-rich and the other CO_2-rich. Addition of polyamidoamine (PAMAM) dendrimer of generation 0 to IL [bmim][DCA] improved the system performance at higher temperatures. The solubilities of CO_2 and He were determined in the ionic liquid with or without the dendrimer in solution as well as in the presence or absence of moisture; polyethylene glycol (PEG) 400 was also studied as a replacement for the IL. The solubility selectivity of the ionic liquid containing the dendrimer for CO_2 over helium was considerably larger than that for the pure ionic liquid. The solubility of CO_2 and CO_2-He solubility selectivity of PEG 400 and a solution of the dendrimer in PEG 400 were higher than the corresponding ones in the IL, [bmim][DCA]. A mathematical model was developed to describe the PSMAB process; a numerical solution of the governing equations described successfully the observed performance of the PSMAB process for the pure ionic liquid-based system.

TABLE OF CONTENTS

EXECUTIVE SUMMARY

The goal of this research was to develop via laboratory-based experiments an advanced pressure swing absorption (PSAB) device and a cyclic process to produce purified hydrogen at a high pressure for the combustion turbine of the Integrated Gasification Combined Cycle (IGCC)-Carbon Capture and Storage (CCS) power production plants; the PSAB device and process were expected to yield a purified CO_2 stream containing at least 90% of the CO_2 in the post-shift reactor gas stream and suitable for subsequent sequestration. Additional project goals included development of a mathematical model of the PSAB device and process, validating it against the experimental data to facilitate a scaled up design useful for evaluation of the separation device and process.

Using the nonvolatile ionic liquid (IL) 1-butyl-3-methylimidazolium dicyanamide ([bmim][DCA]) as the absorbent on the shell side of a small membrane module containing either a porous hydrophobized ceramic tubule or porous hydrophobized polyether ether ketone (PEEK) hollow fiber membranes, we achieved CO_2 removal from hot simulated pre-combustion shifted syngas by a pressure swing membrane absorption (PSMAB) process which operates in a cyclic fashion. Helium was used as a surrogate for H_2 in the simulated shifted syngas containing ~40% CO_2 on a dry gas basis. In this cyclic process, the membrane module was used to achieve non-dispersive gas absorption from a high-pressure feed gas (689-1724 kPag; 100-250 psig) at temperatures between 25-100^{0}C (in a few experiments up to 125^{0}C) into a stationary absorbent liquid on the shell side of the membrane module during a certain part of the cycle followed by among other cycle steps controlled desorption of the absorbed gases from the liquid in the rest of the cycle. From the module end opposite to the feed gas introduction end, the He-rich product was obtained. The CO_2-rich product stream was obtained from the feed gas introduction end.

To improve CO_2 separation, a 5-valve system was designed to replace the simpler 3-valve system since we were working with small membrane modules; optimal duration times for the key steps in one cycle e.g., absorption, He-rich product withdrawal etc. were determined. A typical cycle lasting 69 sec consisted of: feed gas introduction, 5 sec; gas absorption, 30 sec; He-rich product withdrawal, 2 sec; middle part gas withdrawal, 2 sec; CO_2-rich product withdrawal, 30 sec. The effects of feed pressure and temperature on the absorption behavior and CO_2 removal were studied. Results showed that although the hydrophobized ceramic membrane tubule did not yield high quality products, it performed stably and provided consistent separation results under a high pressure of 1724 kPag (250 psig) and a high temperature of 125^{o}C. Using two well-designed small (0.117 m^2) PEEK membrane modules (PEEK-S) in series, we achieved a He-rich product containing CO_2 ~ 5.0% and a CO_2-rich product in which CO_2 concentration was enriched to ~80% at lower temperatures and 965 kPag (140 psig). For pure [bmim][DCA] as absorbent, the product qualities were degraded as the feed temperature was increased for a given membrane module. Adding polyamidoamine (PAMAM) dendrimer of generation 0 to [bmim][DCA] enhanced CO_2 solubility. Using 25 wt% dendrimer in [bmim][DCA] and a larger (0.345 m^2) PEEK membrane module (PEEK-L) showed much less effect of temperature on separation up to 100^{o}C compared to that with pure IL. The PSMAB

process performance was stable with time. The PEEK membrane modules performed much better than ceramic membrane modules since PEEK hollow fibers had much higher gas-liquid contacting area per unit gas volume.

The PSMAB process performance depended strongly on the PEEK membrane module design. Decreasing the dead volume in the tube side headers of the module (0.345 m^2) by adding small hollow Teflon balls and increasing the space between contiguous hollow fibers by decreasing fiber packing density improved the PSMAB product qualities substantially. A higher membrane surface area (0.555m^2) PEEK-III module having increased feed gas volume vis-à-vis the module dead gas volume yielded a CO_2-rich product having 90.7% CO_2 from a 1724 kPag (250 psig), 100^oC feed. We studied experimentally a 2-stage PSMAB with a 14.0% CO_2 in He as feed coming from stage 1, and showed that a He-rich product having 5.50% CO_2 could be achieved at 100^oC. Simultaneous production of a He-rich stream having less than 5% CO_2 and a CO_2-rich stream containing 95% CO_2 will require putting two/three redesigned PEEK membrane modules in series. The experimentally observed preliminary performances of the inexpensive solvent PEG 400 suggest that it could replace the IL as the basic absorbent.

Measurements of the solubility of pure CO_2, pure He, and a mixture of 40% CO_2-He balance in the IL ([bmim][DCA]) and in its solution containing 20 wt% and 30 wt% PAMAM dendrimer Gen 0 with and without moisture were carried out in a pressure-decay-dual transducer apparatus at temperatures of 323, 353, 363, and 373K and at pressures up to 1.38 MPa (~200 psig). Henry's law constants of pure CO_2 and pure He were determined for the pure IL. Pseudo Henry's law constants for each of CO_2 and He in a 40-60% feed gas mixture were also determined. Solubility selectivity of CO_2 to He for all liquid absorbents were also calculated at each temperature. A 30 wt% dendrimer in [bmim][DCA] with moisture yielded the highest CO_2/He selectivity of 55 at 50^oC and 10 at 100^oC . Replacing the IL with PEG 400 yielded higher CO_2 solubility and CO_2/He selectivity. Diffusion coefficients of CO_2 and He were also determined for the pure IL.

A mathematical model was developed to predict the behavior of the simpler 3-valve PSMAB process and compare the predictions with the experimental results for pure [bmim][DCA] as absorbent. Numerical model simulations employed the solubilities and diffusivities of CO_2 and He obtained experimentally. The pressure drop observed experimentally during the absorption step could be predicted reasonably well for both ceramic and the PEEK-II membrane modules and systems. The flow rates and compositions of the two product streams were also predicted. The deviations in the experimentally observed compositions of the two product streams from the model predictions reflect dilution from the dead volume effect; the experimentally observed PEEK-III module performances having reduced dead volume were closer to the model simulations. Achieving 90% plus recovery of CO_2 in the CO_2-rich stream and getting two product streams with required purity appears achievable by employing either a two stage process or a number of membrane modules in series. Redesigned membrane modules having reduced dead volume and a lower packing density to provide space for absorbent between contiguous hollow fibers will facilitate achieving the desired performance goals.

REPORT DETAILS

This report is going to have the following major sections:

1. Introduction
2. Experimental Methods
3. Results and Discussions
4. Conclusion
5. Notation, Tables and Illustrations
6. References
7. List of Acronyms and Abbreviations
8. Acknowledgements

1. INTRODUCTION

Continuous emission of large amount of greenhouse gases to the atmosphere has brought obvious changes such as higher earth surface temperature and more frequent and severe climatic disturbances. Among all greenhouse gases, CO_2 is believed to make the largest contribution about 80% (Lashof et al., 1990). Scientists have confirmed that the atmospheric concentration of CO_2 has increased globally by about 100 ppm (36%) over the last 250 years mostly due to human activities (Pachauri et al., 2007).

CO_2 capture and storage (CCS) is widely thought to be the most important technique to deal with global climate change in short term (Azar et al., 2006; Rubin et al., 2007). For coal-based power plants, three fields widely investigated for CO_2 removal are oxygen-enriched combustion, post-combustion and pre-combustion (Kanniche et al., 2010). Oxygen-enriched combustion has the advantage that CO_2 concentration in flue gas can be as high as 90%; it can be very easily concentrated further; however, it faces the difficulty of oxygen-enriched gas production and high energy cost (Tan et al., 2002). For post-combustion, due to the low flue gas pressure and much lower CO_2 concentration, the capture of CO_2 is difficult and requires high capital investment and high energy cost (Merkel et al., 2010). Compared to post-combustion capture, pre-combustion CO_2 capture from post-shift reactor synthesis gas obtained via integrated gasification combined cycle (IGCC) for coal as a solid fuel is of significant interest since CO_2 is present at a much higher partial pressure. From this point of view, CO_2 removal from pre-combustion shifted syngas will play an important role in global CCS. However, the temperature of this gas is also very high around 150-200^oC+ along with a high pressure.

At present, solvent absorption is still the most successful and widely applied method for CO_2 removal; but it is generally not applied to higher temperatures. For a pre-combustion process, low temperature (L-T) water gas shift reactor product stream is likely to be available at ~15-20 atm and around 150-200^oC. If CO_2 from this stream is to be absorbed in a liquid absorbent, the liquid absorbent must be thermally stable and essentially nonvolatile. Further it must be highly CO_2-selective over H_2 and any other impurities present (such as CO etc.).

Room temperature ionic liquids (RTILs) have been considered green solvents for carbon dioxide capture because of their unique characteristics. RTILs are bulky organic compounds whose cations are organic and anions are either organic or inorganic (Baltus and Moganty, 2010). RTILs are in liquid form at room temperature and are chemically, thermally stable, and non-volatile. Therefore, they can be used to replace volatile organic solvents as absorbents for carbon dioxide separation (Camper et al., 2006). Yokozeki and Shiflet (2007) have tested CO_2 solubilities in different ionic liquids and demonstrated solubility selectivity of CO_2 over H_2 of as much as 30-300 at H_2 partial pressures of 0.5-3MPa at around room and lower temperatures for the ionic liquid of 1-butyl-3-methylimidazolium hexafluorophosphate ([bmim][PF_6]) (Shiflett and Yokozeki, 2005; Yokozeki and Shiflett, 2007). Solubility selectivity tests for CO_2 over other gases also have been carried out by other researchers with different ionic liquids (Yuan et al., 2006; Yuan et al., 2007; Raeissi and Peters, 2009). Sudhir et al. (2004) investigated the high-pressure phase behavior of carbon dioxide with imidazolium-based ionic liquids and they found solubility is strongly dependent on the choice of anion.

Task specific ionic liquids (TSILs) having functional groups which can form complexes with CO_2 have been synthesized and used as facilitated supported liquid membrane (FSLM). Meindersma et al. (2007) reviewed the application of task-specific ionic liquids for intensified separation; they suggested that 1-butyl-3-methylimidazolium dicyanamide ([bmim][DCA]) could be a good choice as a CO_2 absorption solvent. The CO_2/H_2 selectivity achieved by such a FSLM reached up to 10-20 at a temperature of ~85^oC (Myers et al., 2008). The major advantage of such ionic liquids is that they can operate at a high temperature and separate in the absence of water which is not possible in highly CO_2-selective polymeric membranes containing amines in cross-linked poly(vinyl alcohol) and studied in the temperature range of 100-170^oC (Zou and Ho, 2006). A similar study indicated a precipitous drop in CO_2/H_2 selectivity of the polymeric membrane containing amine moieties as the feed gas moisture content decreased (Yegani et al., 2007). A major weakness of the SLMs using ILs is that their overall CO_2/H_2 selectivity is low. It is known that a membrane's selectivity is determined by the product of the solubility selectivity and diffusivity selectivity. Although their solubility selectivity for CO_2 over H_2 is quite high, the diffusivity selectivity favors H_2 or He over CO_2 due to their much smaller size. Therefore unless reversible chemical complexation is introduced, the overall SLM selectivity will be low.

Primary and tertiary amines or compounds containing those amines can be used as reactive carbon dioxide absorbents. Effective CO_2 absorption however requires significant amount of moisture in systems containing tertiary amines. Previous studies have shown that a pure liquid membrane of PAMAM dendrimer Gen 0 with humidified gas streams had a very high selectivity of CO_2 over N_2/O_2 in the range of 15,000-18,000 (Kovvali et al., 2000; Kovvali et al., 2001) at around room temperature and at low CO_2 partial pressures. This amine molecule with a molecular weight of 517 contains four primary amines and two tertiary amines. Additional supported liquid membrane studies using pure PAMAM dendrimer Gen 0 for CO_2 separation have been carried out in other laboratories (Duan et al., 2006; Taniguchi et al., 2008; Duan et al., 2007). This dendrimer Gen 0 has also been used as a reactive absorbent in an aqueous solution in a

hollow fiber membrane contactor at room temperature (Kosaraju et al., 2005). In addition, Rolker et al. have succeeded in achieving high CO_2/N_2 solubility selectivity in nonvolatile hyper-branched oligomeric liquid absorbents (Rolker et al., 2007).

The cost of purified analytical grade PAMAM dendrimer Gen 0 per Aldrich Catalog etc. is quite high of the order of $3000/kg. However, the manufacturer of this chemical proposes to supply industrial grade of this compound in large scale at ~ $10-20/lb (Dendritech, 2012). This price is quite reasonable when we compare it with other specialized amines being studied e.g., piperazine whose bulk price is around $9/lb. The industrial grade dendrimer may have small amounts of impurities all of which are going to be amines highly capable of CO_2 absorption. Further, reactions of this dendrimer amine with CO_2 are completely reversible as we have observed with runs of thousands of cycles of absorption and desorption every day in this project.

Unlike permeation behavior in a separation membrane, an absorption-based process is unlikely to suffer from a deficiency in CO_2-H_2 selectivity since solubility selectivity is likely to be controlling. Actually the post-shift reactor gas stream for coal-based gasification plants can also be purified to recover hydrogen with high purity via the pressure swing adsorption (PSA) process wherein H_2 is purified at near ambient temperature and high pressure using adsorbents such as molecular sieves, silica gel to remove impurities such as CO_2 (Yang et al., 2008). The desorption stream produces purified CO_2. However there is significant loss of H_2 as much as 10% in such regeneration processes along with substantial thermal/cooling needs (Harrison, 2008).

Cyclic thermal-swing sorption-enhanced reaction (TSSER)-based H_2 production processes producing compressed CO_2 as a byproduct gas (Lee et al., 2008) employ a shift reactor which contains a CO_2-selective chemisorbent such as calcium based oxides, K_2CO_3-promoted hydrotalcite etc. (Lee et al., 2008). This process is dynamic and the chemisorbent is regenerated periodically by superheated steam using thermal swing adsorption processes and producing a pure and compressed CO_2 byproduct useful for sequestration. Such a process is not useful for IGCC-CCS processes where a post-shift reactor gas stream is already available at appropriate pressures and temperatures.

Ionic liquids are very viscous. Ionic liquids containing polyamidoamine (PAMAM) dendrimers of lower generation (studies reported later) are even more viscous. Conventional absorption processes where such liquids are mobile face considerable pressure drops. This problem can be avoided if we adopt the novel concept of pressure swing absorption originally proposed in Bhaumik et al. (1996). They carried out a lower-temperature lower-pressure analog of the concept investigated here (rapid pressure swing absorption, RAPSAB) for a 10% CO_2-90% N_2 feed stream at 375 kPag using 19.5 wt% aqueous solution of diethanolamine (DEA) as the absorbent on the shell side of a porous polymeric hollow fiber module 160 cm long containing 840-1200 polymeric hollow fibers. The CO_2 level in the purified N_2 stream was reduced to virtually zero (less than 50 ppm which was the detection limit in the gas chromatograph used). The desorbent stream also produced a highly enriched CO_2 stream. The aqueous solution used was volatile and

had to be regenerated by occasional infusion of the absorbent liquid solution from the shell side. A related technique was pursued in Obuskovic et al. (1998).

In this study we are focusing on designing a cyclic separation process of H_2 purification and CO_2 absorption and recovery which combines the specific advantages of a number of basic separation techniques: selective absorption of CO_2 in a nonvolatile liquid/oligomeric absorbent at temperatures and pressures characteristics of the feed stream under consideration; pressure swing absorption (PSAB) process simulating a PSA process (which however uses adsorbent particles); hollow microporous tubules/fibers providing per unit device volume a very large surface area of nondispersive contact between the post-shift reactor synthesis gas stream flowing through the fiber lumen and the liquid absorbent present as a thin stagnant absorbent liquid layer in between the microporous tubules/hollow fibers on the shell side of the separation device. Helium was used as a surrogate for hydrogen. Employing porous ceramic (inorganic material can endure high pressure and temperature) tubules or PEEK (organic material, easy to be processed with inorganic-like robust characteristics) hollow fiber membrane modules, ionic liquid [bmim][DCA] with or without PAMAM dendrimer of generation 0 (Gen 0) as absorbent, a novel cyclic Pressure Swing Membrane Absorption (PSMAB) process was designed. Based on the determination of the optimal step duration times of various steps in each cycle, the effects of feed pressure and test temperature were systematically investigated. A brief dimensional comparison between two types of membrane modules was also carried out to explain their considerable performance difference. Solubilities of both CO_2 and He in a variety of absorbent liquids were measured; the absorbent liquids include [bmim][DCA], PEG 400 and their mixtures with PAMAM dendrimer Gen 0 with or without water; diffusion coefficients of He and CO_2 were also obtained for pure ionic liquid [bmim][DCA]. Separation performance was also briefly studied with dendrimer-containing PEG 400 in a membrane module. A mathematical model was developed for a pure non-chemically interacting absorbent liquid, e.g., ionic liquid for a simple PSMAB process; the model results were compared with experimental data.

1.1 **Pressure Swing Membrane Absorption (PSMAB) Process**

Figure 1(a) shows a microporous ceramic tubule or a porous polymeric hollow fiber. In the separator device, there will be many such tubules or hollow fibers as in Figure 1(b). Surrounding the tubule/fiber is the absorbent (e.g., ionic liquid) filling the shell side of the membrane gas-liquid contactor. The pores in the wall of the ceramic tubule or polymeric hollow fiber are gas-filled. In the test apparatus (Figures 1(c) and 1(d)), the membrane contactor module is put inside an oven to maintain a certain temperature. The shell side of the module was filled with a certain absorbent such as ionic liquid supplied from the absorbent container connected to a N_2 cylinder to maintain the desired pressure. Feed gas was introduced into the membrane tube side where it contacted the absorbent through the micropores to be absorbed. Usually the absorbent pressure in the shell side was kept about 138 kPag (20 psig) higher than the feed gas pressure in tube side to avoid any possible gas bubbling in to the shell-side absorbent liquid. Figure 1(e) shows the apparatus used for gas solubility measurements which will be discussed later.

In a typical pressure swing membrane absorption process (Bhaumik et al., 1996) usually a 3-valve control system is applied as shown in Figure 2(a); there will be 4 steps in each absorption cycle:

Step 1: Valve 1 open, valves 2 and 3 closed, feed gas was introduced into tube side of the membrane module for a certain time to develop the desired pressure (a sharp pressure increase in tube side);

Step 2: All 3 valves closed, absorption between feed gas in tube side and absorbent in shell side takes place mainly at the interface of micro-pores during this period (pressure in tube side will decrease gradually in this step due to gas absorption);

Step 3: Valves 1 and 2 closed, valve 3 opened for certain time to withdraw He-rich product (sharp pressure decrease in tube side because of product withdrawal);

Step 4: Valves 1 and 3 closed, valve 2 opened for certain time to withdraw CO_2-rich product at a lower pressure (sharp pressure decrease in tube side because of product withdrawal).

In the absorption process described in Figure 2(a), feed gas in the tube side was separated into two parts as He-rich product and CO_2-rich product. This design will work well if we have ideally porous membrane fibers (here ideally means fibers are as thin as possible and as porous as possible to increase contacting area between feed gas and absorbent, micro-pores should be as small as possible to withstand high pressure operation) and absorbent with high capacity and selectivity. Further the membrane length has to be quite long to simulate the kind of long bed used in pressure swing adsorption. However since we have short lengths of membrane modules located in smaller size ovens, additional modifications of this cycle are needed since the 3-valve system that usually separates the feed gas into two parts will face a tradeoff situation. If better quality He-rich product is preferred (only take a very limited amount of gas in the tube side as He-rich product), low quality CO_2-rich product will have to be accepted; vice versa, if we want better CO_2-rich product, we should take gas in tube side as much as possible to be a He-rich product, and that will definitely cause a lower product quality for helium side. In order to overcome this tradeoff problem, we have designed a new 5-valve system for the pressure swing membrane absorption process as shown in Figure 2(b).

There are 6 steps in each cycle in case of 5-valve system as listed below.

Step 1: Valve 1 opened and all other valves closed; fresh feed gas was introduced into tube side until desired pressure established;

Step 2: All valves closed, absorption happened between gas and absorbent IL;

Step 3: Valve 3 opened and all others closed, He-rich product withdrawal;

Step 4: Valve 4 opened and all others closed, middle part gas withdrawal;

Step 5: Valve 2 opened and all others closed, CO_2-rich product withdrawal;

Step 6: Valve 5 opened and all others closed, middle part gas was recycled into membrane tube side as initial feed gas before fresh feed gas is introduced in the next cycle.

The main difference between the two arrangements is as follows. With a 5-valve system after the gas absorption step we can divide the gas mixture in the membrane module tube side into three parts: He-rich product, middle part gas and CO_2-rich product. In other words, an extra step (middle part gas withdrawal step) was added between step 3 and step 4 of the 3-valve system. Actually the composition of the middle part gas can be controlled close to feed gas so it could be collected and recycled into tube side at the beginning of next cycle. Both processes were studied in this project.

1.2 **Absorbents and Membranes**

For the proposed process, the membrane module and the liquid absorbent are two of the most important factors to determine if the PSMAB process will be useful. An ideal membrane contactor would have: a high breakthrough pressure; appropriate surface hydrophobicity; low pore transport resistance; significant gap between neighboring fibers so that there is sufficient liquid for absorption without sacrificing a high surface area per unit volume. Two types of membrane modules were studied: porous hydrophobized ceramic tubule; porous hydrophobized polyether ether ketone (PEEK) hollow fiber membranes (although polytetrafluoroethylene hollow fibers were also employed, they did not have the pressure capability). The design of the membrane modules turned out to be very influential in determining the process/separation performance. The influences of the tube side header dead volume and hollow fiber packing density in the membrane contactor on the PSMAB process were therefore studied in the project.

In terms of absorbent, as we mentioned earlier, ionic liquid will be a good choice: Ionic liquids (ILs) have high thermal stability, essentially no vapor pressure and most important CO_2 has much higher solubility in ILs compared to hydrogen as it has been widely reported which provides a basic advantage for applicability for the proposed PSMAB process (Shiflett and Yokozeki, 2005; Yokozeki and Shiflett, 2007; Yuan et al., 2006; Yuan et al., 2007; Raeissi and Peters , 2009; Sudhir et al., 2004; Baltus et al.,2004). More detailed information about the RAPSAB process in such a context has been provided in Bhaumik et al. (1996), Obuskovic et al. (1998).

The influence of experimental temperature on the product quality of PSMAB process when [bmim][DCA] was used as absorbent was systematically investigated. Continued attempt of adding dendrimer to IL to enhance PSMAB performance especially at higher temperatures was also carried out. Comparison among different absorbents solutions with variable dendrimer concentration was investigated to determine an optimal absorbent composition. Further, reactions of this dendrimer amine with CO_2 are completely reversible as was observed with runs of thousands of cycles of absorption and desorption every day in this project. A few studies employed PEG-400 with dendrimer.

Influence of feed gas pressure up to 1723 kPag (250 psig) on product quality at high temperature was studied to investigate the stability of this system and the membrane module itself. An analysis of the influence of the tube-side header dead volume was carried out and a calculation was made to show what the actual product quality should be if tube-side dead volume was eliminated. To achieve satisfactory product qualities on both sides of the membrane module, namely, for the He-rich stream and the CO_2–rich stream, a 2-stage PSMAB process was proposed.

Solubilities of many gases in ionic liquids have been studied and published by utilizing a number of different techniques that include a gravimetric method (Muldoon et al. 2007; Shiflett and Yokozeki, 2005; Shiflett et al., 2006; Shiflett and Yokozeki, 2007; Anthony et al., 2002), a pressure decay method (equilibrium pressure and volume techniques) (Blanchard et al., 2001; Kamps et al., 2003), a quartz crystal microbalance method (Baltus et al., 2004), and gas uptake into a thin ionic liquid film technique (Hou, 2006; Hou and Baltus, 2007; Moganty, 2009). This project utilized the pressure decay method to find solubilities of pure carbon dioxide and pure helium in [bmim][DCA]. We have already indicated that this ionic liquid is a good absorbent for CO_2; more importantly we have found that it has a very good solubility for PAMAM dendrimer Gen 0 unlike some others. Solutions of PAMAM dendrimer Gen 0 in [bmim][DCA] having 20 wt% dendrimer and 30 wt% dendrimer with and without moisture have also been investigated at different feed gas pressures up to 1.38 MPa (200 psig) and at 323, 353, 363, and 373K. Solubilities from a CO_2-He feed gas mixture (40% CO_2, He balance) have also been obtained.

The apparent reaction equilibrium constants for reactions with primary amine functional groups in dendrimer have been determined for dry gas systems subject to particular assumptions. The range of reaction possibilities include only one primary amine consumed to all primary amines consumed since PAMAM contains a total of four primary amines. Most studies of CO_2 absorption with amines in a liquid absorbent employ an amine or two having a single amine functionality, primary, secondary, or tertiary. The dendrimer of this study has multiple amine functionalities, four primary and two tertiary amines. Therefore, the analysis of the data to determine the reaction equilibrium constant is complicated with considerable uncertainties.

Ionic liquids are quite expensive. Therefore the solubilities of CO_2 and He in an alternate solvent namely, polyethylene glycol, PEG 400, were also investigated. This solvent is also nonvolatile and does not undergo thermal degradation in the absence of oxygen. PEG is not very stable in air at $>80^0$C; however in the absence of oxidation agents, no degradation is expected (Han et al., 1995).

In addition, a mathematical model was also developed to predict the extent of separation of the feed gas mixture into two product streams, one He-rich and the other CO_2–rich. This model required both the diffusivity and solubility of various gas species in the ionic liquid. The experimental data obtained during the solubility determination was utilized to determine the diffusivities of the gases as well. Further the production rates of the He-rich and the CO_2-rich streams were also estimated from a numerical

solution of the model. These calculations were primarily implemented using the 3-valve configuration and a pure ionic liquid as an absorbent. Limited calculations for scale up were also considered.

2. EXPERIMENTAL METHODS

2.1. Materials and Chemicals

Ionic liquids (ILs), [bmim][DCA] and [Emim][Tf_2N], were purchased from EMD Chemicals (Philadelphia, PA) and used as received. The IL [bmim][DCA] was selected as the absorbent because of its excellent CO_2 absorption behavior as reported; further it is stable in the presence of moisture at a high temperature. As the results will indicate, it is also highly miscible with PAMAM dendrimer which will enhance the absorption process and improve the final separation results.

PAMAM dendrimer (generation 0) was purchased from Dendritech (Midland, MI). It was received as a dendrimer-methanol solution in which dendrimer concentration was 62.35wt%. To get pure dendrimer, the solution was vacuumed for certain time under relatively high temperature to remove methanol. PEG 400 was obtained from Chemicals Direct, Roswell, GA.

Simulated pre-combustion syngas gas containing 40.67% CO_2, helium balance as surrogate for H_2 was purchased from Air Gas (Salem, NH). This dry gas was used as feed gas quite often. When dendrimer and ionic liquid mixture is used as absorbent, the feed gas was humidified to enhance the absorption behavior.

All membrane modules used in this study are summarized in Tables 1a, 1b, and 1c. Four ceramic membrane modules were purchased from Media and Process Technology (Pittsburgh, PA) (Table 1a). Each module contains a single ceramic tubule in a stainless steel housing. The ceramic tubule had a γ-alumina coating on an α-alumina substrate with all surfaces hydrophobized with nonafluorohexylsilane coating; the outside surface had a pore size ~5 nm; the inside layers had larger pores. During all tests a solid Teflon rod was inserted into the tube side of the ceramic membrane tubule to reduce the tube side volume. The diameter of Teflon tube was 1/8 inch and about 47.5% volume in the ceramic tube side was reduced. Therefore in every cycle much less feed gas will enter the tube side to be treated leading to better separation results since the tubule had limited surface area.

Three Teflon membrane modules were supplied by Applied Membrane Technology Inc., Minnetonka, MN (Table 1b). These hollow fibers were based on porous Teflon hollow fibers from Markel Corporation, Plymouth Meeting, PA; Applied Membrane Technology Inc. reduced the pore sizes by plasma polymerization on the fiber O.D. All polyether ether ketone (PEEK) membrane modules were obtained from Porogen (Woburn, MA). These are listed in Table 1c. Two basic types of PEEK membrane modules were obtained. One type is small PEEK module (identified as PEEK-S) - it contains certain number of straight micro-porous hydrophobized PEEK hollow fibers in cylindrical stainless steel housing with additional 1 to 1.5 inch on each open end of the fibers for stainless steel fittings. The other type (sometimes identified as PEEK-L; at

other times as PEEK-I, PEEK-II and PEEK-III) has exactly the same type but much longer fibers or higher surface area in a stainless steel housing. The main difference from the small PEEK-S modules is that all fibers in the large PEEK-L module are often helically wound so that the length of the whole PEEK-L module is around 50 cm which is shorter than the actual fiber length. Further the fibers are sometimes tightly bunched together as if they are in a strap. Details of membrane module differences between PEEK-S and PEEK-L modules are listed in Table 1d.

The difference between PEEK-I and PEEK-II modules lies in their packing density (Table 1e). PEEK-II module has a much lower packing density; there is significant space between the consecutive fibers for the liquid absorbent compared to that in PEEK-I. The PEEK-III module (Table 1c) has much larger membrane surface area than the other PEEK-L modules; therefore the internal gas volume in PEEK-III is significantly larger than those in other modules.

Teflon balls with a diameter of 1/8" were bought from Engineering Laboratories, Inc (Oakland, NJ). During the PSMAB test, these small balls were sometimes added to both ends of the PEEK-L modules to reduce the existing dead volume in the tube-side headers as much as possible; Figure 1(d) illustrates the location of these balls in the module placed inside the oven.

2.2. Breakthrough Pressure test for membrane modules

Before newly received membrane modules could be used, it is important to test their breakthrough pressure for the ionic liquid [bmim][DCA]; the value of this breakthrough pressure will determine how high the feed gas pressure for PSMAB studies could reach. Breakthrough pressure was determined primarily by two factors: pore size of membrane fibers/tubules at the liquid-membrane interface on the shell side and the surface tension of the IL or any other liquid used to test. During the test, one port on the shell side of the membrane module was connected to a small cylinder containing [bmim][DCA] or any other liquid used (the other port kept closed) and the module shell side was filled with the IL (or any other liquid). The IL cylinder was also connected to a nitrogen cylinder to supply the desired pressure. The membrane module tube side had a low N_2 flow to bring any possible breakthrough of IL out when the liquid side pressure was gradually increased. When there is a leak, the IL could be detected from the tube side and the test pressure was defined as the breakthrough pressure. Liquids other than [bmim][DCA] were also tested to explore the capabilities of the membranes as well as compare its performance against other potential liquids such as [emim][Tf_2N], PEG 400.

2.3. Pressure swing membrane absorption (PSMAB) Process

The experimental arrangements to study the PSMAB process are shown in Figure 1c for a 3-valve process and in Figure 1d for a 5-valve process. In each case, the membrane contactor module with or without dead volume reduction was put inside a PV-222 oven (Espec Corp, Hudsonville, MI) so that the exact temperature could be set and controlled. The shell side of the module was filled with a certain absorbent such as ionic

liquid supplied from the absorbent container connected to a N_2 cylinder to maintain the desired pressure. Feed gas was introduced into the membrane tube side where it contacted the absorbent through the micropores to be absorbed. Usually the absorbent pressure in the shell side was kept about 138 kPag (20 psig) higher than the feed gas pressure in tube side to avoid any possible gas breakthrough. When a mixture of dendrimer and ionic liquid mixture was used as absorbent, feed gas may enter water bath before entering the tube side and be humidified to investigate water vapor influence on the absorption behavior; HP 1100 model water pump (Waldbronn, Germany) was used to inject water into the system. The humidity level was monitored with humidity probe HMP 76 (Vaisala Inc., Woburn, MA). The CO_2 product side was connected to a vacuum pump to supply driving force for product withdrawal; three or five pneumatic valves were used to control exactly the time period for different steps in one absorption cycle (3-valve system or 5-valve system). This valve control system was realized via a Programmable Logic Controller (PLC) scheme installed by PneuMagnetic (Quakertown, PA).

Both He-rich and CO_2-rich product streams were analyzed by HP 5890A GC (Santa Clara, CA). One Hayesep D 100/120 packed column from Alltech Associates (Deerfield, IL) was used to analyze the gas product. Helium was used as the carrier gas, oven temperature was kept at 100^{o}C and TCD temperature was kept at 125^{o}C. Due to the need for rapid monitoring of the gas stream compositions, a Quantek Model 906 CO_2 Analyzer (Grafton, MA) was primarily used so that the data collected allow estimation of real time CO_2 concentration fluctuations in the two product gas streams. Product flow rate values were low and were fluctuating due to the cyclic process. No attempt was therefore made to collect them. Instead they were allowed to collect in a small cylinder and rapidly allowed to go out through the CO_2 Analyzer which needed a certain minimum gas flow rate to determine the CO_2 composition on a real time basis. With a larger flow rate, one can collect it in a larger cylinder and then have a small steady flow rate taken out of it under constant pressure.

A pressure transducer installed inside the oven and directly connected to the feed gas end of the tube side of the membrane module revealed detailed pressure changes during the absorption process. This allowed a better understanding of the pressure swing membrane absorption process. For example, from the pressure drop in the absorption step, one can estimate how much gas was absorbed and find out which absorbent was better. Changes in pressure versus time were read and recorded by the pressure transducer unit which included one pressure transducer (Model PX32B1-300GV), one assembly cable (Model CA-6TE24-010-PX32), and one universal input Ethernet (Model DP41-B-EI) purchased from Omegadyne Inc., Sunbury, OH.

All PSMAB process data reported here were taken after at least 30 cycles running. Also all tests were repeated 3 times to confirm their accuracy.

2.4 Solubility Apparatus and Measurements

The gas solubility measurements were made using a pressure decay method. The schematic of the apparatus is shown in Figure 1e. The gas solubility measurement system mainly contained a cell volume, a reference volume, a programmable temperature oven (Model PH-202, ESPEC North America Inc., Hudsonville, MI), and a gas cylinder**.** A volume of 10 mL of liquid absorbent was measured, weighed, and added to the cell. The whole system was then degassed for about 5 hours using a vacuum pump (KNF, model UN 726.3 FTP, Trenton, NJ) with all valves (R.S. Crum & Company, product # SS-2P4T-BK, Mountainside, NJ) opened. For solubility measurement involving moisture, a predetermined amount of water was weighed and added along with the absorbent liquids to make up to 10 mL in a graduated cylinder. The solution was then transferred into the cell (stainless steel cylinder). After the connection to the cell cylinder was closed with an open/close valve 4, the system was degassed for 3 hours without the cell cylinder to prevent water being evacuated during the degassing process. Then the cell cylinder was attached onto the system and was degassed for 15 minutes. The same process was repeated for the case of gas mixtures.

After the degassing process, the desired gas (CO_2 or He or a mixture of both) was loaded into the reference stainless steel cell cylinder (R.S. Crum & Company, product # 304L-05SF4-150, Mountainside, NJ) with valves 1, 3, and 4 closed to a pre-determined pressure while valve 2 was opened. The oven was turned on to allow temperature of the gas to reach a desired temperature in the reference volume after opening valve 4. Then, valve 3 was opened and controlled by a pneumatic controlling unit (PneuMagnetic, Quakertown, PA) while valves 1 and 2 remained closed. The pneumatic controlling unit allows any user to open and close valve 3 with a toggle switch that is easily accessible and positioned outside the oven. Valve 3 can be opened for up to 99 hours which is long enough to ensure that equilibrium is fully established between both cylinders. The final pressure difference was used to calculate the number of moles of gas absorbed by the absorbent liquid.

Changes in pressure versus time were also read and recorded by pressure transducer units in both cell and reference cylinders. The rate of change of the pressure indicates the rate of absorption of CO_2; from such data one can also calculate the diffusion coefficient using the assumption that the depth of the liquid in the test cell is infinite (Hou, 2006; Moganty, 2009). Such calculations are not reported here; they are part of transport modeling and are discussed in section 3C. The pressure transducer units included two pressure transducers (Model PX32B1-250GV), two assembly cables (Model CA-6TE24-010-PX32), and two universal input Ethernets (Model DP41-B-EI) purchased from Omegadyne Inc., Sunbury, OH. The pressure in the transducers ranges from zero to 1.72 MPa (~250 psig) with 0.25% linearity accuracy. The transducers can withstand a temperature of up to 115^{o}C (388K). This provided an upper limit to the measurements.

For CO_2/He gas mixture, the equilibrium gas mixture composition was determined by a gas chromatograph (Shimadzu Scientific Instruments, Model GC-2014, Somerset, NJ). A CarboxenTM-1010 PLOT Capillary (Sigma-Aldrich Inc., product #: 25467, Saint Louis, MO) was used in the analysis of the gas mixture at equilibrium. Nitrogen was used as the carrier gas; column and TCD temperatures were kept at 180^{o}C and 230^{o}C respectively. The temperature of the split injector was kept at 200^{o}C with a

linear velocity flow control and a split ratio of 5. The run time for the analysis was set at ten minutes.

2.5 Absorbent Degradation Analysis

These analyses were carried out at Dendritech Inc., Midland, MI. Samples of our fresh absorbent ionic liquid [bmim] [DCA] were sent to Dendritech. Further samples of ionic liquid containing dendrimer at certain levels were withdrawn from the membrane module after considerable use and sent for analysis: these are designated NJIT-1 and NJIT-2. The following list represents the sample identifications:

NJIT-1 20% G(0)/BMIM:DCA, unknown history

NJIT-2 30% G(0)/BMIM:DCA, unknown history

G(0):IL-1 20.1% G(0)/BMIM:DCA(NJIT-007), freshly prepared

G(0):IL-2 29.8% G(0)/BMIM:DCA(NJIT-007), freshly prepared.

G(0) freshly prepared sample of "standard" G(0)

IL BMIM:DCA(NJIT-007), freshly prepared.

All samples were prepared at 2% (wt/wt) concentration in HPLC water. All prepared samples were injected (1.0 μL) into a Waters HPLC system comprised of an autoinjector, gradient pump, column oven (30^{o}C), and UV/Vis detector (210 and 300 nm). The column was Waters symmetry C18, 3.6μ, 150 x 4.6 mm. The eluents were: A) 0.010M sodium pentane sulfonate (pH=2.5). B) acetonitrile; Gradient: 95/5(A/B)—5min→95/5—12min→70/30—4min→0/100—5min→0/100; Reequilibration (95/5) 10 min. The software used was: Waters Breeze 2. Eluted peaks were operator defined.

3. RESULTS AND DISCUSSIONS

3A. PSMAB Process Studies

3A.1. Breakthrough Pressure

All breakthrough pressure test results for three types of membrane modules with different liquids are listed in Tables 2a, 2b and 2c; the comparative results are summarized in Table 2d. Four kinds of liquids were used for testing while essentially only [bmim][DCA] with or without dendrimer was applied as the absorbent (except for a few studies with PEG 400). A total of four ceramic membrane modules, three Teflon and seven PEEK membrane modules were tested (Tables 2a, 2b, 2c and 2d). Table 2a shows that in general the ceramic modules could withstand a breakthrough pressure of 2068 kPag (300 psig). From Table 2b it is clear that membrane modules of Teflon did not perform well; they could not go up to the desired pressure. As a result, these modules were not tested at all in the PSMAB setup. As we can see from the results in Table 2c,

when ionic liquid [bmim][DCA] was used as solvent, for PEEK-S (30-105-21), the feed pressure can go only up to 965 kPag (140 psig). PEEK-I (2P6296), PEEK-II (SN421) and PEEK-III (SN459) modules could easily withhold the ionic liquid at much higher pressure up to 1723 kPag (250 psig). When we provide a symbol >300 psig it means no leakage up to 2068 kPag (300 psig) but tests at higher pressure were not done.

Table 2d summarizes the results for ceramic and PEEK modules and different absorbents. For ceramic membrane modules, the feed pressure can go up to 2068 kPag (300 psig) while for PEEK-S membrane modules, the highest test pressure was 965 kPag (140 psig); some minor liquid leakage could be found when liquid on shell side was pressurized to 160 psig. However PEEK-L modules could easily withhold liquids at higher pressure up to 2068 kPag (300 psig).

3A.2. Solubility of PAMAM Dendrimer Gen 0 in Various Absorbents

Table 2e summarizes the experimentally observed results of solubility of PAMAM dendrimer Gen 0 in various solvents at room temperature. It is clear that PAMAM dendrimer Gen 0 is highly soluble in [bmim][DCA], PEG 400 and glycerol carbonate; however it has very low solubility in [emim][Tf_2N]. This is one more reason for selecting [bmim][DCA] as our ionic liquid for the project.

3A.3. The 5-valve System Design and Its Comparison with the 3-valve System

As described in Section 1.1, the advantage of the 5-valve system is that we can have a similar He-rich product and an improved CO_2-rich product at the same time. Experimental data listed in Table 3 clearly reveal the advantages of the 5-valve system. With one PEEK-S membrane module and pure [bmim][DCA], tests were carried out at room temperature with a feed pressure of upto 689 kPag (100 psig). As expected the newly designed 5-valve system showed better performance. With feed gas pressure at 100 psig, using the 5-valve system we can have He-rich product with a CO_2 concentration of 8.31% and a CO_2-rich product with CO_2 concentration of 70.10%. While if using 3-valve system, a CO_2 concentration of 8.00% in helium side will bring a product with a CO_2 concentration as low as 38.40% at CO_2 side; on the other hand, if CO_2-rich product with a CO_2 concentration of 70.95% was achieved, a helium-rich product with CO_2 concentration as high as 30.90% is what we will get at the other side.

A look at the quality of the CO_2-rich product for the 3-valve system for cases where the He-rich product has low CO_2 concentration around 8 - 10.7% shows that the CO_2 concentrations are less than 40%. For the 3-valve system if we want to have a high quality He-rich product, only a very small amount of gas in the tube side will be taken out as the He-rich product. The CO_2-rich product is composed of two parts: the large amount of He-rich gas remaining in the tube side and the CO_2-rich gas absorbed in solvent; the first part is in much larger proportion since not enough desorption was carried out. In this case the readout from CO_2 analyzer was determined primarily by the first part since

complete desorption was not carried out. As a result the CO_2-rich stream's concentration is a bit lower than that of the feed gas since it has experienced considerable absorption.

3A.4. Determination of Optimal Duration Time for Cycle Steps

Once the preliminary absorption cycle design was completed, it was necessary to determine the optimal duration time for each step. As mentioned above, in a typical 3-valve pressure swing membrane absorption process, there are four essential steps described as feed in, absorption, He-rich product withdrawal (there will be a middle part gas withdrawal step in the case of a 5-valve system) and CO_2-product withdrawal. The aim of the first step (feed gas in) is establishing the desired feed pressure in the tube side of the membrane module; there is also some absorption-based purification at the front end of the gas stream which has the highest contact time. During our tests, for all membrane module combinations applied, 5 s was long enough to establish the desired feed pressure up to 1728 kPag (250 psig). Therefore the duration of the first step will be 5s in all continuing tests. Also it is easy to find out the optimal time for the desorption step since we can directly read out the pressure change during this step. Usually to make sure that most of the CO_2 absorbed in ionic liquid will be desorbed during the vacuum step, this step will be maintained as long as 30s or 45s for different modules respectively. For middle part gas withdrawal time, usually we will maintain it as long as 20s since we want to have a higher quality CO_2-rich product. A longer middle part gas withdrawal time will let us take more helium-rich gas in tube side out; therefore a higher CO_2 concentration could be achieved in the CO_2-rich product. In some experiments only 2 s was used for middle part gas withdrawal.

3A.4.1. Determination of optimal duration time for the absorption step

3A.4.1.1. Optimal absorption step duration time for ceramic module system

Here a combination of three ceramic membrane modules in series (unless otherwise mentioned) mode was employed; pure ionic liquid [bmim][DCA] was used as the absorbent. The absolute pressure change in the tube side tests during the long time absorption step was carried out at different temperatures with a fixed feed pressure of 1034 kPag (150 psig).

As shown in Figure 3(a), during the long duration absorption step, pressure in tube side gradually decreased due to absorption of CO_2 and helium into the shell-side absorbent. From the pressure drop during 900 s absorption time, we can determine the optimal duration time for absorption step. It is obvious that longer absorption time will bring more CO_2 absorption and therefore a better product quality. But too long an absorption step will reduce the treatment capacity of the system. We will have to find a balance between absorption time and treatment capacity. From Figure 3(b) it is seen that at 120 s of absorption step time, i.e. ~13.3% of total 900 s duration, the system has achieved about 55~65% CO_2 absorption for different temperatures. Thus the optimal

absorption step duration for this system was chosen as 120 s. Further higher temperatures lead to a faster absorption at the beginning.

Absorption at higher pressures was also carried out with four ceramic modules in series at room temperature. These results for 900 s absorption time (shown in Figure 3(c)) indicate that during the long duration absorption step, the pressure in tube side gradually decreased due to absorption of CO_2 and helium in feed gas into the shell-side absorbent. When a higher feed pressure was introduced into the tube side, due to higher CO_2 partial pressure in the feed, more absorption will happen and this will bring about a sharper pressure drop. If we consider the ratio between the pressure drop and the absolute feed pressure, we find that the ratios are close for all test pressures (For 250 psig, 12.5%; for 200 psig, 12.6%; for 150 psig, 11.5%; for 100 psig, 10.9%). Since for all tests with different feed pressures, the same membrane modules (same contacting area) and absorbent were used, feed gas pressure will be a major influencing factor for final absorption performance. Absorption of CO_2 into the ionic liquid may be described by Henry's law; thus it is easy to understand why we got very close ratios between pressure drop and absolute feed pressure for different feed pressures.

Now from the pressure drop phenomena during 900 s absorption time, we can determine the optimal duration time for absorption step. It is obvious that longer absorption time will bring more CO_2 absorption and then better product quality. But too long a step will reduce the treatment capacity of the system, that is to say we will have to sacrifice the product quantity. Just like the tradeoff between permeability and selectivity for a membrane, we will have to pursue a balance between absorption time and treatment capacity. If we examine the data in Figure 3c carefully, we find as before that at 120 s of absorption step time, the pressure drop for all 4 feed pressures is about half of the total drop in 900s respectively. This means that compared with 900 s absorption time, 120 s absorption time using around 13.3% of the time the system achieved about 50% CO_2 absorption. This confirms our selection of the duration of the absorption part of the cycle as 120 s for the configuration of 4 ceramic membrane modules in series as well.

3A.4.1.2. Optimal absorption step duration time for PEEK-S module system

Similar to the tests described above, two PEEK-S membrane modules were connected in series; feed pressure was kept at 689 kPag (100 psig), and absorption behavior of 900 s for the PEEK-S membrane module system was studied at different temperatures.

As shown in Figure 4(a), the extended time absorption behavior for the PEEK membrane module system was quite different from the ceramic module system. Actually with the hollow fiber based PEEK-S modules the absorption of gas was much faster.

Most of the absorption was completed within 100 s. If we set the optimal absorption step duration time as 30 s around 3.33% of the total extended absorption time, we see from Figure 4(b) that 55~65% of total absorption has taken place. Based on these results, for two PEEK modules in series mode system, its optimal absorption step duration time could be fixed as 30 s much shorter than 120 s for the ceramic system.

Due to the very high surface area per unit volume of the PEEK system, much more rapid absorption takes place into the surrounding liquids compared to that in the ceramic tubule system. In PSMAB process rapid initial absorption is important. After this initial period, there is slow diffusion and absorption into the large volume of the surrounding liquid as we see in Figures 3 and 4.

3A.4.2. Optimal duration time for the He-rich product withdrawal step

Next we determined the He-rich product withdrawal time. For PSMAB process, we should increase the contacting opportunity between the gas and the absorbent. From this point of view, a longer and thinner hollow fiber will be favorable since the surface area per unit volume can be increased a lot. Therefore during a cycle when the absorption step is completed over a short duration, gas composition in the tube side will not be same, we are more likely to have a concentration distribution along the length. Since the gas at the module end for He-rich product withdrawal passed through the whole fiber and had more contacting opportunity with the absorbent in shell side, its CO_2 concentration should be much lower than the other end that is why we took gas out from this exit as the He-rich product. In this case we would like to investigate the influence of helium withdrawal time on its product quality. Since the PEEK-S-based and ceramic membrane modules have very large variation in the internal diameter of the membrane hollow fibers/tubules, here we will investigate their influence one after the other.

3A.4.2.1. Influence of He-rich product withdrawal time in PEEK-S modules

For tests described below, two PEEK-S membrane modules were put together in series mode and pure [bmim][DCA] was used as absorbent. All tests were carried out at room temperature with a feed pressure of 965 kPag (140 psig). For this system using the method described in section 3A.4.1.2 the optimal absorption step time employed was 30s.

Figure 5a presents pressure changes in tube side within one complete cycle. It started from a negative pressure, and then reached 965 kPag (140 psig) after feed gas introduction. At the end of 30 s absorption time, pressure in the tube side dropped to 133 psig. Next by adjusting the He-rich product withdrawal time, different pressure drops were observed. Next middle part gas release left tube side at one atmosphere pressure and the last step of CO_2–rich product withdrawal brought tube side to a negative pressure again.

Different He-rich product withdrawal durations will lead to different pressure drop in the tube side. Longer duration will bring more pressure drop that means more gas in the tube side will be taken out as He-rich product and thus product quality will be influenced. As shown in Figure 5a, starting from 133 psig, when pressure at the end of helium withdrawal step decreased to 100 psig (1 s), we had helium product with CO_2 concentration as low as 5.5%; while when pressure was reduced to 78 psig (2 s), CO_2 concentration in helium-rich product increased to 7.7%; 65 psig pressure generated 10.0% concentration (3 s); 47 psig brought a 13.5% concentration (5 s) and 30 psig led to the poorest product with CO_2 concentration up to 17.5% (10 s). In terms of the CO_2-rich product, since it was withdrawn from the same atmospheric pressure in tube side, its quality was stable maintaining a CO_2 concentration at 77.9~78.4%. Figure 5b clearly illustrates the effect of duration of helium product withdrawal on the quality of the two product streams.

Based on these results there should be a tradeoff between the He-rich product quantity and its quality. We need to find a balance between these two factors by determining a proper He-rich product withdrawal duration time in a practical application.

3A.4.2.2. Influence of He-rich product withdrawal time in ceramic modules

In tests with PEEK-S hollow fiber membrane modules mentioned earlier, with an optimal absorption time of 30 s, the product withdrawal time showed great effect on the product quality. Compared with PEEK-S hollow fibers, ceramic membrane module has a tubule with a much larger diameter. To find out if this will have any impact, similar tests were carried out with 4 ceramic membrane modules in series and the feed pressure was 689 kPag (100 psig). As determined earlier the optimal absorption time was set as 120 s in each cycle.

As shown in Figure 6a, unlike the PEEK-S module test results, He-rich product withdrawal time showed very little influence on its product quality in the case of ceramic modules except for the longest 6 s withdrawal time. For the first 3 different withdrawal times tested (1 s, 2 s and 4 s), we achieved almost the same He-rich and CO_2-rich products. When the withdrawal time was set as 6 s, CO_2 concentration in the He-rich product increased obviously since we almost took all gas in tube side as He-rich product. If we consider the product output that could be revealed by the pressure drop in product withdrawal time, all started from around 95 psig (that meant about 5 psig CO_2 pressure drop caused by absorption in absorbent during the absorption step), as shown in Figure 6b for 1 s withdrawal time, its pressure drop was about 31 psig; for 2 s, pressure drop was about 50 psig; for 4 s, about 62 psig. This meant compared with the PEEK-S system, because of its much larger tubule diameter, even though we had a Teflon rod inside the ceramic tube to reduce the gas volume, there was still too much feed gas in the tube side waiting to be treated. Only a very small part of the feed gas could be satisfactorily absorbed due to limited gas-liquid contacting area. As we know from Figures 3 and 4, CO_2 absorption in PEEK-S modules is a much faster process than that in the ceramic

module case; therefore when feed gas in PEEK-S fibers reached the other end during feed introduction in step 1, it had experienced already considerable CO_2 absorption. Therefore in the ceramic case it is more likely that the gas concentration distribution along the tube length was not well developed as in the PEEK modules after the absorption step. So for ceramic membrane module test we can take much more gas in tube side out as helium-rich product, while its quality was not as good as that produced by PEEK-S modules under similar test conditions. So for the four ceramic modules in series mode, 4 s will be a better choice as helium-rich product withdrawal time.

3A.5. Influence of Temperature and Feed Pressure on the PSMAB Process

3A.5.1. Influence of feed pressure on PEEK-S module system

To study the effect of feed gas pressure, we maintain the optimal cycle time distribution as (5; 30; 3; 15; 30 s). Two PEEK-S membrane modules were put together in series mode, pure [bmim][DCA] was used as absorbent and all tests were carried out at room temperature.

As shown in Figure 7a, with an increase of feed gas pressure, the helium side product quality decreased a little bit while on the CO_2 side the product quality had some improvement. For example, when the feed gas pressure was 80 psig, helium-rich product had a CO_2 concentration of about 5.5% that was much lower than 10.0% when feed gas pressure was increased to 140 psig. For the former condition CO_2-rich product had a concentration about 75.0% that was lower than 78.8% when feed gas pressure was 140 psig. The reason for this difference is as follows. When feed gas pressure was increased, more CO_2 will be absorbed in absorbent that will definitely bring a better CO_2 product. In other words, higher feed pressure or CO_2 partial pressure will favor better CO_2-rich product. While since the absorption capability of PEEK-S modules based absorption system was limited, when feed gas pressure increased, possibly this would give the present system too much burden and insufficient capability to absorb the increased feed gas as much as it can at a low pressure. This will explain why helium product quality decreased a little bit when the feed pressure increased. Figure 7b represents the pressure changes in tube side with different feed gas pressures to help understand final gas product partition in tube side.

As discussed in Section 3A.4, at the end of absorption step in each cycle, there was likely a concentration distribution along the length of the module fibers. When the feed gas passed through longer length inside the fibers, it had more contacting possibility with IL on shell side that means more CO_2 absorption; therefore its CO_2 concentration should be lower. Based on this consideration, we can conclude longer fibers bring better absorption results. Comparison of results from Table 3 (one PEEK-S module) and Figure 7a (two PEEK-S modules) proved this assumption was reasonable. For example, with the feed gas pressure at 80 psig, one PEEK-S module could produce a helium-rich product with CO_2 concentration about 6.81% based on 15 psig pressure drop caused by product withdrawal; when two PEEK-S modules in series were applied a helium-rich product with CO_2 concentration about 5.50% based on 35 psig pressure drop caused by product

withdrawal could be achieved. This comparative performance definitely reveals the advantages of a longer PEEK fiber: relatively more product output with better quality.

3A.5.2. Effects of temperature and feed pressure on ceramic module system

As mentioned in the introduction, pre-combustion shifted syngas has a high temperature and pressure. Therefore it is important to investigate if the PSMAB system will still show satisfactory separation under severe testing conditions. Similar to the method used to optimize the absorption step duration time, 900 s absorption step time was set to find out the influences of temperature and pressure in four ceramic membrane modules in series.

As shown in Figures 8a-d, it can be seen that with an increase of temperature, CO_2 absorption in the ionic liquid decreases. This is reasonable since usually temperature increase will bring a negative influence to the solubility of gases in a solvent. However, increase of feed gas pressure will cause more CO_2 absorption since CO_2 partial pressure is higher and thus more gas will be absorbed following Henry's law. One interesting item to be pointed out is that at the beginning period of absorption the solubility difference is not so much; this is beneficial for our test since the optimized absorption time will be kept as 120 s. What should be mentioned more is that under higher feed pressure, influence of temperature was not so obvious, in other words, weak. When feed pressure was 1723 kPag (250 psig), the absorption capability was almost the same under different temperatures tested. The results are especially meaningful for treatment of pre-combustion shifted syngas available only at a high temperature of 150-200^{o}C.

3A.5.2.1. Influence of temperature on PSMAB performance of ceramic module system

Since the low temperature (L-T) water gas shift reactor product stream is likely to be available at a high pressure and temperature, in this part with the feed gas pressure kept at 1723 kPag (250 psig), the influence of temperature on four ceramic modules in series mode was investigated in the range of 25 to 125^{o}C. The product quality results are presented in Figure 9. The test temperature showed very little influence on the PSMAB effect in the ceramic module system. This was in accordance with absorption behavior results in 3A.3.2.1. For all testing temperature of 25 to 125^{o}C, He-rich product showed a CO_2 concentration all around 35.0%. Condition at CO_2 side seemed to be a little different since CO_2 concentration did show a slight increase from 46.5% (25^{o}C) to 48.5% (125^{o}C). This may be caused by easier desorption of absorbed CO_2 from absorbent at a higher temperature. Absolute pressure change records during one complete cycle from different test temperatures are listed in Figure 10; they essentially yielded the same pressure change condition which explains why close separation results were achieved.

3A.6. PSMAB Performance with Middle Part Gas Recycled using Ceramic Membrane Module System

In order to investigate if recycling middle part gas will influence the product quality of the PSMAB system, with three ceramic membrane modules in series and pure

[bmim][DCA] as absorbent, one set of tests with middle part gas being recycled was carried out at 250 psig at different temperatures. In the middle part gas withdrawal step of a 5-valve system, the final pressure in tube side will be determined by the ratio between middle part gas collecting cylinder volume and membrane tube side volume. Thus by adjusting the ratio between cylinder volume to module tube side volume the final pressure in the tube side after middle part gas withdrawal step could be controlled that will determine CO_2-rich product quality (in this set of tests we chose a small cylinder for collecting middle part gas, its volume was very similar with tube side volume that means the ratio is close to 1.0). Then when the CO_2-rich product withdrawal step was finished, the module tube side will have negative pressure; therefore at this time middle part gas in collecting cylinder could be introduced into tube side as initial feed gas followed by additional high pressure feed gas introduction.

There are 6 steps in one 5-valve system cycle as listed below, totally 169 s as shown in Figure 11a:

Step 1: Middle part gas recycled into membrane tube side as initial feed gas, 5 s;

Step 2: Fresh feed gas was introduced to tube side until desired pressure established, 5 s;

Step 3: Absorption between gas and absorbent IL, 120 s;

Step 4: Helium-rich product withdrawal, 4 s;

Step 5: Middle part gas withdrawal, 5 s;

Step 6: CO_2-rich product withdrawal, 30 s.

If we compare the results between Figure 9 and Figure 11b, it is clearly seen that middle part gas recycling to the system did not show obvious influence on the He-rich product side since the recycled middle part gas was very limited compared with the final 250 psig feed gas in module tube side; another reason was its composition was not far different from that of the feed gas. For CO_2-rich product side, conditions seemed to be different since its CO_2-product quality changed just a little bit. This difference could be easily explained. In the case without middle part gas recycling, CO_2-rich product was withdrawn from atmospheric pressure as shown in Figure 10; while in the middle part gas recycled case, as shown in Figure 11a, CO_2-rich product was withdrawn from about 20 psig above atmospheric pressure. Since for the latter case more CO_2-rich product could be achieved thus its quality would not be as good. Similar to the earlier results from Section 3.5.2, temperature did not show obvious influence to PSMAB process with ceramic membrane modules in case of middle part gas being recycled; absorption performance from room temperature to 125 ^oC was quite stable.

3A.7. Influence of Dendrimer on CO_2 Solubility and Absorption Performance

As reported earlier (Kovvali et al, 2000; Kovvali et al., 2001; Kosaraju et al., 2005), polyamidoamine (PAMAM) dendrimer can react with CO_2; therefore addition of dendrimer to solvent [bmim][DCA] will enhance its CO_2 solubility performance. To

investigate the influence of dendrimer in the PSMAB process, a set of tests with a PEEK-L module was carried out with pure [bmim][DCA] and its 25 wt% dendrimer solution as absorbent. Feed pressure was kept as 1034 kPag (150 psig) and different temperatures were applied. For both tests, middle part gas was collected and then recycled to the feed zone at the beginning of the next cycle as described in section 3A.6.

It could be clearly seen from Figure 12 that when pure [bmim][DCA] was used as absorbent, the increase of test temperature showed obvious influence on the helium side product quality. Under similar pressure drop in each cycle that meant comparable amount of gas was taken out as helium product, at room temperature about 28^{o}C, pure [bmim][DCA] could produce a helium product with CO_2 concentration about 5.0%; when the test temperature was increased to 100^{o}C, as we know higher temperature will lead to gas solubility decrease in the absorbent liquid, a helium product with a much higher CO_2 concentration of around 16.3% was produced. Compared with pure [bmim][DCA], when 25 wt% dendrimer solution was used as absorbent and under similar test conditions, a much more stable performance could be seen in Figure 12. At room temperature, helium product from dendrimer mixture had a CO_2 concentration about 7.1% that was higher than the value 5.0% for pure [bmim][DCA]. We can explain this difference from consideration of viscosity. At room temperature adding dendrimer to IL will greatly increase its viscosity that will show negative effect for gas transfer. When temperature increased the viscosity of mixture will decrease thus this negative influence will disappear and what is more dendrimer will selectively react with CO_2 in feed gas and play a positive role to enhance CO_2 solubility. As shown in Figure 12, even when test temperature was increased to 100^{o}C, with 25 wt% dendrimer in DCA as solvent, a helium product almost same as 50^{o}C (that showed a CO_2 concentration about 9.0%) was achieved. Here because quite a large part of the gas was released as CO_2 product as we can see from Figures 13a and 13b, the achieved CO_2 concentration was around 55~60% . Results of improving CO_2 side product quality are reported later.

Figures 13a and 13b show the pressure change in membrane tube side with the two different liquids as absorbent. If we compared the pressure drops during absorption step, one finds that when pure [bmim][DCA] was used as absorbent, the pressure drop was obviously influenced by the test temperature. When dendrimer mixture was used as absorbent, as we can see from Figure 13b, all pressure drop curves from absorption step were parallel which meant similar pressure drops. This could explain their different performances under various temperatures.

3A.8. Comparison of PEEK and Ceramic Membrane Module Systems

From results presented earlier, we see that there is considerable difference in the performance between the PEEK module and the ceramic module systems. Obviously the performance of PEEK system is much better. The reasons are as follows. In PSMAB process, membrane contacting module plays an important role by providing non-dispersive contacting area for feed gas in the tube side and the liquid absorbent on the shell side. What should be done first is to compare the dimensional parameters of thes two types of modules. Since hollow fibers in PEEK modules were arranged in parallel

mode and the same absorption process happened in each fiber at the same time so dimensional calculation will be carried out using only one fiber. Detailed comparisons are provided in Table 4.

Only one hollow fiber was used for calculation since multiple hollow fibers in one module can only increase its treatment capacity without directly affecting the absorption behavior. In the PSMAB process, absorbent capability and membrane module contacting area will be the two main factors that will determine the final separation effect for a given cycle configuration. According to dimensional parameters listed in Table 4, in terms of the ratio between the contacting area in one hollow fiber and the corresponding feed gas containing volume, for ceramic module (with a Teflon rod in tube side case) it is only 8.19 cm^{-1} which is much lower than 54.71 cm^{-1} valid for a PEEK hollow fiber. This could directly explain why in Section 3A.4 PEEK membrane module showed much faster absorption behavior than the ceramic module. This also explains why PEEK modules have much better PSMAB performance than the ceramic modules. In other words, if ceramic modules with similar dimensions as PEEK fibers could be successfully prepared, much better separation results and promising application potential for this kind of modules that show stable separation results under high temperature could be expected.

If we compare the results from PEEK-S and any of the PEEK-L membrane modules, it could be concluded that even if they are using exactly the same fibers, with much shorter fibers PEEK-S could achieve comparable and sometimes even better separation results than PEEK-L. This performance difference is to be attributed to their different module configurations. The most possible explanation is that fibers in PEEK-L module were bundled very tightly thus there was very limited absorbent between fibers; therefore during absorption the surrounding liquid was getting close to saturation very soon and developed reduced absorption ability.

3A.9. Effect of Membrane Module Design on PSMAB Performance

Membrane module design involves other aspects beyond a simple incorporation of a large gas-liquid contacting membrane surface area per unit system volume. First, it is important to have the hollow fibers placed in the module such that there is adequate space around each fiber for enough of the absorbent liquid to absorb the gas dissolving at the gas-liquid interface. If the fibers are placed too close to each other, there may not be enough absorbent liquid in between them for absorption leading to reduced performance. Therefore the fiber packing density in the module has to be modulated to take care of this need. This is especially true of the 6 fibers-in-a-strand design originally supplied to us by the membrane manufacturer, Porogen. Second, hollow fiber modules have dead volumes in so far as shell-side gas absorption is concerned. There are two regions of dead volume in a hollow fiber module in the present context: the tube-side header at both ends of the hollow fiber module and related connections; two potted section of the hollow fiber module at two ends of the fiber. Gas mixtures present in these regions do not participate in the gas-liquid absorption-desorption process with the shell-side absorbent liquid. Further they contaminate and affect the compositions of the two product streams

withdrawn from two ends of the hollow fiber device during different parts of the cycle. We will look at these two effects now one after another.

3A.9.1 Comparison between PEEK-I and PEEK-II modules when running at different temperatures

A look at Tables 1c and 1e shows that the main difference between PEEK-I and PEEK-II membrane modules is that the latter has a much lower fiber packing density around 21.8% compared to 67% in PEEK-I. This means that much more absorbent liquid will exist in the space between the hollow fibers in PEEK-II. From Figure 14 we observe that under the same testing conditions larger pressure drop as a result of higher gas absorption is visible in PEEK-II compared to that in PEEK-I. In order to investigate how this packing density will influence the PSMAB process and its product qualities, a set of tests were carried out at different temperatures with same feed gas pressure of 1034 kPag (150 psig). Pure [bmim][DCA] was used as absorbent. The pressure drops in the absorption step are shown in detail in Figures 15a and 15b. It is clear that PEEK-II has much higher pressure drop than that in PEEK-I. Figure 16 shows that the separation performances for both product streams are better with PEEK-II compared to those of PEEK-I.

If we compare pressure drops in Figure 15 (a) and 15(b), the first conclusion we can make is that compared with PEEK-I, under same running conditions, PEEK-II showed larger pressure drop. This is in accordance with the results shown in Figure 14. In terms of temperature influence, PEEK-I showed obviously different behavior from PEEK-II. Pressure drop in tube side of PEEK-I did not vary very much under different test temperatures. Different from PEEK-I, test temperature showed great influence to PEEK-II. Higher temperature brought larger pressure drop in tube side. This could be explained by the fact that there is very limited amount of absorbent surrounding the hollow fibers in PEEK-I thus it will be very easy to be saturated thus we cannot see an obviously difference from different temperature. Unlike PEEK-I, PEEK-II has a much lower packing density thus there is much more absorbent existing among fibers thus different pressure drops from different test temperature have an opportunity to be presented. Another possible reason for much higher pressure drop at higher temperature for PEEK-II could be at higher temperature gas absorption will be facilitated so gas pressure drop rate will increase. Usually temperature increase will decrease CO_2 solubility in solvents. On the other hand helium will have an opposite tendency when temperature increases: its solubility in liquids will increase. Our 60 s absorption duration is a short period and far away from the gas-liquid system to reach an equilibrium state thus during this period it looks like the rate of gas absorption will mainly be rate-controlling and this could explain the results in Figure 15 (b).

Influence of running temperature on product qualities from both PEEK-I and PEEK-II membrane modules are shown in Figure 16. At first we will discuss the influence of temperature on product qualities. Unlike feed gas pressure that is in favor of CO_2-rich product while negative for He-rich product, test temperatures showed negative effects for both products that meant when running at higher temperature both helium-rich

product and CO_2-rich product will face quality degradation. We will show soon that at higher temperature solubility selectivity of CO_2 over helium in IL will decrease. This should be the reason for product quality degradation at higher temperatures.

If we compare product qualities from PEEK-I and PEEK-II under same testing conditions, it can be clearly seen that both CO_2-rich product and He-rich product qualities of PEEK-II were better than those from PEEK-I. The difference for the two product qualities was different: helium-rich product qualities of PEEK-II were only a little bit better than PEEK-I while for CO_2-rich product quality, PEEK-II was much better than PEEK-I. This could be explained as follows. Because of its much lower packing density, PEEK-II has much more absorbent surrounding fibers thus much more gas will be absorbed during each cycle. More absorption will of course bring a better CO_2-rich product quality. The reason we did not see an obvious helium-rich product quality between PEEK-I and PEEK-II may be attributed to this two points: firstly compared with absorbed gas, there is still much larger amount of gas in the module tube side; secondly we almost took most of this tube-side gas out as helium-rich product. This super large withdrawal quantity masked the influence of test temperature on product quality.

3A.9.2. Performance improvement by reducing dead volume of PEEK-II module

Of the two regions of dead volume in a hollow fiber module, nothing can be done to the potted section dead volume. However, for the tube-side header section of the membrane module and related connections, we can greatly reduce it by adding small diameter Teflon balls. To find out how much improvement could be achieved after dead volume was reduced by this method, a set of tests were carried out at room temperature under different feed gas pressures with PEEK-II membrane module. The dead volume formed by header section connections for PEEK-II has been calculated to be about 35.75 cm^3 and the total Teflon balls volume we have added to both ends is around 28.5 cm^3. Pure [bmim][DCA] was used as absorbent. Cycle time was set as 5 s for feed gas introduction; 60 s for absorption; 2 s for helium-rich product withdrawal; 2 s for middle part gas withdrawal; 60 s for CO_2-rich product withdrawal and another 2 s for middle part gas recycle. Detailed pressure changes in module tube side during one complete cycle under different feed gas pressures are summarized in Table 5. Pressure drops within absorption step are presented in Figures 17a and 17b; the compositions of the two product streams have been compared in Figure 18.

From Figure 17 two brief conclusions could be made. First, higher feed gas pressure will lead to more gas absorption thus larger pressure drop in the module tube side can be generated, and this could be clearly seen from both Figures 17a and 17b. Secondly, after the dead volume was reduced, a relatively larger pressure drop in tube side under the same running conditions could be seen since for this case the ratio of the gas in the tube side that has a chance to directly contact with the absorbent on the shell side and get absorbed to the total tube volume will increase.

Figure 18 presents the influence of feed pressure on product qualities and effect of reducing dead volume on membrane module tube side. From Figure 17 we already know increasing feed gas pressure will generate larger pressure drop that means more gas has

been absorbed by shell side liquid, thus it seems reasonable that better CO_2-rich product will be generated at higher feed gas pressure. On the other hand, increasing feed gas pressure will bring a negative effect to He-rich product since more gas will be introduced into module tube side while the contacting area between feed gas and absorbent on shell side remains the same. Much more burden from the higher feed gas pressure will inevitably cause a degradation of He-rich product. The same effect of increasing feed gas pressure could be seen from Figure 18 for PEEK-II module with full and reduced dead volume. Compared with PEEK-II module with full dead volume, after dead volume reduced by adding small Teflon balls on both sides, the PSMAB process generates much better product qualities at both CO_2 and helium sides. For example, when feed gas pressure was kept at 250 psig, CO_2-rich product from reduced dead volume had a CO_2 concentration about 88.2% that was much higher than 79.9% for full dead volume; for He-rich product, its CO_2 concentration after dead volume reduced was around 21.5% that was much lower than 30.25% of full dead volume.

As we have mentioned at the beginning of this section, feed gas existing in the dead volume has no chance to contact the absorbent on the shell side thus it will not undergo any gas absorption. Dead volume reduction means higher ratio of gas in tube side will have an opportunity to contact with the absorbent liquid on the shell side thus better product qualities could be expected. Since we have proven the product quality improvement by reducing dead volume, for tests listed below unless otherwise mentioned, dead volume at both sides of membrane module will be reduced as much as possible by adding small Teflon balls.

Another aspect we should state about the PSMAB results in Figure 18 is that the He-rich product qualities are not very satisfactory. This is because that we deliberately took most of gas in tube side after absorption step out as He-rich product as shown in Table 5. Earlier we have reported that He-rich product quality could be monitored by changing its withdrawal quantity in each cycle. In this section our strategy was to take most gas out as He-rich product thus we can achieve the best CO_2-rich product quality. Continued efforts to improve He-rich product quality will be considered later.

3A.10. Effect of Adding Dendrimer to [bmim][DCA] for High Temperature Performance Improvement of PSMAB Process

Syngas from pre-combustion is generated in a state of high temperature and high pressure; therefore its CO_2 removal will be preferably required to be carried out at high temperature. We already know when pure [bmim][DCA] was used as absorbent, the PSMAB process will inevitably face product quality degradation problems at high temperature. There have been some reports that have revealed amine groups of polyamidoamine (PAMAM) dendrimer can react with CO_2 (Kovvali et al., 2000; Kovvali et al., 2001); therefore addition of dendrimer to [bmim][DCA] and forming a mixed absorbent is expected to enhance its CO_2 absorption performance. Although we have provided some preliminary evidence in Figure 13b, we investigate here in detail if adding dendrimer to IL will improve its separation performance at high temperature; first a set of tests were carried out with a 10.0 wt% dendrimer in [bmim][DCA] mixture as absorbent.

At first 900 s duration absorption tests were carried out at different temperatures with a feed gas pressure of 1034 kPag (150 psig). Corresponding pressure drops in module tube side are illustrated in Figure 19. For the total pressure drop within 900 s, it looks like test temperature did not show too much influence. There is some difference among results from different running temperatures while all data are close in the range of 22 to 24 psig. What we should pay more attention to is the process of pressure drops, especially within the first 60 s for different temperatures since they showed obviously difference. Temperature increase greatly improved its gas absorption behavior within the beginning short period. For example, at the point of 60 s absorption, room temperature running had a pressure drop around 8.5 psig; when temperature was increased to 50 ^{o}C, a larger pressure drop about 9.8 psig could be seen; test running at 75 ^{o}C showed a much larger pressure drop about 15.2 psig and continued 100 ^{o}C test had a slightly increased pressure drop about 15.8 psig. This could be possibly explained by two facts: first as stated earlier high temperature will increase the gas absorption rate at the beginning period; secondly adding dendrimer to pure IL will greatly increase its viscosity while temperature increase will lead to liquid viscosity decrease that is favorable for gas absorption. Larger pressure drop in tube side means more gas absorption happened at a higher running temperature. From this point of view it seems with a dendrimer-IL mixture absorbent a higher running temperature will be more favorable for the PSMAB process.

Continued PSMAB studies were carried out at different temperatures and 150 psig with same cycle step durations as described in Section 3A.8. Pressure changes in tube side were close to the second line of data in Table 5. Detailed pressure drops during the initial absorption step are presented in Figure 20. It has been revealed that test temperature showed greatly influence over gas solubility when dendrimer-IL mixture was used as absorbent. At room temperature because of the high viscosity of the mixed absorbent, gas solubility was restricted thus a pressure drop of 6.45 psig could be seen. When temperature was increased to 50^{o}C pressure drop in absorption step increased to 8.73 psig correspondingly since high temperature will decrease mixture viscosity. Continued high temperature tests at 75 and 100^{o}C did not show great difference since both had a higher pressure drop around 12.5 psig. In terms of product qualities, as shown in Figure 21, temperature increase shows obviously positive effect when dendrimer-IL mixture was used as absorbent. At room temperature He-rich product with CO_2 concentration as high as 29.3% and CO_2-rich product with CO_2 concentration around 59.8% were generated when a 10 wt% dendrimer in [bmim][DCA] mixture as absorbent. When temperature was increased to 75^{o}C, CO_2 concentration in He-rich product got reduced to 22.8% and CO_2 concentration in CO_2-rich product got increased to 80.5%. We can see a great improvement at both sides. When temperature was increased to 100^{o}C, a slightly product quality degradation could be seen. Even from Figure 13b we can see a very close pressure drop in tube side during absorption step for 75 and 100^{o}C tests, while we believe compositions of absorbed gas have been altered a lot because of temperature change. Based on these test results, continued question will be: Will dendrimer concentration in IL increase help improving PSMAB performance at high temperature further?

3A.11. Influence of Dendrimer Concentration in Absorbent Mixtures on PSMAB Process Performance at High Temperatures

Adding dendrimer to ionic liquid has been proven to be a possible choice to improve PSMAB process performance at high temperature. To find out an optimal dendrimer concentration in IL that provides the best enhancing effect, a set of tests using dendrimer-IL mixtures with different dendrimer concentrations were carried out at 100 ^{o}C and 150 psig.

Similar to what we have done before, at first 900 s duration absorption process tests were studied and detailed pressure drops in the module tube side with time were recorded as shown in Figure 22a. It can be clearly see that at high temperature up to 100 ^{o}C, adding dendrimer could greatly improve gas solubility in absorbent. That is to say, in Figure 22a, a larger pressure drop was generated. When pure [bmim][DCA] was used as absorbent, a pressure drop around 21.3 psig could be seen at the end of 900 s absorption duration; under same test conditions, a 10.0 wt% dendrimer-IL mixture could generated a larger pressure drop about 24.6 psig; this value increased to 27.3 psig when a 20.0 wt% dendrimer-IL mixture was used as absorbent; continued concentration increase did not bring a larger pressure drop, a 30.0 wt% dendrimer-IL mixture led to a lower pressure drop around 26.0 psig. We would like to attribute this abnormal phenomenon to a very high viscosity of 30.0 wt% dendrimer-IL mixture even at a high temperature. It could be possible that a much higher temperature test may show its enhancing effects better.

Based on the long duration absorption test results, PSMAB process tests were carried out using dendrimer-ionic liquid mixtures with different dendrimer concentration at 100 ^{o}C with a feed gas pressure of 1034 kPag (150 psig). Detailed pressure drops during absorption step are presented in Figure 22b. Similar to what we can see from Figure 22a, when pure [bmim][DCA] was used as absorbent, lowest pressure drop around 12.1 psig could be seen; a 10.0 wt% dendrimer-IL mixture showed a slightly larger pressure drop about 12.5 psig; when dendrimer concentration in [bmim][DCA] increased to 20.0 wt%, we found a much larger pressure drop of 14.8 psig; continued dendrimer concentration increase to 30.0 wt% did not bring a pressure drop increase since it showed a value around 14.3 psig. All these results were in accordance with the long duration absorption test results in Figure 22a.

Although it may not be very true, we can still say that product qualities from the PSMAB process could be partially predicted by the pressure drop behavior during its absorption step. Influence of dendrimer concentration on PSMAB performance in terms of product quality is presented in Figure 23. It could be clearly seen that adding dendrimer to IL greatly improved the product qualities at high temperature. Among all tested absorbents, pure [bmim][DCA] generated products with the worst qualities: CO_2 concentration in He-rich product was as high as 26.2% and at the same in CO_2-rich product it was only 76.5%. When 10.0 wt% dendrimer-IL mixture was used, the former value decreased to 24.8% and the latter value increased to 78.5%, both have been improved. Continued dendrimer concentration increase to 20.0 wt% did show further improvement since CO_2 concentration in He-rich product decreased to 22.3% and CO_2

concentration in CO_2-rich product increased up to 84.9%. When dendrimer concentration was increased to 30.0 wt%, we did not see an obvious further improvement since both product qualities showed a little bit of degradation when compared with the 20.0 wt% mixture. This could be explained from the fact that 30.0 wt% dendrimer-IL mixture has a much larger viscosity as pointed out earlier.

Based on these test results, it is very clear that adding dendrimer to pure IL to form a mixed absorbent will greatly improve its absorption capability at high running temperatures. Among all mixtures we have tested, 20.0 wt% dendrimer in IL showed the best performance; thus we are going to use it as the main absorbent for continued investigations unless stated otherwise.

3A.12. High Feed Pressure Running Performance of PSMAB Process with 20.0 wt% Dendrimer in [bmim][DCA] Mixture as Absorbent

It could be seen that most of our tests have been running at a relatively low feed pressure of 150 psig. Since pre-combustion syngas will be generated with a state of high temperature and high pressure at the same time, thus it is important to carry out the PSMAB process at a high temperature with a much higher feed gas pressure. In this section, with 20.0 wt% dendrimer in [bmim][DCA] mixture as absorbent, a set of tests were carried out with feed gas pressure up to 250 psig and temperature as high as 100 ^oC using PEEK-II with dead volume reduced at both ends.

As practiced earlier, at first a set of 900 s duration absorption tests were carried out under different feed gas pressures; the pressure drop results are presented in Figure 24. Feed gas pressure showed greatly influence to the pressure drops in tube side since it was the driving force for gas absorption. Actually this increase was proportional. If we divided the total pressure drop during 900 s absorption by its beginning absolute pressure in tube side, we got almost same values around 17.2~17.5% for different feed pressures.

Pressure changes in the module tube side during one complete PSMAB cycle at different feed gas pressures are presented in Figure 25a. Similar to what we have stated earlier, our strategy is trying to take most gas in the tube side after absorption step out as He-rich product thus we can have a better CO_2-rich product (since we do not have much membrane area or length). Detailed pressure drops in the tube side during the absorption step at different feed pressures are also listed in Figure 25a. Similar to the results in Figure 24, we can clearly see a proportional increase in pressure drop when the feed gas pressure was increased.

In terms of product qualities shown in Figure 25b, similar to the room temperature tests in section 3A.9.2 (Figure 18), feed gas pressure increase showed a positive effect for CO_2-rich product quality while a negative influence on helium-rich product quality. Feed gas pressure increase in the tube side means that there will be more feed gas needed to be treated with fixed gas-liquid contacting area and absorbent amount; therefore thereis a higher burden which will degrade He-rich product quality. With a feed gas pressure of 100 psig, He-rich product with a CO_2 concentration around 18.7% was generated; when feed gas pressure was increased to 150 psig, we got an increased He-rich product with

CO_2 concentration around 22.3%; continued feed gas pressure increase to 200 psig led to helium-rich product degradation to 23.6% and 250 psig generated helium-rich product with highest CO_2 concentration around 24.7%. For CO_2-rich product side, we can see an obvious quality improvement when feed gas pressure was increased from 100 psig to 150 psig since the corresponding CO_2 concentration increased from 76.9% to 84.9% (this could be attributed to a large increase of absorbed gas quantity) in the CO_2-rich stream. Continued feed gas pressure increase did not show any obvious improvement to product quality since all CO_2 concentrations were around 84.9~85.7% even though we did see a pressure drop increase during the absorption step. This is due to the fact that at a high temperature such as 100^{o}C, solubility selectivity of CO_2 over helium in IL is much lower than that at room temperature and may influence the final product quality. Larger pressure drop in absorption step means more gas has been absorbed by absorbent while absorbed gas compositions determined by gas solubility selectivity are quite close.

3A.12.1 Separation performance of ceramic modules in series

Helium-rich and CO_2-rich products generated from different absorbents at different temperatures for a feed gas pressure of 150 psig could be observed in Figure 26a and Figure 26b. When pure IL was applied as the absorbent, temperature shows obvious negative influence. Even though we did not see an obvious pressure drop difference during the absorption step, composition of gas absorbed has been altered since temperature increase has different effects on CO_2 and helium. CO_2 concentration in helium-rich product increased from 33.6% of room temperature to 36.1% of 100 ^{o}C; at the same time, CO_2-rich product suffered a concentration drop from 51.7% of room temperature to 47.6% of 100 ^{o}C. When dendrimer was added into IL and used as absorbent, unlike pure IL, temperature increase shows positive effect. Increasing temperature decreased CO_2 concentration in He-rich product and increased CO_2 concentration in CO_2-rich product under most conditions. Among all tested absorbents, 15wt% dendrimer-IL mixture shows best performance at 100 ^{o}C. It yielded a helium-rich product with CO_2 concentration of 34.1% and CO_2-rich product with CO_2 concentration of 50.6%, both were much better than pure IL generated products at 100 ^{o}C.

As mentioned earlier, the ceramic membrane module has a limited effective surface area and a large volume of feed gas in the tube side; therefore we did not see great improvements when dendrimer-IL mixture was applied as absorbent at high temperature. The suitability of ceramic modules for use at high temperature enables us to carry out tests listed above and the results are encouraging enough for us to learn how dendrimer will facilitate the whole PSMAB process and improve the products. This will be very helpful for further investigations.

3A.12.2 Separation Performance of PEG 400 as Absorbent with Dendrimer

As will be seen later in Section 3B, PEG 400 has a higher CO_2 solubility and a higher CO_2-He solubility selectivity compared to the IL [bmim][DCA] with dendrimer. Therefore a few preliminary tests were carried out regarding the absorption step and the separation behavior with PEG 400 containing the dendrimer using PEEK-L II (SN 421) with dead volume reduced by PTFE balls. Figure 26c illustrates the absorption behavior

over a 900 sec absorption behavior. Since the initial period is important, we observe that due to its higher viscosity, absorption in PEG 400 is somewhat slower; yet it shows that it has ultimately a higher solubility than [bmim][DCA]. Higher temperature operation will reduce this effect of viscosity and we will observe better absorption behavior. Figure 26d illustrates the separation behavior vis-à-vis the IL for 20 wt% dendrimer system. We observe a slightly lower performance compared to the IL-based system. At higher pressures and higher temperatures we expect comparable if not better performance from the PEG 400 – based systems.

3A.13. Additional Analysis and Second-stage Tests for PSMAB Product Qualities Improvements

Based on the test results from using 20.0 wt% dendrimer in IL solution as absorbent, when one stage PSMAB process is run using a PEEK-II module (with dead volume reduced) at 100°C and 1723 kPag (250 psig) feed gas pressure, we can have a He-rich product with CO_2 concentration around 24.7% and CO_2-rich product with CO_2 concentration around 85.7%. These product qualities need to be improved. In Section 3A.9.2, we demonstrated how much the presence of dead volume in the tube side affected the final product qualities at both helium and CO_2 side. Although we have greatly reduced the dead volume in the tube side by adding small Teflon balls and achieved improved product qualities, it should be noticed that there is still quite large dead volume left; thus a detailed calculation and analysis should be carried out based on this fact.

As stated earlier the dead volume in the module tube side is composed of two parts: the tube-side header section and related connections of the membrane module and the potted section of the module at both ends. The first part has been reduced from 35.75 cm^3 to 7.25 cm^3 by adding 28.5 cm^3 small Teflon balls on both sides; for potted section, tube side volume of PEEK-II membrane module has been calculated to be 58.29 cm^3 with an actual length of 20.0 cm, total length of potted section on both sides are 8.0 cm thus we can easily calculate dead volume for this section is 23.32 cm^3. Total dead volume on tube side will be 30.57 cm^3 that is about 52.4% of the effective tube side volume of 58.29 cm^3 (feed gas in this space has an opportunity to contact with absorbent on shell side and being absorbed).

Here we need to make an assumption: we will assume feed gas in the dead volume will keep its composition unchanged from the original during the PSMAB process since it has no chance to contact the absorbent. Based on this assumption, and according to the ratio of the dead volume and effective volume for absorption, it can be easily figured out that the actual CO_2 concentration in the He-rich product will be around 16.7% that is much better than 24.7% that we got by mixing of the purified desorbed highly CO_2-rich gas with much less CO_2-rich gas in various dead volumes in the system. It is also clear that the actual CO_2 concentration in CO_2-rich product also should be higher as we can see from Figure 18 that means a better quality even though it is difficult for us to make estimation for this side.

We have to admit even the actual CO_2 concentration in helium-rich product around 16.7% cannot be thought as a desired value. One reason is our strategy to generate a best CO_2-rich product degrades the He-rich product quality; on the other side pre-combustion syngas treatment requires to be carried out at a high temperature and pressure that will bring too much burden for the presently available PEEK-II module. One possible way to improve the He-rich product is to introduce a second absorption stage. With 20.0 wt% dendrimer in [bmim][DCA] as absorbent, 14.0% CO_2 with helium balance as feed gas for second absorption stage, similar PSMAB process tests were carried out at 100^{o}C and the results are listed in Table 6.

As Table 6 shows, PSMAB process tests with 14.0% CO_2 in helium as feed gas were carried out at 689 kPag (100 psig) and 1034 kPag (150 psig). This feed pressure range is mostly like what we are going to get from the first stage PSMAB process with feed gas pressure up to 1723 kPag (250 psig). From pressure change between 2nd and 3rd steps it is clear that most gas in tube side has been taken out as helium-rich product. The CO_2 concentration in He-rich products from two test feed pressures are very close around 8.30~8.55%. If we deduct the dead volume influence, the actual CO_2 concentration in helium-rich product will be 5.46%. This means after two-stage PSMAB processing, we can achieve a He-rich product with helium concentration higher than 94.0%. For CO_2-rich product side, 1034 kPag (150 psig) feed gas pressure generated a CO_2 concentration around 26.2% that was higher than 20.9% of 689 kPag (100 psig) feed gas pressure. Both products could be recycled as feed gas to avoid helium loss.

What should be mentioned more is that for practical applications membrane module with much larger effective area (longer fiber) will be required that means dead volume ratio over effective absorption volume is going to be much lower thus its influence on product quality will be greatly eliminated and a better product quality close to its actual state will be achieved. This could satisfactorily explain the meaning of our efforts for dead volume analysis here.

3A.14. Performance of An Improved PEEK-L Module: PEEK-III

One of the problems this research faced was obtaining the right membrane module. Although PEEK modules from Porogen Inc. appear to satisfy the requirements, we have shown convincingly that there are some important deficiencies in the existing hollow fiber membrane module designs provided to us by Porogen Inc. for the resources we provided to them (we had budgetary limitations since Porogen membranes were not included in the original budget). The last module that we could obtain near the end of the project from Porogen is PEEK-III (Table 1c). It had a much larger membrane volume (a membrane surface area of 5500 cm^2 for the same hollow fibers) in the same size shell casing compared to other PEEK-L modules. This implies that the gas volume in the internal fiber lumen region is substantially larger than those in the other modules. Therefore the dilution that the two product streams namely, the He-rich and the CO_2-rich streams, will encounter from the dead volume regions will be significantly reduced. From data obtained with pure ionic liquid [bmim] [DCA] and a 5-valve cycle shown in Table 7a we can see that at 25^{0}C, the CO_2-rich product stream achieves 92.9% CO_2 at 250

psig; at 50^0C at the same pressure it is reduced to 91.0% and so on. It becomes clear that the reduction of the CO_2 concentration seen at higher temperatures may be effectively counteracted if we had 20 wt% dendrimer in the ionic liquid. Table 7b illustrates such a result with a 20 wt% dendrimer solution. For example, we see that at 100^0C and 1723 kPag (250 psig) feed gas pressure the CO_2-rich product stream has a CO_2 composition of around 90.7%. We did not reduce the dead volume in this module with Teflon balls. Therefore we believe that with an improved module design having a substantial reduction in the dead volume and a well-distributed fiber assembly, the purity of the CO_2-rich stream can exceed 95% CO_2. Putting two such modules in series with a much larger gas volume in terms of the flow path in the fiber lumen, we can achieve simultaneously a highly purified He-rich product stream as well; our results with two PEEK-S modules in series support such a contention. All we have to do is make sure that the middle part gas volume does not contaminate the two product streams; the 5-valve scheme devised in this project can ensure such an outcome.

3B. Solubility Measurements

3B.1. Data Analysis for Pure Ionic Liquid

Solubilities of pure carbon dioxide and pure helium as well as their mixtures were determined in various absorbents at different temperatures and pressures up to 1.38 MPa. The gas mole fractions in absorbent liquids were calculated from the differences in the values of the initial and final pressures. The general equation of state based on the compressibility factor was used to calculate the number of moles of gas. The total number of initial moles of the desired gas at pressure P_1 is given by

$$n_T = \frac{P_1 V_{ref}}{Z_i RT} \tag{1}$$

The number of moles in the cell volume and the reference volume after equilibrium is reached at a pressure P_2 is given by

$$n_1 = \frac{P_2 (V_{ref} + V_{cell} - V_{IL})}{Z_f RT} \tag{2}$$

The moles of gas absorbed is

$$n_2 = n_T - n_1 \tag{3}$$

Here P_1 is the initial feed pressure of the desired gas in the reference cylinder; P_2 is the final equilibrium pressure; V_{ref} and V_{cell} are the volumes of reference and cell cylinders, respectively; V_{IL} is the volume of absorbent added in the cell cylinder; Z_i and Z_f are compressibility factors at pressures P_1 and P_2. The compressibility factor value at a temperature and a pressure point can be found in an IUPAC handbook (Angus et al., 1976; Angus et al., 1977).

Henry's law constants for pure CO_2 and pure He were calculated by extrapolating the solubility data of each pure gas to zero pressure and are shown in Table 8a for the ionic liquid [bmim] [DCA] at 50, 80, 90, and 100^oC. The values of a Pseudo Henry's law constant for each gas was also determined for the case where we had a gas mixture: since Henry's law constant is defined for a pure component only, the result determined is being called a Pseudo Henry's law constant when a gas mixture is used. Table 8b lists these values; we will deliberate on these later.

3B.2. Solubilities of Pure Gases at Various Temperatures

Table 8a shows that as the temperature was increased the solubility of CO_2 decreased in the pure ionic liquid which is represented by an increase in Henry's law constant. The temperature-solubility trend observed agrees with literature results for CO_2 (Husson-Borg et al., 2003; Sanchez, 2008). Henry's law constants of CO_2 in [bmim][DCA] at 30^oC, 60^oC, and 71^oC reported by Sanchez are 60.3, 94.4, and 111.4 bar, respectively (Sanchez, 2008). Although the measurement conditions in our study are somewhat different from these conditions, the literature values are in the expected range of the values obtained in this project. The solubility of helium in the studied absorbent, on the other hand, increased with increasing temperature. This trend can be explained based on thermodynamic relationships. For helium increasing temperature corresponds to a positive change in the enthalpy of absorption and the entropy of absorption leading to higher solubility in liquid absorbents (Brian III et al., 1988) For CO_2 increasing temperature results in a negative change in the enthalpy of absorption and the entropy of absorption which leads to lower solubility (Finotello et al., 2008) In other words, for low-solubility gases (N_2, He, H_2, etc.), the solubility increases when the temperature increases. The reverse trend is observed for the high-solubility gases such as CO_2 (Finotello et al., 2008). The same temperature-solubility trends, in terms of mole fractions, for carbon dioxide and helium in the ionic liquid [bmim][DCA] are shown in Figure 27 for a variety of pressures and four temperatures.

3B.3. Solubilities of Pure Gases as a Function of Pressure

The solubilities of carbon dioxide and helium in [bmim][DCA] at the same temperature increased with increasing pressure as shown in Figures 28 to 31 (for two temperatures 50^oC and 100^oC). Table 8b shows the mole fraction values of carbon dioxide in [bmim][DCA] at 30^oC for various pressures reported by Sanchez (Sanchez, 2008). In this study, solubility measurement was carried out at the lowest temperature of 50^oC. For general comparison purpose, the mole fraction values of CO_2 in the same ionic liquid at 50^oC for similar pressures, also shown in Table 8b, show trends similar to those of Sanchez's at 30^oC, namely the solubility increased with increasing pressure and further the values are in the same range.

Table 9a (Table 9b provides a complete data set) shows the values of CO_2 mole fraction in [bmim][DCA] at various feed pressures and temperatures. The data show that carbon dioxide mole fraction values are directly proportional to the feed pressures. In addition, for the same feed pressure, the mole fraction ratio (= the ratio of mole fractions

at the two pressures) at different temperatures is the same. The same trend could be observed for other liquid absorbents in this study.

3B.4. Solubilities of Pure Gases in Ionic Liquid Absorbent containing PAMAM Dendrimer

Solubilities of carbon dioxide in various absorbents at 50 and 100^{o}C are shown in Figures 28 and 29 respectively. Among those different liquid absorbents, carbon dioxide was least absorbed in pure [bmim][DCA]. CO_2 solubility in the absorbent increased with increasing dendrimer concentration in the absorbent solutions since a PAMAM dendrimer (generation 0) molecule contains four primary amine groups and two tertiary amine groups (Figure 32), which helps increase the carbon dioxide absorption. Only primary and secondary amine groups can react with carbon dioxide without any water present. The reaction between primary amine groups in a dendrimer molecule with CO_2 has been shown in equation (4):

$$2\ R(NH_2)_4 + 4\ CO_2 \leftrightarrow R(NHCOO^-)_4 + R(NH_3^+)_4 \quad (4)$$

There is spectroscopic evidence (IR) shown in Figure 33 indicating the presence of carbamate species in the dendrimer Gen 0 system with ionic liquid exposed to CO_2. Figure 34 shows that pure [bmim][DCA] did not have any band at around 1655 cm^{-1} on the IR spectra while 20 wt% dendrimer Gen 0 in [bmim][DCA] without any exposure to CO_2 had the band at 1655 cm^{-1} due to the presence of the amines in the solution. Figure 33 shows that the band at the wavenumber of 1651 cm^{-1} decreased in intensity while the bands at 1567 and 1170 cm^{-1} increased in intensity after CO_2 was introduced to the 20 wt% dendrimer Gen 0 in [bmim][DCA]. This indicates that CO_2 reacted with the primary amine groups to form carbamate species. The bands at approximately 1550 and 1100 cm^{-1} correspond to the C=O asymmetric and symmetric stretching bands of NH_2COO^- (Park, et al., 2008; Krevelen et al., 1949).

In addition, CO_2 solubility increased significantly when moisture was added to the dendrimer-ionic liquid solution due to the contribution of the tertiary amine groups contained in dendrimer besides the primary amine groups. Equation (5) shows the reaction of tertiary amine groups in the presence of water with carbon dioxide (Kovvali et al., 2001; Danckwerts, 1979):

$$2\ CO_2 + R_2\text{-N-R-N-}R_2 + 2H_2O \leftrightarrow 2HCO_3^- + R_2\text{-}NH^+\text{-R-}NH^+\text{-}R_2 \quad (5)$$

The effect of water in [bmim][DCA] containing dendrimers on CO_2 solubility was largest at 50^{o}C, as shown in Figure 28. Some water evaporated at the higher temperature; as a result, the presence of water in [bmim][DCA] containing dendrimer solutions was less effective, corresponding to a smaller increase in CO_2 solubility.

In aqueous systems, the physical solubility of CO_2 is affected by the presence of various ions. When reactive absorption of CO_2 takes place it is difficult to know what the concentration of free CO_2 is. A method followed in literature (Park, et al.. 2008; Krevelen et al., 1949) involves determining the change in solubility of an inert gas due to the

presence of various ions. The ratio of this change in solubility of this inert gas due to various ions is used to correct the free CO_2 concentration by the same factor. Normally N_2O is used to this end (Versteeg et al, 1996; Blauwhoff et al., 1983); here we have used the solubility ratio of inert He to correct the concentration of free CO_2 in the reactive absorbent liquid:

$$H_{CO2T} = H_{CO2}\frac{H_{HeT}}{H_{He}} = \frac{P_f}{x} \tag{6}$$

where H_{CO2T}: Henry's law constant of CO_2 due to physical absorption in the IL containing dendrimer

H_{CO2}: Henry's law constant of CO_2 in pure IL

H_{HeT}: Henry's law constant of He in the IL containing dendrimer

H_{He}: Henry's law constant of He in pure IL

x: mole fraction of free CO_2.

Due to the radically different charge climate in an ionic liquid as opposed to water (for example), the effect is expected to be minor. We find this correction to be around 5-8%.

3B.5. Solubilities of Gases Present in a Mixture

Table 10 summarizes the Pseudo Henry's law constants for an initial feed gas mixture containing 40% CO_2, He balance for different absorbent liquids and at different temperatures. Here we define Pseudo Henry's law constant as the value of the slope of the curve of the gas partial pressure vs. mole fraction of species in liquid as this mole fraction tends to zero. The Pseudo Henry's law constants for each of CO_2 and He in the gas mixture were slightly higher than Henry's law constants of pure CO_2 and He. The Henry's law constants for pure CO_2 and He in pure [bmim][DCA] at 50^oC are 74.4 and 751.8 bar respectively whereas the Pseudo Henry's law constants for CO_2 and He in the gas mixture at 50^oC are respectively 78.2 and 761.5 bar. The differences between those values are within 5%. In addition, all the solubility trends with temperature, pressure, and absorbent liquids observed with the pure gases were also observed here. This was also a way to verify that the results are consistent and reproducible.

3B.6. CO_2-He Solubility Selectivity

Solubility selectivity of CO_2 over He is defined in this study as the ratio of Henry's law constant of pure helium to that of pure carbon dioxide at a given temperature for [bmim] [DCA]. For other reactive absorbents the solubility selectivity is defined as the ratio:

$$\text{Solubility selectivity}\,(CO_2/He) = \frac{\text{Pseudo Henry's law constant for He}}{\text{Pseudo Henry's law constant for } CO_2} \quad (7)$$

Here we define as before Pseudo Henry's law constant as the value of the slope of the curve of the gas partial pressure vs. mole fraction of species in liquid as this mole fraction tends to zero. When we have a reactive absorbent, Henry's law constant defined for physical absorption in the limit of zero mole fraction in the liquid phase is misleading. However, in all four dendrimer-containing absorbents studied (Figures 28-31) there is essentially a linear behavior over almost the whole range of pressures and certainly as the pressure is lowered.

Figure 35 shows the solubility selectivity of CO_2 over He in a number of liquid absorbents at four temperatures. The solubility selectivity decreased with increasing temperature for all liquid absorbents. The highest selectivities were observed at 50°C. Solubility selectivity of carbon dioxide over helium in pure [bmim][DCA] decreased from ~10 at 50°C to ~2.8 at 100°C. Furthermore, a solution of 30 wt% dendrimer in [bmim][DCA] with moisture gave the highest CO_2/He solubility selectivity among the three studied absorbents and five systems: a value of 55 at 50°C and 10 at 100°C.

3B.7. Apparent Equilibrium Constant for the Reaction in Reactive Absorption

The PAMAM Gen 0 molecule has four primary amines and two tertiary amines (Figure 32). For a dry system, we need to focus only on primary amines. The reaction scenario is complicated by the fact that under conditions of excess CO_2, we can have all four primary amines in a molecule consumed. However, if we have limited amount of CO_2, we can envisage a scenario where only one primary amine in a molecule has been consumed (In reality there will be a variety of intermediate conditions). Here we will develop appropriate equations for these two extreme cases so that we can extract values of the corresponding apparent equilibrium constants. First we focus on the situation where all four primary amines in a PAMAM Gen 0 have been consumed:

$$2R(NH_2)_4 + 4CO_2 \leftrightarrow R(NHCOO^-)_4 + R(NH_3^+)_4 \quad (8)$$

The approach for determining the equilibrium constant from the measured data is as follows. For 20 wt% dendrimer in [bmim][DCA] with a known mass (m) and volume of 0.01L (V_{IL}), the number of moles of dendrimer and [bmim][DCA] are respectively

$$n_{den} = \frac{0.2m}{517.0} \quad (9)$$

$$n_{IL} = \frac{0.8m}{205.26} \quad (10)$$

The number of moles of CO_2 absorbed in the IL containing dendrimer, n_2, was calculated from the experimental data via equation (3). The Henry's law constants for CO_2 due to physical absorption in the IL containing dendrimer are calculated via equation (6).

This approach is adopted since the physical solubility of CO_2 in the IL will be influenced by the presence of other electrolytes/compounds such as dendrimer. The effect of these compounds on the solubility of He will provide some guidance on the correction needed for CO_2 solubility. If N_2O was used instead of He, the correction may have been more accurate (Versteeg et al., 1996; Blauwhoff et al., 1983). However, as mentioned earlier due to the radically different charge climate in an ionic liquid as opposed to water (for example), the effect is expected to be minor.

For mole fraction of free CO_2 in the liquid

$$x = \frac{n}{n + n_{IL} + n_{den}} = \frac{P_f}{H_{CO2T}} \tag{11}$$

Therefore, $$n = \frac{x(n_{IL} + n_{den})}{1 - x} = \text{moles of free } CO_2 \text{ in solution} \tag{12}$$

Now, n_{CO2r}, the moles of CO_2 reacted with primary amines present in dendrimer, is equal to

$$n_{CO2,r} = n_2 - n \tag{13}$$

From equation (4), the apparent reaction equilibrium constant, K_C, may be written as:

$$K_C = \frac{\dfrac{n_{R(NHCOO^-)_4}}{V_{IL}} \dfrac{n_{R(NH_3^+)_4}}{V_{IL}}}{\left(\dfrac{n_{CO_2|free}}{V_{IL}}\right)^4 \left(\dfrac{n_{R(NH_2)_4}}{V_{IL}}\right)^2} \tag{14}$$

where we have assumed that any dendrimer molecule has all four primary amine groups reacting with CO_2 per equation (4). Obviously

$$n_{R(NHCOO^-)_4} = \frac{n_{CO2,r}}{4} = n_{R(NH3^+)_4} \tag{15}$$

Also the number of moles of unreacted dendrimer molecules, $n_{R(NH_2)_4}$ are related to

$$n_{R(NH_2)_4} = n_{den} - \frac{n_{CO_2,r}}{4} - \frac{n_{CO_2,r}}{4} = n_{den} - \frac{n_{CO_2,r}}{2} \tag{16}$$

Substituting relations (12), (15), and (16) in (14), we get

$$K_C = \frac{\left(\frac{n_{CO_2,r}}{4}\right)^2}{n^4\left(n_{den} - \frac{n_{CO_2,r}}{2}\right)^2} V_{IL}^{\ 4} \tag{17}$$

Since all of the quantities on the right hand side are known, K_C can be determined.

In the other limit, we may have only one primary amine of each dendrimer molecule reacting with CO_2. In reality, we have a variety of scenarios. However, one can calculate the K_C value in the limit where only one primary amine of each dendrimer reacts with CO_2:

$$CO_2 + 2\ R(NH_2)_4 \leftrightarrow R(NH_2)_3HNCOO^- + R(NH_2)_3NH_3^+ \tag{18}$$

The apparent reaction equilibrium constant, K_C, in this case could be expressed as (a detailed derivation is provided in the appendix):

$$K_C = \frac{\left(n_{CO_2,r}\right)^2}{n\left(n_{den} - 2_{nCO2,r}\right)^2} V_{IL} \tag{19}$$

One can calculate the theoretical capacity of CO_2 absorption by PAMAM dendrimer molecules under dry conditions as well as under wet conditions. We have calculated this value for example for dry conditions for a certain concentration of PAMAM in the ionic liquid. By taking into account the total CO_2 absorbed minus the amount due to CO_2 solubility in the ionic liquid under the selected condition, one can then find out what fraction of this theoretical absorption capacity has been consumed under this particular condition. If we are very close to the theoretical capacity, we can argue that equation (8) describes the situation. On the other hand, if we are very far away from the theoretical capacity, the case for reaction (18) improves.

In Table 11a (for a complete table which includes many pressures at any temperature, refer to Table 11b for additional details), we have provided the percent theoretical capacity consumed for a few pressures at a given temperature for 20 wt% dendrimer in the ionic liquid. At 14.66 bar, we find that the absorption amount is 97.69% of the theoretical capacity at 50°C. Therefore equation (17) may be used to estimate the apparent equilibrium constant K_C; the value is 29972 L^4/mol^4. At 2.41 bar, the absorption amount is 10.56% of the theoretical capacity at 50°C. We may therefore use equation (19) to estimate K_C; the value is 6100 L/mol. In addition, at 80, 90, and 100°C, equation (19) is used to calculate the apparent equilibrium constants due to the small percent amine saturation. The K_C values for 20 wt% dendrimer in [bmim][DCA] at 80, 90, and 100°C are 2804, 2227, and 1790 L/mol respectively.

We can carry out similar calculations for the 30 wt% dendrimer in the ionic liquid at different temperatures and pressures; the results are shown in Table 12a (for a

complete table, refer to Table 12b). Since the percent amine saturation for most cases at all the temperatures studied is small, equation (19) is used to calculate the apparent equilibrium constants at different temperatures. The K_C values for 30 wt% dendrimer in [bmim][DCA] at 50, 80, 90, and 100^oC are 6659, 3061, 2431, and 1954 L/mol respectively. At 50^oC and 14.66 bar, the % saturation is 69.58%. Therefore, equation (17) may be used to calculate K_C: the value is 10329 L^4/mol^4. Due to lower % saturation this value is quite different from 29972 L^4/mol^4 calculated for 20 wt% case with 97.69% saturation at 50^oC.

What we observe is as follows: the apparent reaction equilibrium constants decreased as the temperature was increased. Further the value of K_C for the case of only one primary amine being consumed is likely to be independent of the dendrimer concentration at all four temperatures.

3B.8. Solubilities in PEG 400 as the Absorbent with or without PAMAM Dendrimer

Table 13a shows that Henry's law constants for PEG 400 for pure CO_2 at four temperatures are somewhat smaller than those for pure [bmim] [DCA] (Table 8a). On the other hand, the PEG 400 values for He are just about very close to or larger than those for the ionic liquid. This would indicate that PEG 400 is somewhat more selective for CO_2 over He. The measured solubilities are also shown in Figures 36a and 36b for pure PEG 400 and that containing 20 wt% dendrimer (the Pseudo Henry's constants for the latter are shown in Table 13b).With the addition of dendrimer in the absorbent, the solubility data shown in Table 13b may be converted into solubility selectivity. We see clearly in Figure 36c that over all four temperatures, PEG 400 system with dendrimer is somewhat more selective than [bmim] [DCA] containing the same level of the dendrimer.

3C. Mathematical Modeling

3C.1. Model for the 3-Valve PSMAB Process

A mathematical model has been developed that describes the PSMAB process performance in terms of the pressure drop in the absorption step and the compositions of the two product gas streams. The product stream flow rates have also been calculated. In the model, the hollow fibers are assumed to be arranged in a regular pitch and the analysis based on a single fiber can be extended to the whole module. The mathematical model utilized the Happel free surface model (Happel, 1959) as originally applied to membrane contactors by Karoor and Sirkar (1993) and shown in Figure 37. This figure shows two concentric cylinders: the inner cylinder consists of one hollow fiber and the outer cylinder consists of the absorbent liquid with a free surface across which there is no mass transfer. The following assumptions are introduced to develop a mathematical model for the PSMAB system using a non-reactive absorbent (Bhaumik et al., 1994)

1. Ideal gas law is valid.
2. The absorption process is isothermal.
3. Diffusion and solubility coefficients are constant and independent of concentration.
4. No reaction takes place between the liquid and any gas component.

5. The components of the gas phase are in equilibrium with the absorbed components at the gas-liquid interface and Henry's law is valid.
6. The flow pattern within the fiber bore can be described by the model of plug flow with axial diffusion.
7. The mass transfer mechanism from the bulk gas phase to the outside surface of the fiber where the gas-liquid interface is located may be described by a first order model based upon a constant mass transfer coefficient and a concentration difference between the two locations.
8. The pressure drop in the fiber lumen is governed by Hagen-Poiseuille equation for the compressible fluid without any effect of radial absorption.
9. The deformation of the fibers due to the higher external pressure of the liquid is negligible so that the fiber size and the void fraction remain unchanged.
10. End effects are negligible.
11. Volume of gas in the pores is negligible compared to that in the fiber lumen.
12. Feed gas concentrations do not change during the first step of the cyclic PSMAB process.

The void fraction of the fiber bundle containing N hollow fibers,ε, is defined in equation (20):

$$\varepsilon = 1 - \frac{\textit{shell side cross sectional area occupied by the hollow fibers } (N\pi r_0^{\,2})}{\textit{total cross sectional area of the shell side } (\pi r_S^{\,2})} \tag{20}$$

Then the equivalent radius, r_e, can be calculated:

$$r_e = \left(\frac{1}{1-\varepsilon}\right)^{1/2} r_0 \tag{21}$$

When the gas pressure drop in the fiber lumen is not negligible, the governing balance equations and boundary conditions for any species j (He, CO_2) in a single hollow fiber can be written as (Bhaumik et al., 1994):

Gas Phase:

$$\frac{\partial C_{jg}}{\partial t} = D_{jg}\frac{\partial^2 C_{jg}}{\partial z^2} - \frac{\partial}{\partial z}\left(v_g C_{jg}\right) - \frac{4K_{jg}d_0}{d_i^{\,2}}\left(C_{jg} - C_{jg}^{\,i}\right) \tag{22}$$

where

$$v_g = -\frac{RTd_i^{\,2}}{32\mu_{mix}}\sum_{j=1}^{n}\frac{\partial C_{jg}}{\partial z} \tag{23}$$

$$C_{jg}^{\,i} = \frac{C_{jl}\big|_{r=r_0}}{H_j RT} \tag{24}$$

Initial condition:

$$\text{At } t = 0, C_{jg} = 0 \ (0 \le z \le L) \tag{25}$$

Boundary conditions:

$$v_g C_{jg}\big|_u = v_g C_{jg}\big|_{z=0} - D_{jg}\left.\frac{\partial C_{jg}}{\partial z}\right|_{z=0} \tag{26}$$

$$D_{jg}\left.\frac{\partial C_{jg}}{\partial z}\right|_{z=L} = 0 \tag{27}$$

The corresponding governing balance equation and boundary conditions for the liquid phase for species j are:

$$\frac{\partial C_{jl}}{\partial t} = D_{jl}\left(\frac{\partial^2 C_{jl}}{\partial r^2} - \frac{1}{r}\frac{\partial C_{jl}}{\partial r}\right) \tag{28}$$

Initial condition:

$$\text{At } t = 0, C_{jl} = 0 \ (0 \le z \le L \text{ and } r_0 < r < r_e) \tag{29}$$

Boundary conditions:

$$-D_{jl}\left.\frac{\partial C_{jl}}{\partial r}\right|_{r=r_0} = K_{jg}\left(C_{jg} - \frac{C_{jl}\big|_{r=r_0}}{H_j RT}\right) \tag{30}$$

$$\left.\frac{\partial C_{jl}}{\partial r}\right|_{r=r_e} = 0 \tag{31}$$

These equations in dimensionless forms were numerically solved using the method of lines technique and programs developed using MATLAB. The method of lines technique was used to discretize the spatial component of the partial differential equations (PDEs), hence, reducing the system of PDEs to a coupled system of ordinary differential equations (ODEs) (Brian III et al., 1998).

The decrease of the pressure and the change in composition of the gas in the tube side during absorption has to be determined. Similarly the quality of the two product streams has to be determined by solving the governing equations. For both cases we need to use appropriate initial conditions and boundary conditions as identified below.

For Absorption step:

Initial condition:

$$\text{at } t = 0, C_{jg} = C_{jg\ feed} \tag{32}$$

Boundary conditions:

$$\left.\frac{\partial C_{jg}}{\partial z}\right|_{z=0} = 0 \tag{33}$$

$$\left.\frac{\partial C_{jg}}{\partial z}\right|_{z=L} = 0 \tag{34}$$

For He-withdrawal step:

Initial condition:

at $t = 0, C_{jg} = C_{jg\ in\ tube\ side\ after\ absorbtion}$ (35)

Boundary conditions:

$$\left.\frac{\partial C_{jg}}{\partial z}\right|_{z=0} = 0 \quad (36)$$

$$v_g C_{jg}\Big| = v_g C_{jg}\Big|_{z=L} - D_{jg}\left.\frac{\partial C_{jg}}{\partial z}\right|_{z=L} \quad (37)$$

For CO_2-withdrawal step:

Initial condition:

at $t = 0, C_{jg} = C_{jl\ in\ \text{shell}\ side\ after\ absorbtion}$ (38)

Boundary conditions:

$$v_g C_{jg}\Big|_u = v_g C_{jg}\Big|_{z=0} - D_{jg}\left.\frac{\partial C_{jg}}{\partial z}\right|_{z=0} \quad (39)$$

$$\left.\frac{\partial C_{jg}}{\partial z}\right|_{z=L} = 0 \quad (40)$$

The CO_2 compositions in percentage of the two product streams are calculated using the equations below:

$$\%\, CO_2\ in\ He-rich\ stream = \frac{C_{CO2\,in\ He-rich\ stream}}{C_{He-rich\ stream}} x100\% \quad (41)$$

$$\%\, CO_2\ in\ CO_2-rich\ stream = \frac{C_{CO2\,in\ CO2-rich\ stream}}{C_{CO2-rich\ stream}} x100\% \quad (42)$$

The He compositions in percentage of the two product streams are then determined:

$$\%\, He\ in\ He-rich\ stream = 100\% - \%\, CO_2\ in\ He-rich\ stream \quad (43)$$

$$\%\ He\ in\ CO_2 - rich\ stream = 100\% - \%\ CO_2\ in\ \mathrm{CO}_2 - rich\ stream \tag{44}$$

One needs also information on CO_2 solubility and diffusivity in the ionic liquid to numerically predict the performance of the PSMAB process. Therefore, measurements of the solubilities of pure carbon dioxide, pure helium, and a feed mixture of 40% CO_2-He balance were also carried out in the ionic liquid, ([bmim][DCA]) as mentioned earlier in Section 3B (and in its solution containing 20 wt% and 30 wt% poly(amidoamine) (PAMAM) dendrimer Gen 0 with and without water). From the pressure changes versus time collected in the solubility studies, the diffusion coefficients of CO_2 and He in pure [bmim][DCA] can be found via equation (45) shown below (Hou and Baltus, 2007):

$$\ln\left(\frac{P}{P_0}\right) = \left(\frac{k}{H_{CO2}}\right)\sum_{n=0}^{\infty}\frac{1}{(2n+1)^2}\left\{\exp\left[-\frac{(2n+1)^2\pi^2 D_{CO2}t}{4L^2}\right]-1\right\} \tag{45}$$

where $k = \dfrac{8RTV_{IL}\rho_{IL}}{\pi^2 V(MW)_{IL}}$

P_0: initial feed gas pressure

V: volume of gas

ρ_{IL}: density of ionic liquid

V_{IL}: volume of ionic liquid

L: height of ionic liquid

$(MW)_{IL}$: molecular weight of ionic liquid.

This equation has two unknowns: H_{CO2} and D_{CO2}. Fitting the equation above to the experimental P vs. time data in MATLAB, the unknowns are determined. The units for k and H_{CO2} in equation (45) are atm. The unit for H_{CO2} and H_{He} used in the numerical model is mol/atm*m^3. From the solubility measurement data, Henry's law constants of CO_2 and He can be calculated using equation (46) below:

$$H_{CO2} = \frac{moles\ of\ CO_2\ absorbed\ in\ the\ IL}{V_{IL}(P_f)} \tag{46}$$

where P_f: equilibrium pressure obtained in the solubility measurement

V_{IL}: volume of ionic liquid.

3C.2. Optimal Absorption Duration for PSMAB Cycle

Absorption is one of the important steps; it directly determines how long the feed gas will be in contact with the ionic liquid in the shell side and will undergo gas absorption. To find out the optimal absorption time, at first we set the absorption time in

one cycle as long as 900 seconds to examine the pressure drop caused by gas absorption into pure [bmim][DCA] in the shell side of the membrane module during this step. The experimental pressure drop during the absorption will be compared with that generated by the numerical model. The optimal absorption duration for different membrane modules was determined earlier. For ceramic membrane modules, the optimal absorption step duration for this system was chosen to be 120 second (Section 3A.4.1.1). For the PEEK membrane module, the optimal absorption step duration was 30-60 second (Section 3A.4.1.2). Due to the very high surface area per unit volume of the PEEK-L system, much more rapid absorption takes place into the surrounding liquid compared to that in the ceramic tubule system. In the PSMAB process, rapid initial absorption is important.

3C.3. Diffusion Coefficients and Henry's Law Constants of CO_2 and He in Pure [bmim][DCA]

As mentioned earlier, equation (45) has two unknowns: H_{CO2} and D_{CO2}. Fitting this equation to the experimental pressure vs. time data in Matlab, the unknowns are determined. Similarly, H_{He} and D_{He} can also be determined. Henry's law constant for pure carbon dioxide and pure helium were also experimentally determined from the solubility measurements (Sections 3B.2/3B.3); these values can be used to compare and check with the Henry's law constants generated by the Matlab program to ensure that they are comparable. Table 14 summarizes the diffusion coefficients and Henry's Law constants in [bmim][DCA] for CO_2 and He at room temperature (25 ^oC), 50 ^oC, and 100 ^oC. The carbon dioxide diffusion coefficients in [bmim][DCA] at room temperature and at 50 ^oC are in range with the diffusion coefficients for CO_2 in [emim][Tf_2N] reported by Camper et al. (2006).

3C.4. Pressure Drop during the Absorption Step

3C.4.1. Ceramic membrane module system

Three ceramic membrane modules were connected in series and were employed with pure ionic liquid [bmim][DCA] as the liquid absorbent. The absolute pressure changes in the tube side tests during the 900 second absorption step were measured at 25 ^oC, 50^oC, and 100^oC for a fixed initial feed gas pressure of 1034 kPag (150 psig). The pressure drops measured from the experimental runs and predicted by the numerical models are shown in Figures 38, 39, and 40 respectively. The pressure drop in the absorption step was plotted against the normalized (dimensionless) absorption time ($\frac{D_{ll}t}{r_e^2}$). The pressure drops generated by the numerical model were close to those measured in the experimental runs at all temperatures. We will later find out that there are two reasons for it vis-à-vis the PEEK hollow fiber module. First, there is no ambiguity about the value of r_e. The second reason for this agreement is that the ceramic membrane modules had much less dead volume compared to those in the PEEK membrane module vis-à-vis the feed gas volume (as will be discussed later).

3C.4.2. PEEK-L-II Membrane Module

One large PEEK membrane module (PEEK-L of type PEEK-II) was used with pure [bmim][DCA] as the liquid absorbent for the absorption test. The experiments were carried out at 689 kPag (100 psig) and 1379 kPag (200 psig) feed gas pressures and at room temperature. The pressure drop was plotted against dimensionless time and the results are shown in Figures 41 and 43 (Figures 42 and 44 will be dealt with soon). Unlike in the ceramic case, the pressure drops generated by the numerical model were larger than those of the experimental runs. There are two reasons. First, the fibers in the module were wound helically in a strand; therefore the calculation of r_e via Happel's approach (equation (21)) will introduce some error since the fibers were artificially packed closer together. The actual r_e values should be smaller than those calculated in Happel's approach. When inputting a smaller value of Happel's approach-based radius into the numerical model, the theoretical curves got closer to those of the experimental results as shown in Figures 42 and 44. Secondly, there was a significant amount of dead volume in the two ends of the hollow fiber module which will increase the module end pressure monitored by the pressure indicator; the gas in these large dead volumes in the PEEK membrane module will not undergo absorption. Therefore the measured pressure drops will be lower.

Round PTFE balls were used to fill both ends of the tube-side headers of the PEEK-L (II) module to reduce the dead volume. The same absorption experiment was carried out at 100 psig and room temperature. Figure 45 shows a much improved prediction of the model with respect to the experimental run. This shows that the dead volume strongly affects gas absorption, which also ultimately affects the products quality when desorption takes place.

3C.5. Quality of Product Streams in Terms of % CO_2 Concentration in Both He-rich and CO_2-rich Streams

3C.5.1. Three ceramic modules in series

The ceramic membrane module has a membrane tubule with a much larger inner diameter. In order to find out if this will have any impact, tests were carried out with three ceramic membrane modules in series at a few temperatures; the feed pressure was 689 kPag (100 psig). As determined earlier the optimal absorption time was set as 120 seconds in each cycle. Figure 46 shows the percent carbon dioxide concentrations (%) in both product streams as the He-rich stream withdrawal and then CO_2-desorption steps were carried out. He-rich stream was first desorbed for 2 seconds; and then CO_2-rich stream was under vacuum for 30 seconds.

We have seen earlier that even with 3 ceramic membrane modules the product qualities for both streams were poor because of its much larger tubule diameter, which results in a lot of feed gas that is required to be absorbed. In addition, due to limited contacting area along the tube side, only a small amount of feed gas could be absorbed. Therefore, it is more likely that the gas concentration distribution along the tube length was not fully developed for a ceramic system. The model predictions for compositions of the two product streams differ from experimental measurements by about 3% on an average.

Figure 46 also shows as expected the adverse effect of temperature on the product concentrations with pure IL. As the temperature increases, less carbon dioxide and more helium would be absorbed by the ionic liquid. As a result, the % carbon dioxide in the He-rich product stream increased from 33% to 36% when temperature was increased from 25 ^{o}C to 100 ^{o}C (Figure 46(a)). The % carbon dioxide in the CO_2-rich product stream decreased from 52% to ~48% over the same range of temperature (Figure 46(b)).

3C.5.2. One PEEK-L (II) module filled with PTFE balls in the module headers

After the performance of the absorption step was studied, a set of PSMAB process tests with the PEEK-L (II) module having PTFE balls reducing the dead volume in the module headers was carried out at different feed pressures and temperatures. The concentrations of the two product streams are shown in Figure 47. This figure shows that an increase in feed gas pressure leads as expected to an increase in % CO_2 concentration in the CO_2-rich product stream for the same temperature. Higher feed gas pressure means more gas would be introduced into the membrane tube side and contacted with ionic liquid (IL) to be absorbed. The % CO_2 concentration in the CO_2-rich product increased from ~81% at 689 kPag (100 psig) and 25^{o}C to 87% at 965 kPag (140 psig) and 25^{o}C.

In addition, the PEEK-L module provided better results as compared to the ceramic module due to it having a much larger effective contacting area and the correspondingly longer feed gas length. Table 15 provides the dimensional features of the two types of membrane modules. Table 4 had already shown clearly that the effective surface area per unit volume for the ceramic module is only 8.19 cm^{-1}; it is much lower than 54.71 cm^{-1} for a PEEK hollow fiber. This could directly explain why PEEK module showed much higher absorption rates than the ceramic membrane module. As a result, PEEK modules have much better PSMAB performance than the ceramic modules. The % CO_2 in the CO_2-rich product in PEEK-L module was 81% compared to 56% for ceramic module system at 689 kPag (100 psig) feed and 25^{o}C.

The modeling results showed that the predicted compositions are around 7-10% different from the measured values. For the CO_2-rich product the model results predict considerably higher CO_2 concentration in the CO_2-rich product just as the model results predict considerably lower CO_2 concentration in the He-rich product. Part of this discrepancy should be ascribed to the effect of residual dead volume in the module. If one considers the results we have obtained with PEEK –L III module shown in Table 7a, it will show that these experimental results are closer to the simulation results obtained here.

3C.6. Flow Rates of Product Streams and % CO_2 Recovery

The molar flow rate of the He-rich product stream per cycle can be estimated based on the change in the pressure during He-withdrawal process using equations (47) and (48). Knowing the pressure drop during the withdrawal step at a certain temperature, one can first calculate the number of moles using the equation of state:

$$\Delta n = \frac{(\Delta P) * V}{R * T} = \frac{(\Delta P) * \left(\pi * r^2 * L * N\right)}{R * T} \tag{47}$$

where r is the inner radius of one hollow fiber, L is the effective fiber length, and N is the number of fibers in a module.

Therefore, the He-rich molar flow rate per cycle is:

$$\dot{n}_{He} = \frac{\Delta n}{t} \tag{48}$$

where t is the cycle time.

The CO_2-rich molar flow rate per cycle, $\dot{n}_{CO2}$, can be calculated using the CO_2 species balance on the system since the compositions of the product streams are known for a feed gas stream of known composition:

$$0.4 * (\dot{n}_{He} + \dot{n}_{CO2}) = \dot{n}_{He} * x_1 + \dot{n}_{CO2} * x_2 \tag{49}$$

where x_1 and x_2 are the CO_2 compositions in the He-rich and CO_2-rich product streams,

respectively. The % CO_2 recovery in the CO_2-rich stream may be estimated from the

$$\%CO_2 \text{ Recovery} = \frac{y * \dot{n}_{CO2}}{y * \dot{n}_{CO2} + x * \dot{n}_{He}} x100\% \tag{50}$$

where y is the % CO_2 in CO_2-rich stream, x is the % CO_2 in He-rich stream, $\dot{n}_{CO2}$ is the CO_2-rich molar flow rate per cycle, and $\dot{n}_{He}$ is the He-rich molar flow rate per cycle.

Tables 16 and 17 summarize the estimated molar product flow rates per cycle for both CO_2-rich and He-rich streams in ceramic and PEEK-L II modules respectively under different experimental conditions. The compositions of both of these product streams are also indicated there. The Tables also provide an estimate of the % CO_2 recovery in the CO_2-rich stream.

3C.7. Product Flow Rates, Compositions and % CO_2 Recovery for Two PEEK-L (III) Modules in Series with Pure IL as Absorbent -- Simulation Results

Table 18 provides the simulation results when two PEEK-L III modules are connected in series and pure [bmim][DCA] is used as the absorbent. It just demonstrates what addition of membrane area can do in terms of the considerable improvement in product qualities without affecting the production rate. Obviously increased temperature affects the product quality; but increased membrane area provides some compensation which suggests that even with a pure ionic liquid we may be able to achieve high purity in the gas streams and high CO_2 recovery.

The % CO_2 recovery achieved is somewhat low since the CO_2 concentration in the He-rich product stream is high. By adding appropriate membrane length or a 2-stage process, the He-rich product quality can be substantially improved and the desired % CO_2 recovery can be achieved.

3D. Absorbent Degradation

Syngas has a few impurities such as H_2S, CO etc. It is useful to enquire whether there are any downsides to using ionic liquids in the presence of H_2S. We have not located any literature indicating adverse chemical reactions of H_2S with the IL under consideration. Literature data on solubility of H_2S in a variety of ILs are available (Pomelli et al., 2007; Jalili et al., 2009; Shiflett et al., 2010). In case there are any adverse reactions with trace H_2S amount, the PSMAB device allows easy discharge and replenishment of IL through two valves on the shell side as and when necessary. The same comments are valid for PEG-400 although there are no literature reports for any interaction of PEG-400 with these acid gases.

Results of an analysis of the absorbent degradation are indicated in Figures 48 and 49. Figure 48 shows the HPLC chromatograms from fresh samples. Figure 49 illustrates what was observed with dendrimer-IL absorbent samples taken out of the shell side of the PEEK-L-II membrane module after a few months of use vis-à-vis freshly prepared samples. It is clear that the primary peak area of the dendrimer has been substantially reduced in the used NJIT samples and other species have shown up. This will indicate that there has been significant degradation of the PAMAM dendrimer Gen0 into some other species. It is not known whether the ionic liquid is responsible for this degradation or the higher temperature is. Some of the breakdown products may be volatile also leading to reduced peak area. That ionic liquids are powerful solvents with some reactivity is known; for example, ionic liquids have been studied extensively for biomass treatment. There are a number of ways to counteract such a tendency. One could use the automatic solvent replenishment arrangement available in the PSMAB process (see Figures 1c and 1d) where fresh absorbent may be supplied from the solvent reservoir automatically. Alternately if Ils are responsible for degradation, one could replace the IL with PEG 400 etc.

3E. Comments on Process Scale Up Aspects

As seen from the simulation results illustrated in Table 18 for a pure ionic liquid-based system, best CO_2 recovery and CO_2–rich as well as He-rich (surrogate for H_2) product qualities were observed at the low pressure 689 kPag (100 psig) and low temperature (23^oC) operation. Increasing the temperature reduced the product qualities and CO_2 recovery (unless dendrimer absorbents are added). Operation at higher pressure increased the processing capacity of the module as well as the CO_2 product quality. However, operation at higher pressures decreased the CO_2 recovery and He (surrogate for H_2) product quality. For syngas CO_2 capture application it would be desirable to operate the PSMAB system at maximum possible pressure and temperature investigated which are currently limited to 1723 kPag (250 psig) and 100^oC temperature operation for the PEEK modules used. However the simulations were carried out up to 1379 kPag (200 psig) only.

As indicated earlier, one way to improve the performance of the 3-stage PSMAB process is to add a second stage. An attempt was therefore made to predict the performance of a two-stage system operating at 1379 kPag (200 psig) and 100^oC as being the most desirable feed gas conditions. While the second stage could be operated at a

lower pressure as dictated by a He-rich (surrogate for H_2-rich) gas release pressure used in the first stage (demonstrated experimentally in this project), it was also assumed to be operated at 1379 kPag (200 psig) and 100^oC conditions to allow extrapolation of model simulation results of a single stage at these conditions. The single stage performance for a pure IL at 1379 kPag (200 psig) and 100^oC is shown in Figure 50 and that for the two-stage system both being operated at same conditions is shown in Figure 51. The net feed gas flow rate in both cases is 1 gmole/s.

The two-stage simulation shown above indicates that adding the second stage provides substantial improvement in the overall CO_2 recovery as well as He-rich (for H_2-rich) gas product quality without changing the high CO_2 product quality achieved in the first stage. The feed gas flow rate to the second stage is 70% of that of the first stage thus the membrane area required for the second stage would be 70% of that of the first stage (since the amount of CO_2 to be removed is significantly lower due to much lower CO_2 composition, actually the area required should be lower). The combined processing capacity of the two-stage system, however, is reduced by 21% to 0.79 gmole/sec. Significantly greater (115%) membrane area would therefore be needed for the two-stage operation for the same feed capacity in order to achieve the performance improvement. The two-stage simulation shown above is for illustrative purposes only and does not necessarily represent an optimal process configuration which will require more detailed analysis of several combinations.

The 5-valve PSMAB system provides an inherent flexibility for improving product qualities as well as CO_2 recovery. Target H_2-rich product purity of 95% was experimentally confirmed for He-based system in these studies by partial He-rich (H_2-rich) product withdrawal to 689 kPag (100 psig) pressure from 965 kPag (140 psig) feed pressure (Figure 5a). Less product withdrawal will allow increasing hydrogen purity while increased withdrawal will reduce hydrogen purity. Similarly high CO_2 product purity may also be achieved by controlling the extent of the intermediate gas release. The intermediate gas released is returned to feed stream after completing the CO_2 withdrawal step.

Using the model simulation results presented in Table 18, estimates may be made of the membrane area needed for syngas CO_2 capture application. For baseline IGCC plant with CO_2 capture, e.g., E-Gas IGCC plant, the flow rate of post shift reactor syngas containing 41.2% CO_2 is estimated at 56,835 lbmol/hr with a net power generating capacity of 518 MW, or about 13.85 gmol/s/MW. The membrane areas were estimated for four selected cases for relative comparison:

A) Single-stage PSMAB with 200 psig pressure, 100 ^oC temperature – CO_2 recovery – 67.7%, H_2-rich product – 18.4% CO_2, CO_2-rich product – 90.6% CO_2. Membrane area – 79.7 x 10^3 m^2/MW.

B) Two-stage PSMAB with 200 psig pressure, 100 ^oC temperature – CO_2 recovery – 86.6%, H_2-rich product – 8.6% CO_2, CO_2-rich product – 91.7% CO_2. Membrane area – 171.4 x 10^3 m^2/MW.

C) Single-stage PSMAB with 200 psig pressure, 23 ^{o}C temperature – CO_2 recovery – 79.7%, H_2-rich product – 12.1% CO_2, CO_2-rich product – 97.3% CO_2. Membrane area – 49.8 x 10^3 m^2/MW.
D) Single-stage PSMAB with 100 psig pressure, 23 ^{o}C temperature – CO_2 recovery – 88.5%, H_2-rich product – 7.3% CO_2, CO_2-rich product – 95.1% CO_2. Membrane area – 99.8 x 10^3 m^2/MW.

Above technical evaluation of the PSMAB process indicates that potential ways to achieve the CO_2 capture targets of CO_2 recovery as well as product gas purities in the 3- valve or the 5-valve PSMAB processes are possible either by adding a second stage or by adjusting product withdrawal ratios. Detailed process simulations, however, need to be conducted with the available range of variables to identify the optimal process parameters for achieving those process targets. The identified optimal process parameters should then be verified by well designed experiments.

We believe however that the membrane module design employed so far is inadequate. Suggested directions of membrane module improvement having observed basis in the performance of modified membrane modules in this project is most likely to yield the needed product quality in an one stage device; further the production rate for given product quality specifications and CO_2 recovery will also go up. Employing inexpensive nonvolatile base absorbents (e.g., based on PEG-400) having higher selectivity and sorption capacity will lead to further reduction in the membrane surface area needed.

4. CONCLUSION

Using the nonvolatile ionic liquid 1-butyl-3-methylimidazolium dicyanamide ([bmim][DCA]) as the absorbent on the shell side of a small membrane module containing either porous hydrophobized ceramic tubule or porous hydrophobized polyether ether ketone (PEEK) hollow fiber membranes, this project achieved successfully considerable CO_2 removal from hot simulated pre-combustion shifted syngas by a pressure swing membrane absorption (PSMAB) process which operates in a cyclic fashion. Helium was used as a surrogate for H_2 in the simulated shifted syngas containing ~40% CO_2 on a dry gas basis. In this cyclic process, the membrane module was used to achieve non-dispersive gas absorption from a high-pressure feed gas (689-1724 kPag; 100-250 psig) at temperatures between 25-100^{0}C (in a few experiments up to 125^{0}C) into a stationary absorbent liquid on the shell side of the membrane module during a certain part of the cycle followed by among other cycle steps controlled desorption of the absorbed gases from the liquid in the rest of the cycle. A novel 5-valve cycle was found to perform better than the simpler 3-valve cycle. An illustrative 5-valve cycle time distribution is as follows: Feed gas introduction, 5 s; gas absorption, 30 s; He-rich product withdrawal 2 s; middle part gas withdrawal, 2 s; CO_2-rich product withdrawal, 30 s. The PEEK hollow fiber-based membrane modules possessing a much higher surface area per unit volume of 54.6 cm^{-1} compared to the low value of 8.19 cm^{-1} for the ceramic membrane modules demonstrated much better gas separation performance due to the high gas-liquid contacting area per unit gas volume.

The PSMAB process could achieve a CO_2 concentration as low as 5-8% at 100^0C in the He-rich product stream obtained from the module end opposite to the feed gas introduction end; the highest CO_2 concentration in the CO_2-rich product stream obtained experimentally from the feed gas introduction end of the module at 100^0C was 90.6%. These observed product stream compositions were significantly reduced due to dilution with the feed gas mixture present in the large dead volumes in the PEEK hollow fiber membrane modules used. One small membrane module did not allow achievement of the desired product qualities in both streams at the same time. Either multiple modules in series or a two-stage process was needed. Improved PEEK membrane module design which reduces the tube-side header dead volumes, increases the gas processing volume in the tube-side of the hollow fiber module, and provides adequate space between contiguous fibers for the absorbent liquid on the shell side is likely to allow achievement of high product stream purities from one module and a higher gas processing capacity. To meet the desired process performance level, such a design is expected to eliminate the need for a two-stage process.

The solubilities and diffusivities of CO_2 and He were measured in the pure ionic liquid [bmim][DCA] as well as PEG 400 over 50-100^0C and up to a pressure of 1.38 MPa (~200 psig). Gas solubility measurements were made using a pressure decay method. The experimentally obtained values were employed in a mathematical model that was developed for the PSMAB process for a non-reactive system. Simulation results from a numerical solution of the governing equations appear to describe the observed behavior well. Addition of PAMAM dendrimer of Gen 0 to the ionic liquid or PEG 400 drastically enhanced the solubility of CO_2 and the solubility selectivity of CO_2 over He. Presence of moisture leads to further enhancement in these quantities. It appears that PEG 400 has a higher performance than the IL, [bmim][DCA], with or without the dendrimer. The presence of PAMAM dendrimer in the base absorbent leads to enhanced membrane module separation performance at higher temperatures where the performance of pure absorbents like IL or PEG 400 deteriorates. A dendrimer concentration of around 20% in the base absorbent appears to be optimum for the conditions investigated. The extended term stability of the dendrimer in the IL at higher temperatures needs to be investigated.

5. NOTATION, TABLES AND ILLUSTRATIONS

5A. Notation

C_{jg} = concentration of species j in the gas phase, mol/m^3
C_{jl} = concentration of species j in the liquid phase, mol/m^3
d_i = inside diameter of a hollow fiber, m
d_o = outside diameter of a hollow fiber, m
D_{jg} = diffusion coefficient of species j in the gas phase, m^2/s
D_{jl} = diffusion coefficient of species j in the liquid phase, m^2/s
H_j = solubility coefficient of gas species j in a liquid, mol/(m^3.Pa)
L = effective fiber length, m
r = radial distance, m
r_e = equivalent radius of free surface, m
R = universal gas constant, (m^3Pa)/(mol.K)

t = time, s
T = temperature, K
v_g = gas velocity in fiber lumen, m/s
z = longitudinal distance, m
N = total number of hollow fibers in a module

Greek letters

ε = void fraction of the fiber bundle, m^2/m^3
μ = viscosity, Pa.s
π = 3.14

Superscript and subscripts

i = interface
g = gas phase
j = component j
l = liquid phase
u = upstream section

5B. Tables

Table 1a. Dimensional Characteristics of the Hydrophobized Ceramic Tubule-Based Membrane Absorption Modules

Module*	OD [a]; cm	ID [b]; cm	L [c]; cm	Pore Size; Å	VVF [d]	Fiber Number	Surface area [e]; cm^2	Packing density [f], %
Ceramic I	0.57	0.37	44.0	~50	0.35-0.4	1	78.75	NA
Ceramic II	0.57	0.37	44.0	~50	0.35-0.4	1	78.75	NA
Ceramic III	0.57	0.37	44.0	~50	0.35-0.4	1	78.75	NA
Ceramic IV	0.57	0.37	44.0	~50	0.35-0.4	1	78.75	NA

[a] OD: outer diameter of fiber; [b] ID: inner diameter of fiber; [c] L: effective fiber length; [d] VVF: void volume fraction; [e] Calculation was based on outer diameter of fibers; [f] Packing density was defined as the ratio between actual volume of all fibers and the real volume they occupied in modules (actual volume plus space among fibers). * Ceramic membrane modules were supplied by Media and Process Technology Inc., Pittsburgh, PA.

Table 1b. Dimensional Characteristics of Teflon Membrane Absorption Modules

Module*	OD [a]; cm	ID [b]; cm	L [c]; cm	Pore Size; Å	VVF [d]	Fiber Number	Surface area [e]; cm^2	Packing density [f], %
Teflon I (S/N: 1004)	0.108	0.053	58.0	NA		29	570	NA
Teflon II (S/N: 1005)	0.108	0.053	58.0	NA		29	570	NA
Teflon III (S/N: 1006)	0.108	0.053	58.0	NA		29	570	NA

[a] OD: outer diameter of fiber; [b] ID: inner diameter of fiber; [c] L: effective fiber length; [d] VVF: void volume fraction;
[e] Calculation was based on outer diameter of fibers; [f] Packing density was defined as the ratio between actual volume of all fibers and the real volume they occupied in modules (actual volume plus space among fibers).
* Teflon membrane modules were supplied by Applied Membrane Technology Inc., Minnetonka, MN.

Table 1c. Dimensional Characteristics of PEEK Membrane Absorption Modules

Module*	OD [a]; cm	ID [b]; cm	L [c]; cm	Pore Size; Å	VVF [d]	Fiber Number	Surface area [e]; cm^2	Packing density [f], %
PEEK-S 30-105-20	0.0452	0.0290	34.3	<20	~0.4	240	~1168	NA
PEEK-S 30-105-21	0.0452	0.0290	34.3	<20	~0.4	240	~1168	NA
PEEK-L 2PG295	0.0452	0.0290	117	<20	~0.4	208	~3452	67.0
PEEK-I 2PG296[h]	0.0452	0.0290	117	<20	~0.4	208	~3452	67.0
PEEK-L 2PG261[g]	0.0452	0.0290	117	<20	~0.4	208	~3452	37.1
PEEK-II SN421[i]	0.0452	0.0290	41.0	<20	~0.4	568	~3420	21.8
PEEK-III SN459	0.0470	0.0272	41.0	<20	~0.4	980	~5500	27.2

[a] OD: outer diameter of fiber; [b] ID: inner diameter of fiber; [c] L: effective fiber length; [d] VVF: void volume fraction;
[e] Calculation was based on outer diameter of fibers; [f] Packing density was defined as the ratio between actual volume of all fibers and the real volume they occupied in modules (actual volume plus space among fibers); [g] Inter-fiber space is larger for 2PG261. Packing density of fibers in modules: 67.0% (2PG295 and 2PG296), 37.1% (2PG261). Here packing density is defined as the ratio between actual volume of all fibers and the real volume they occupied in modules; [h]PEEK-I is identified as 2PG296; [i] PEEK-II is indentified as SN421.
* PEEK membrane modules were supplied by Porogen, Inc., Woburn, MA.

Table 1d. Dimensional Characteristics of the Membrane Absorption Modules

Module [1]	OD; cm	ID; cm	L [2]; cm	Pore Size; Å	VVF [3]	Fiber Number	Surface area [4]; cm^2
Ceramic	0.57	0.37	44.0	~50	0.35~0.4	1	78.75
PEEK-S[6]	0.0452	0.0290	34.3	~20	~0.4	240	1168
PEEK-L [5]	0.0452	0.0290	117	~20	~0.4	208	3452

[1] OD: outer diameter of fiber; ID: inner diameter of fiber; [2] L: effective fiber length; [3] VVF: void volume fraction; [4] Based on outer diameter of fibers; [5] PEEK-L is PEEK SN421 module has a packing density (defined as the ratio between actual volume of all fibers and the real volume they occupied in module) around 37.1%.
; [6] PEEK-S is PEEK 30-105-20 or 30-105-21 as they are identical.

Table 1e. Comparative Dimensional Characteristics of PEEK Membrane Modules for Absorption Process

Module	OD [a]; cm	ID [b]; cm	L [c]; cm	Pore Size; Å	VVF [d]	Fiber Number	Surface area [e]; cm^2	Packing density [f], %
PEEK-I	0.0452	0.0290	117	~20	~0.4	208	3452	67.0
PEEK-II	0.0452	0.0290	41.0	~20	~0.4	568	3420	21.8

[a] OD: outer diameter of fiber; [b] ID: inner diameter of fiber; [c] L: effective fiber length; [d] VVF: void volume fraction; [e] Calculation was based on outer diameter of fibers; [f] Packing density was defined as the ratio between actual volume of all fibers and the real volume they occupied in modules (actual volume plus space among fibers).

Table 2a. Breakthrough Pressure Test Results for Ceramic Membrane Modules

Module type	Water	[bmim][DCA]	[emim][Tf2N]	PEG 400	20% Dendrimer in PEG 400	20% Dendrimer in [bmim][DCA]
Ceramic I	210 psi	*No leakage up to 300 psi	N/A	N/A	300 psi	N/A
Ceramic II	*No leakage up to 300 psi	*No leakage up to 300 psi	180 psi	*No leakage up to 300 psi	N/A	N/A
Ceramic III	*No leakage up to 300 psi	*No leakage up to 300 psi	*No leakage up to 300 psi	N/A	N/A	N/A
Ceramic IV	*No leakage up to 300 psi	*No leakage up to 300 psi	*No leakage up to 300 psi	N/A	N/A	N/A

* Tests were not carried out at higher pressure; all tests were carried out at room temperature.

Table 2b. Breakthrough Pressure Test Results for Teflon Membrane Modules

Module type	Water	[bmim][DCA]	[emim][Tf2N]	PEG 400	20% Dendrimer in PEG 400	20% Dendrimer in [bmim][DCA]
Teflon I (S/N: 1004)	*No leakage up to 100 psi	100 psi	N/A	80 psi	N/A	100 psi
Teflon II (S/N: 1005)	140 psi	40 psi	N/A	80 psi	N/A	40 psi
Teflon III (S/N: 1006)	*No leakage up to 140 psi	60 psi	N/A	80 psi	N/A	60 psi

* Tests were not carried out at higher pressure; all tests were carried out at room temperature.

Table 2c. Breakthrough Pressure Test Results for PEEK Membrane Modules

Module type	Water	[bmim][DCA]	[emim][Tf2N]	PEG 400	20% Dendrimer in PEG 400	20% Dendrimer in [bmim][DCA]
PEEK 2PG295	*No leakage up to 200 psi	*No leakage up to 200 psi	*No leakage up to 200 psi	*No leakage up to 200 psi	N/A	N/A
PEEK 2PG296	*No leakage up to 260 psi	*No leakage up to 260 psi	N/A	*No leakage up to 260 psi	N/A	N/A
PEEK 2PG261	N/A	*No leakage up to 250 psi	N/A	N/A	N/A	N/A
PEEK (S/N:30-105-20)	*No leakage up to 200 psi	40 psi	N/A	140 psi	N/A	N/A
PEEK-I 2PG296	>260 psig	>260 psig		>260 psig		
PEEK-II SN421	>300 psig	>250 psig		>250 psig		
PEEK-III SN459	>300 psig	>250 psi				

* Tests were not carried out at higher pressure; all tests were carried out at room temperature.

Table 2d. Breakthrough pressure test results

	Water	[bmim][DCA]	[emim][Tf_2N]	PEG 400
Ceramic No.1	210 psig	> 300 psig	N/A	300 psig
Ceramic No.2	> 300 psig	> 300 psig	180 psig	>300 psig
Ceramic No.3	> 300 psig	> 300 psig	> 300 psig	N/A
Ceramic No.4	>300 psig	> 300 psig	> 300 psig	N/A
PEEK-S No.1	> 200 psig	160 psig	N/A	140 psig
PEEK-S No.2	>200 psig	160 psig	80 psig	180 psig
PEEK-L	>300 psig	>250 psig	N/A	N/A

Table 2e. Solubility of Dendrimer Gen 0 in various absorbent liquids

Liquids Tested / Dendrimer in solution (%)	[emim][Tf_2N]	[bmim][DCA]	PEG400	Glycerol Carbonate
1	Soluble	Soluble	Soluble	Soluble
5	Not Soluble	Soluble	Soluble	Soluble
10	Not Soluble	Soluble	Soluble	Soluble
15	Not Soluble	Soluble	Soluble	Soluble
20	Not Soluble	Soluble	Soluble	Soluble
25	Not Soluble	Soluble	Soluble	Soluble
30	Not Soluble	Soluble	Soluble	Soluble
35	Not Soluble	Soluble	Soluble	Soluble
40	Not Soluble	Soluble	Soluble	Partially Soluble
45	Not Soluble	Soluble	Soluble	Partially Soluble
50	Not Soluble	Soluble	Soluble	Partially Soluble

Table 3. Comparison of performance between 3-valve and 5-valve Systems for one PEEK-S Module at Room Temperature

Feed pressure psig	System	Cycle time [1] s	He product [2]	CO_2 product [3]
60	5-valve	5; 30; 1; 4; 30	**6.57%**	**63.20%**
60	3-valve	5; 30; 1; 30	9.14%	34.80%
60	3-valve	5; 30; 15; 30	27.50%	57.90%
80	5-valve	5; 30; 1; 4; 30	**6.81%**	**67.20%**
80	3-valve	5; 30; 1; 30	10.70%	36.60%
80	3-valve	5; 30; 15; 30	29.80%	66.30%
100	5-valve	5; 30; 1; 4; 30	**8.31%**	**70.10%**
100	3-valve	5; 30; 1; 30	8.00%	38.40%
100	3-valve	5; 30; 30; 30	30.90%	70.95%

[1]: For a 5-valve system there are 5 steps in each cycle as, for example, feed gas in (5s), absorption (30s), helium-rich product withdrawal (1s), middle part gas withdrawal (4s) and CO_2-rich product withdrawal (30s) in the first row. For a 3-valve system, same time for feed gas in, absorption and CO_2-rich product withdrawal time, while helium withdrawal time varies, if high quality helium-rich product preferred, step time was kept as 1s; otherwise it was kept as long as 30s to achieve better product in CO_2 side.

[2]: For a 5-valve system four pressure values in the tube side identify the pressure at the end of: absorption; helium-rich product withdrawal; middle part gas withdrawal and CO_2-rich product withdrawal. For a 3-valve system no middle part withdrawal step so there are only 3 pressure values.

[3, 4]: All are in terms of CO_2 concentration.

Table 4. Estimated Dimensional Calculations for PEEK Hollow Fiber Module and Ceramic Tubule Membrane-based Modules

Module	OD; cm	ID; cm	L; cm	VVF	V [1]; cm^3	A [2]; cm^2	A / V [3]; cm^{-1}
Ceramic	0.57	0.37	44.0	~0.4	7.33	31.5	4.30
Ceramic [4]	0.57	0.37	44.0	~0.4	3.84	31.5	8.19
PEEK	0.0452	0.0290	34.3	~0.4	0.0356	1.95	54.7

[1] V: feed gas containing volume in one hollow fiber;

[2] A: effective contacting area for one hollow fiber based on outside area;

[3]A/V: ratio between contacting area and feed gas containing volume for one hollow fiber;

[4]A Teflon rod was inserted into the tube side of ceramic membrane module to reduce the volume as described earlier.

Table 5. Pressure Changes in Membrane Module Tube Side during One Complete Cycle under Different Feed Gas Pressures

Feed gas pressure; psig	1st step; psig	2nd step [a]; psig	3rd step; psig	4th step; psig	5th step; psig	6th step; psig
100	102	97.1/96.2	14.0	4.9	-14.5	-5.0
150	153	145.3/144.6	25.0	10.0	-14.5	-2.0
200	207	196.8/195.6	33.0	16.0	-14.5	1.0
250	261	237.5/236.3	43.0	21.0	-14.5	4.0

[a] The first pressure value is for PEEK-II with dead volume and the second value is for reduced dead volume.

Table 6. Pressure Changes in Membrane Module Tube Side during One Complete Cycle and Product Quality Variation under Different Feed Gas Pressures

Feed gas pressure ; psig	1st step; psig	2nd step [1]; psig	3rd step; psig	4th step; psig	5th step; psig	6th step; psig	He-rich product [a]	CO_2-rich product [b]
100	96.8	92.6	9.75	1.42	-14.5	-5.30	8.30%	20.9%
150	149.8	143.6	19.7	6.84	-14.5	-1.07	8.55%	26.2%

[a, b]: All product qualities are in term of CO_2 concentration.

Table 7a. Product Qualities at Different Temperatures and Feed Pressures for PEEK-L III with [bmim][DCA] as the Liquid Absorbent

Temperature (^oC)	Feed Pressure (kPag)	CO_2 product stream (%CO_2)	He product stream (%CO_2)
25	689 (100 psig)	89.9	17.3
	1379 (200 psig)	92.5	19.2
	1724 (250 psig)	92.9	21.6
50	689 (100 psig)	87.0	19.9
	1379 (200 psig)	90.4	22.6
	1724 (250 psig)	91.0	23.6
75	689 (100 psig)	79.4	25.2
	1379 (200 psig)	87.3	27.7
	1724 (250 psig)	87.8	28.9
100	1379 (200 psig)	84.9	27.7
	1724 (250 psig)	85.5	28.8

Table 7b. Product Qualities at Different Temperatures and Feed Pressures for PEEK-L III with 20 wt% Dendrimer in[bmim][DCA] as the Liquid Absorbent for a 5-valve PSMAB System

Pressure (psig)	Temperature (^oC)	CO_2 product stream (% CO_2)	He-Rich Product (% CO_2)
100	50	85.9	20.9
200		88.3	24.7
250		89.5	25.4
100	75	81.9	23.3
200		88.4	24.4
250		89.3	26.5
200	100	89.8	25.2
250		90.7	25.9

Table 8a. Henry's law constants of pure CO_2 and pure He in [bmim][DCA] at different temperatures

Absorbent liquids	Temperature (K)	Henry's law constant (bar)		Reference H_{CO2}[+] (bar)
		H_{CO2}	H_{He}	
[bmim][DCA]	323	74.4±0.5	751.8±5.1	60.3±1.6 @303K
	353	104.2±2.5	521.1±7.2	94.4±3.5@333K
	363	114.3±3.0	440.8±6.4	111.4±4.8 @344K
	373	129.8 ±1.1	365.1±3.0	

[+]Sanchez (2008).

Table 8b. CO_2 mole fractions in [bmim][DCA] for different pressures at 30^{o}C and 50^{o}C

	Pressure (bar)	CO_2 mole fraction
Sanchez[+] at 30^{o}C	2	0.035
	4	0.068
	5	0.08
	7	0.11
	9	0.13
Experimental data at 50^{o}C (This work)	1.14	0.015
	1.78	0.024
	2.45	0.033
	3.11	0.042
	3.78	0.051
	4.42	0.060
	5.11	0.069
	5.85	0.078
	6.48	0.087
	7.17	0.097

+ Sanchez(2008).

Table 9a. CO_2 mole fractions in [bmim][DCA] at various feed pressures and temperatures

Temperature (°C)	Pressure (bar)	CO_2 mole fraction	Pressure Ratio	Mole Fraction Ratio
50°C	2.43	0.015	1.00	1.00
	7.92	0.051	3.26	3.33
	14.77	0.097	6.08	6.35
80°C	2.43	0.015	1.00	1.00
	7.92	0.051	3.24	3.28
	14.77	0.097	6.07	6.21
90°C	2.43	0.015	1.00	1.00
	7.92	0.051	3.28	3.26
	14.77	0.097	6.15	5.92
100°C	2.43	0.015	1.00	1.00
	7.92	0.051	3.39	3.39
	14.77	0.097	6.32	6.42

Table 9b. CO_2 mole fractions in [bmim][DCA] at various feed pressures and temperatures

Temperature (^oC)	Pressure (bar)	CO_2 mole fraction	Pressure Ratio	Mole Fraction Ratio
50^{o}C	2.43	0.015	1.00	1.00
	3.75	0.024	1.54	1.56
	5.16	0.033	2.12	2.16
	6.51	0.042	2.68	2.74
	7.92	0.051	3.26	3.33
	9.23	0.060	3.80	3.92
	10.67	0.069	4.39	4.51
	12.08	0.078	4.97	5.12
	13.39	0.087	5.51	5.70
	14.77	0.097	6.08	6.35
80^{o}C	2.43	0.015	1.00	1.00
	3.75	0.024	1.70	1.73
	5.16	0.033	2.12	2.13
	6.51	0.042	2.68	2.66
	7.92	0.051	3.24	3.28
	9.23	0.060	3.81	3.84
	10.67	0.069	4.38	4.48
	12.08	0.078	4.97	5.05
	13.39	0.087	5.51	5.60
	14.77	0.097	6.07	6.21
90^{o}C	2.43	0.015	1.00	1.00
	3.75	0.024	1.52	1.52
	5.16	0.033	2.14	2.15
	6.51	0.042	2.72	2.74
	7.92	0.051	3.28	3.26
	9.23	0.060	3.85	3.86
	10.67	0.069	4.43	4.39
	12.08	0.078	5.01	4.95
	13.39	0.087	5.58	5.55
	14.77	0.097	6.15	5.92
100^{o}C	2.43	0.015	1.00	1.00
	3.75	0.024	1.63	1.63
	5.16	0.033	2.21	2.21
	6.51	0.042	2.80	2.82
	7.92	0.051	3.39	3.39
	9.23	0.060	4.00	4.05
	10.67	0.069	4.60	4.66
	12.08	0.078	5.17	5.23
	13.39	0.087	5.76	5.81
	14.77	0.097	6.32	6.42

Table 10. Pseudo Henry's law constants of CO_2 and He mixture in [bmim][DCA] at different temperatures

Absorbent liquids	Temperature (K)	Pseudo Henry's law constant (bar)	
		H_{CO2}	H_{He}
[bmim][DCA]	323	78.2±1.7	761.5±3.9
	353	116.9±2.0	537.4±3.1
	363	120.5±3.1	450.3±3.4
	373	135.3±3.3	368.9±3.1

Table 11a. Percent theoretical capacity* of primary amines consumed under different pressures and its corresponding apparent equilibrium constant of primary amine reaction with CO_2 for 20 wt% dendrimer in [bmim][DCA] at different temperatures**

	P_{feed} (bar)	% Saturation (%)	K_C
50°C	2.43	10.56	6100 L/mol
	14.66	97.69	29972 L^4/mol^4
80°C	2.39	5.51	2804 L/mol
90°C	2.41	4.13	2227 L/mol
100°C	2.47	3.84	1790 L/mol

*Theoretical capacity is the theoretical moles of carbon dioxide absorbed due to reacting with primary amines in dendrimer based on the equation (4)

**Dry system

Table 11b. Percent theoretical capacity of primary amines consumed under different pressures and its corresponding apparent equilibrium constants of primary amine reaction with CO_2 for 20 wt% dendrimer in [bmim][DCA] at different temperatures*

	P_{feed} (bar)	% Saturation (%)	K_C
50°C	2.43	10.56	6100 L/mol
	3.74	24.23	
	5.16	31.85	
	6.47	38.89	
	7.90	47.72	
	9.26	53.89	
	10.59	66.74	
	11.96	77.54	
	13.43	75.83	
	14.66	97.69	29972 L^4/mol^4
80°C	2.39	5.51	2804 L/mol
	3.76	9.03	
	5.14	12.88	
	6.53	16.61	
	7.77	18.83	
	9.27	22.85	
	10.67	27.42	
	12.14	32.13	
	13.39	34.83	
	14.83	42.08	
90°C	2.41	4.13	2227 L/mol
	3.87	6.88	
	5.17	9.78	
	6.58	13.28	
	7.93	15.47	
	9.38	19.62	
	10.68	23.08	
	12.07	27.51	
	13.38	29.10	
	14.77	34.36	
100°C	2.47	3.84	1790 L/mol
	3.76	5.73	
	5.16	8.20	
	6.52	10.06	
	7.91	12.65	
	9.27	15.06	
	10.61	17.99	
	11.99	20.52	

	13.43	22.52	
	14.47	26.96	

*Dry system

Table 12a. Percent theoretical capacity* of primary amines consumed under different pressures and its corresponding apparent equilibrium constant of primary amine reaction with CO_2 for 30wt% dendrimer in [bmim][DCA] at different temperatures*

	P_{feed} (bar)	% Saturation (%)	K_C
50°C	2.41	9.29	6659 L/mol
	14.66	69.58	10329 L^4/mol^4
80°C	2.43	4.49	3061 L/mol
90°C	2.43	3.93	2431 L/mol
100°C	2.43	2.98	1954 L/mol

*Theoretical capacity is the theoretical moles of carbon dioxide absorbed due to reacting with primary amines in dendrimer based on the equation (4)

**Dry system

Table 12b. Percent theoretical capacity of primary amines consumed under different pressures and its corresponding apparent equilibrium constants of primary amine reaction with CO_2 for 30wt% dendrimer in [bmim][DCA] at different temperatures*

	P_{feed} (bar)	% Saturation (%)	K_C
50°C	2.41	9.29	6659 L/mol
	3.75	13.18	
	5.16	19.22	
	6.47	25.06	
	7.90	32.37	
	9.26	39.53	
	10.59	47.15	
	11.96	55.09	
	13.43	64.05	
	14.66	69.58	10329 L^4/mol^4
80°C	2.43	4.49	3061 L/mol
	3.62	6.77	
	5.16	10.43	
	6.47	13.08	
	7.90	16.75	
	9.26	20.17	
	10.59	23.02	
	11.96	26.47	
	13.43	31.19	
	14.96	33.84	
90°C	2.43	3.93	2431 L/mol
	3.71	6.00	
	5.16	8.58	
	6.47	10.61	
	7.90	14.08	
	9.26	17.09	
	10.59	19.47	
	11.96	23.00	
	13.43	26.18	
	14.86	28.06	
100°C	2.43	2.98	1954 L/mol
	3.72	4.82	
	5.16	6.72	
	6.47	8.49	
	7.90	10.63	
	9.26	13.00	

	10.59	14.39	
	11.96	16.46	
	13.43	19.78	
	14.66	21.93	

*Dry system

Table 13a. Henry's Law Constants for CO_2 and He in PEG 400 at different temperatures

	T(^{o}C)	H_{CO2} (bar)	H_{He} (bar)
PEG 400	50	65.4 ±3.4	791.0±6.5
	80	91.1±2.3	565.6±10.2
	90	101.5±2.0	463.2±8.6
	100	110.2±4.6	361.4±4.7

Table 13b. Pseudo Henry's Law Constants for CO_2 and He in PEG 400 containing 20wt% Dendrimer at different temperatures

	T(^{o}C)	Pseudo H_{CO2} (bar)	Pseudo H_{He} (bar)
20wt% Dendrimer in PEG 400	50	25.4±2.3	800.0±12.1
	80	40.9±2.0	574.8±12.5
	90	48.3±2.7	473.1±8.4
	100	56.0±2.3	375.7±7.3

Table 14. Diffusion Coefficients and Henry's Law Constants CO_2 and He in [bmim][DCA] at different temperatures

	Diffusion Coefficients (m^2/s)		Henry's Law Constant (mol/m^3*atm)	
Temperature (^{o}C)	D_{CO2}	D_{He}	H_{CO2}	H_{He}
25	$3.54x10^{-10}$	$7.64x10^{-10}$	93.32	2.81
50	$6.55x10^{-10}$	$9.64x10^{-10}$	74.75	6.89
100	$9.52x10^{-10}$	$1.14x10^{-9}$	41.47	14.37

Table 15. Dimensional Characteristics of the Membrane Absorption Modules

Module [1]	OD; cm	ID; cm	L [2]; cm	Pore Size; Å	VVF	Fiber Number	Surface area [2]; cm^2
Ceramic	0.57	0.37	44.0	~50	0.35~0.4	1	78.75
PEEK-L [3,4]	0.0452	0.0290	41.0	~20	~0.4	568	3420

[1] OD: outer diameter of fiber; ID: inner diameter of fiber; L: effective fiber length; VVF: void volume fraction; [2] Based on outer diameter of fibers; [3] PEEK-L module has a packing density around 21.8% that was defined as the ratio between total fiber volume and the real volume they occupied (total fiber volume plus space between the fibers in the fiber strands wound helically in the module); [4] PEEK-L module with PTFE bead-filled tube-side headers in the module.

Table 16. Estimated Molar Product Flow Rates, Compositions and % CO_2 Recovery for 3 Ceramic Modules* in Series at 1034 kPag (150 psig) and Different Temperatures for Pure [bmim][DCA]

Temperature (^oC)	CO_2-rich Molar Flow Rate per Cycle (mol/s)	CO_2-Rich Composition (% CO_2)	He-rich Molar Flow Rate per Cycle (mol/s)	He-Rich Composition (% CO_2)	% CO_2 Recovery (%)
23	4.37E-05	56	7.00E-05	30	53.83
50	3.84E-05	53	6.24E-05	32	50.46
100	2.75E-05	57	5.19E-05	31	49.30

*see Table 1a for module details

Table 17. Estimated Molar Product Flow Rates, Compositions and % CO_2 Recovery for PEEK-L II Module* at Different Pressures and Temperatures with Pure [bmim][DCA]

Pressure (kPag)	Temperature (^oC)	CO_2-Rich Molar Flow Rate per Cycle (mol/sec)	CO_2-Rich Composition (% CO_2)	He-Rich Molar Flow Rate per Cycle (mol/sec)	He-Rich Composition (% CO_2)	% CO_2 Recovery (%)
689 (100 psig)	23	2.27E-05	91	4.13E-05	12	80.64
	50	1.85E-05	88	3.71E-05	16	73.33
	100	1.44E-05	85	3.09E-05	19	67.62
965 (140 psig)	23	2.84E-05	93	5.80E-05	14	76.51
	50	2.45E-05	89	5.21E-05	17	71.08
	100	1.91E-05	87	4.08E-05	18	69.34

*see Table 1c for number of fibers and surface area; PEEK-L II

Table 18. Simulation Results in Terms of Product Qualities at Different Temperatures and Feed Pressures for 2 PEEK-L III Modules in Series with Pure [bmim][DCA] as the Liquid Absorbent and Estimated Products Molar Flow Rates per Cycle

P (psig)	Temperature (^oC)	He-Rich Molar Flow Rate per Cycle (mol/sec)	He-Rich Composition (% CO_2)	CO_2-Rich Molar Flow Rate per Cycle (mol/sec)	CO_2-Rich Composition (% CO_2)	% CO_2 Recovery (%)
100	23	9.58E-05	7.3	5.69E-05	95.1	88.54
	50	8.20E-05	10.1	4.79E-05	91.2	84.03
	100	6.17E-05	14.6	3.26E-05	88.1	76.10
200	23	2.06E-04	12.1	1.00E-04	97.3	79.65
	50	1.67E-04	13.7	8.20E-05	93.5	77.01
	100	1.34E-04	18.4	5.71E-05	90.6	67.71

5C. Illustrations

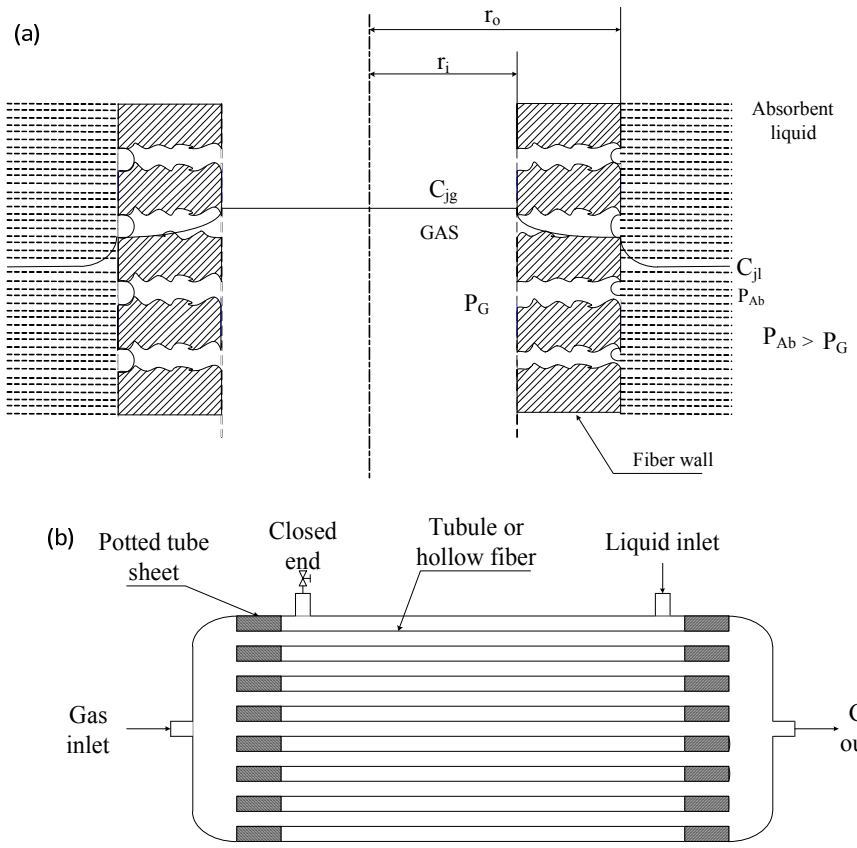

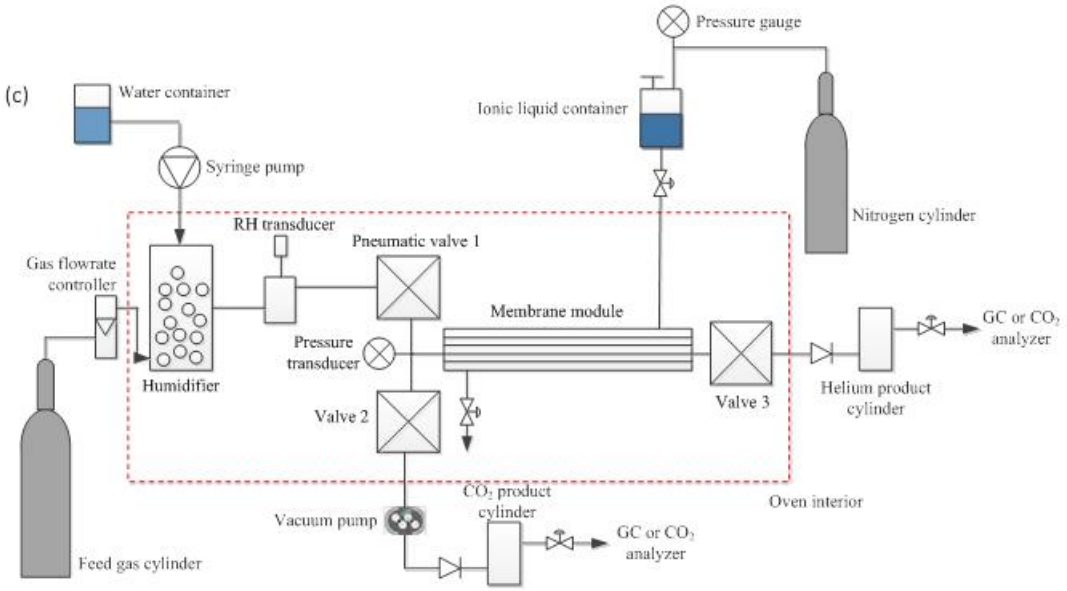

x

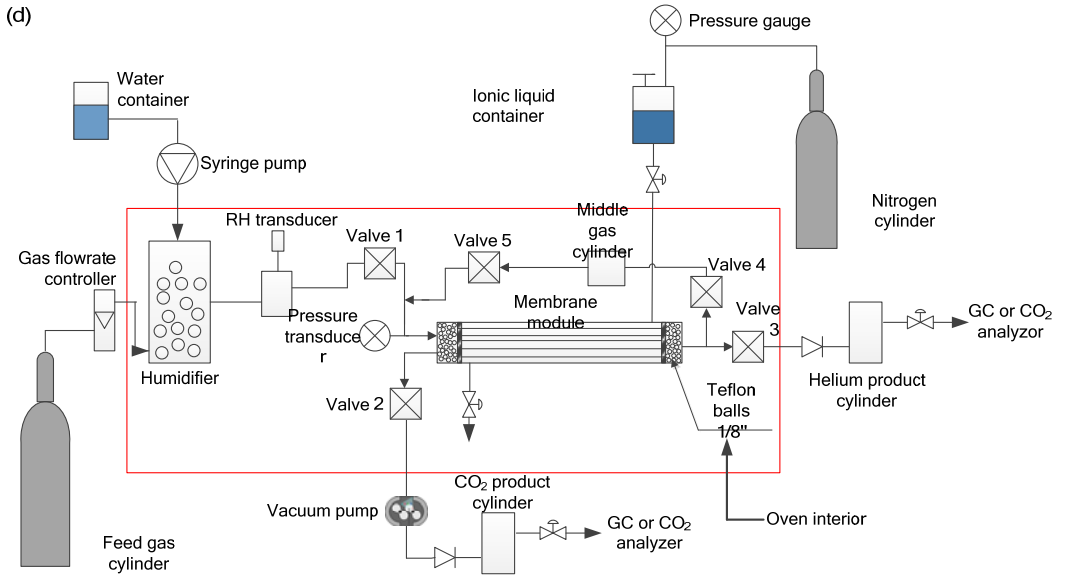

Figure 1. (a) Gas liquid membrane contacting in a membrane contactor; (b) Membrane module of ceramic tubules or hollow fibers; (c) Schematic diagram of pressure swing membrane absorption apparatus; (d)) Schematic diagram of pressure swing membrane absorption apparatus having dead volume reduction.

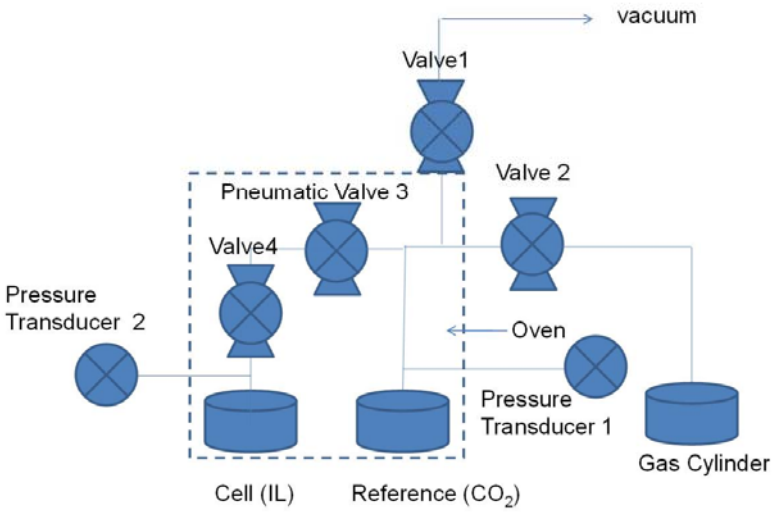

Figure 1(e). Apparatus for measuring gas solubility.

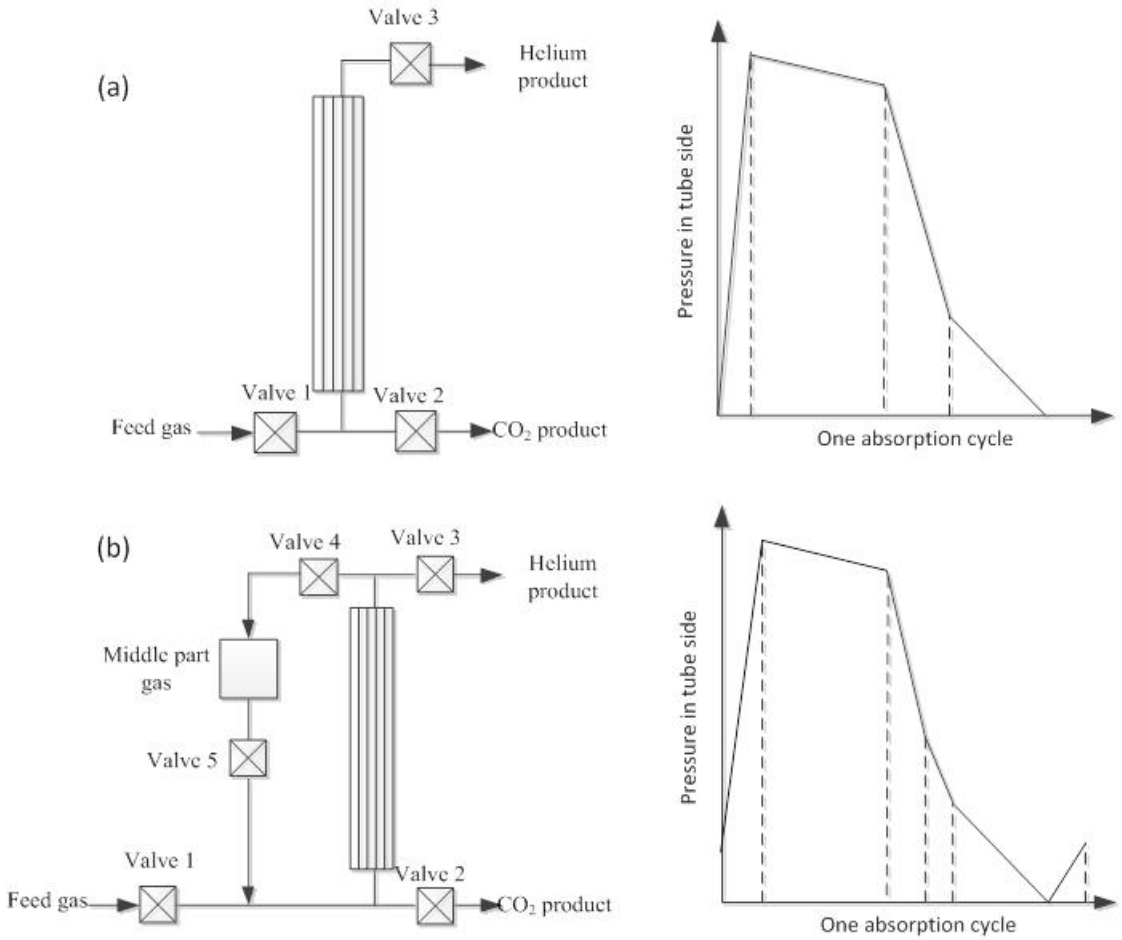

Figure 2. Schematic diagrams of (a) 3-valve and (b) 5-valve pressure swing membrane absorption process.

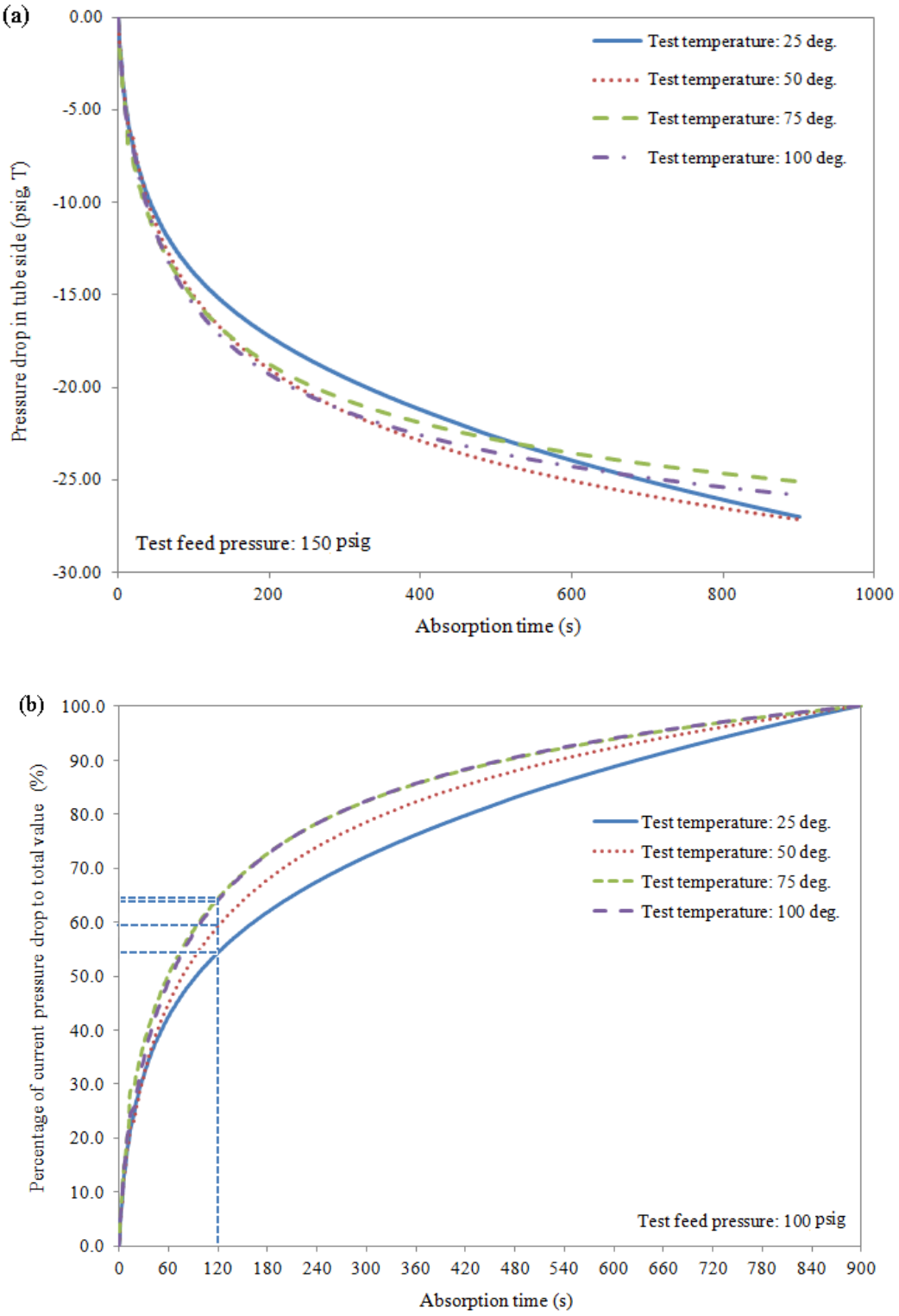

Figure 3. Pressure drops in (a) tube side and (b) pressure drop percentage during extended time absorption step in three ceramic membrane modules connected in series.

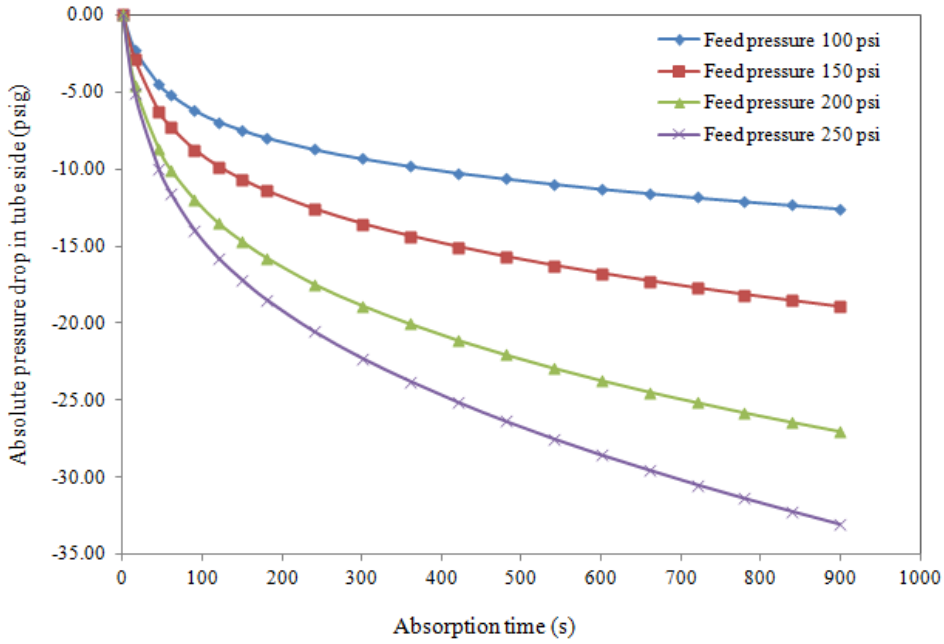

Figure 3(c). Absolute pressure changes in the tube side during extended time absorption step in four ceramic membrane modules connected in series.

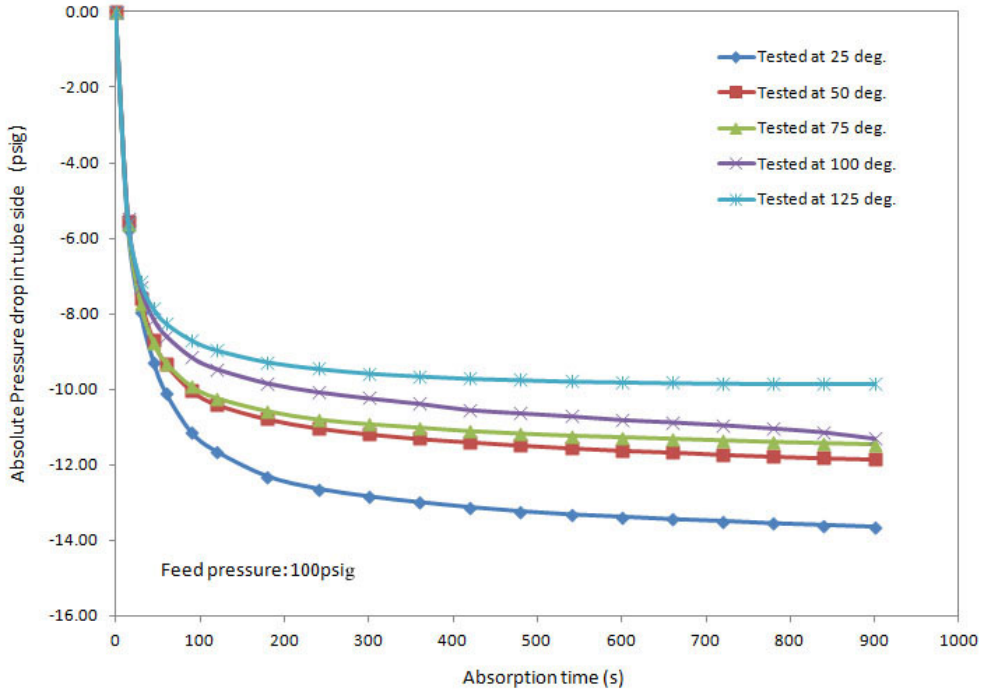

Figure 4(a). Absolute pressure changes in tube side during extended time absorption step in two PEEK-S membrane modules in series.

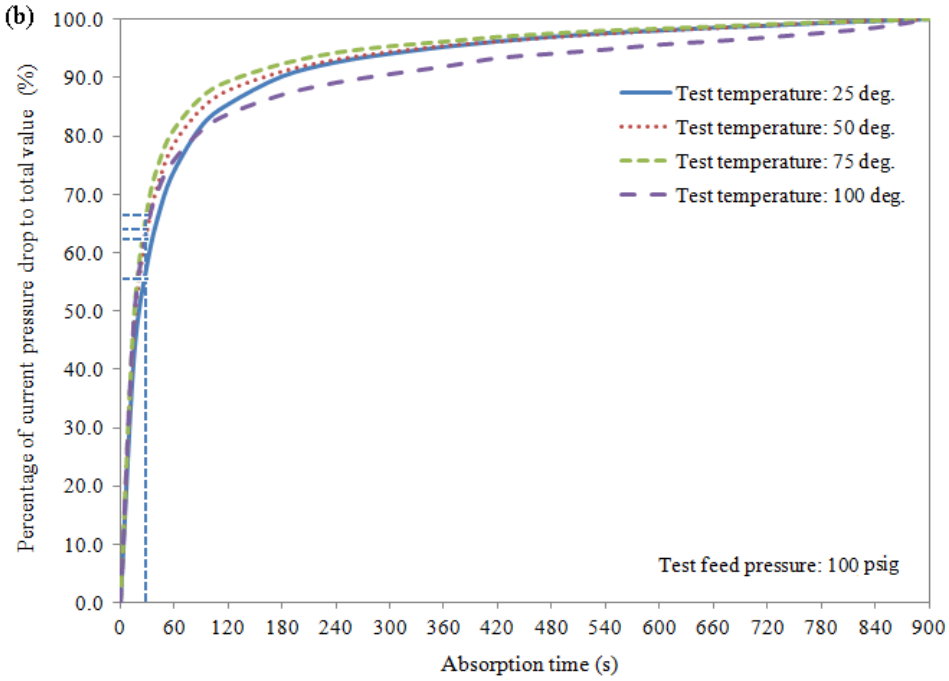

Figure 4(b). Percent pressure drops during extended time absorption step in two PEEK-S membrane modules in series.

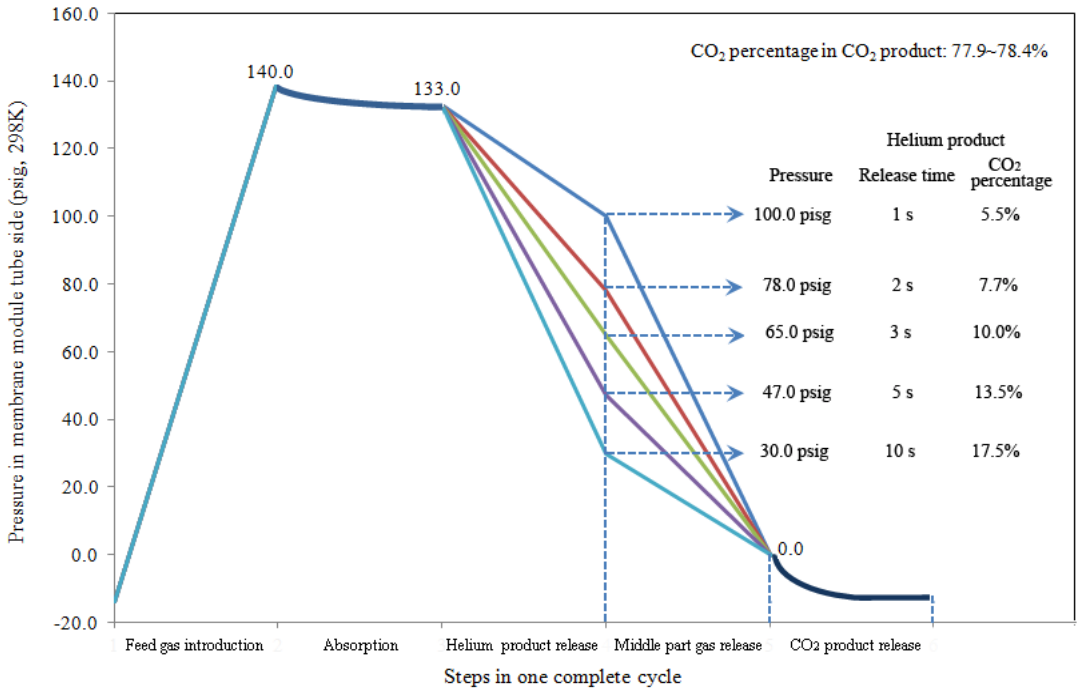

Figure 5a. Pressure change in tube side and product composition for different helium product release amounts for two PEEK-S hollow fiber modules in series.

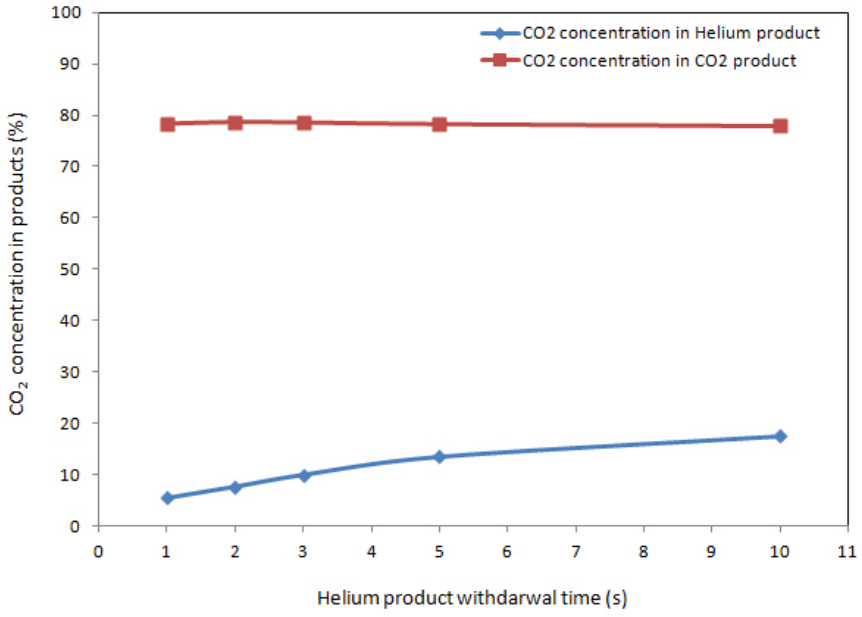

Figure 5b. Influence of helium-rich product withdrawal time on the product quality for two PEEK-S hollow fiber modules in series.

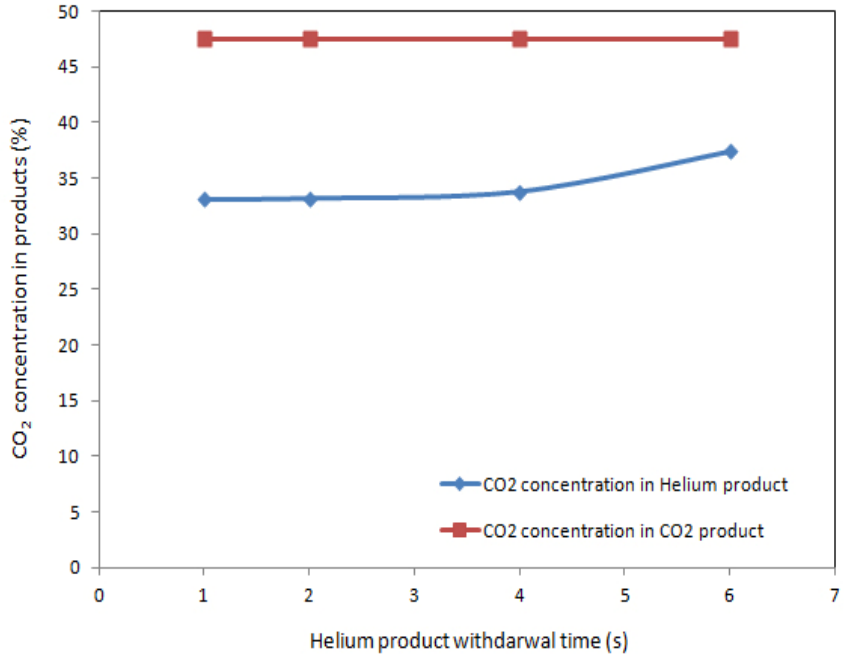

Figure 6a. Influence of helium-rich product withdrawal time on the product quality for four ceramic modules in series.

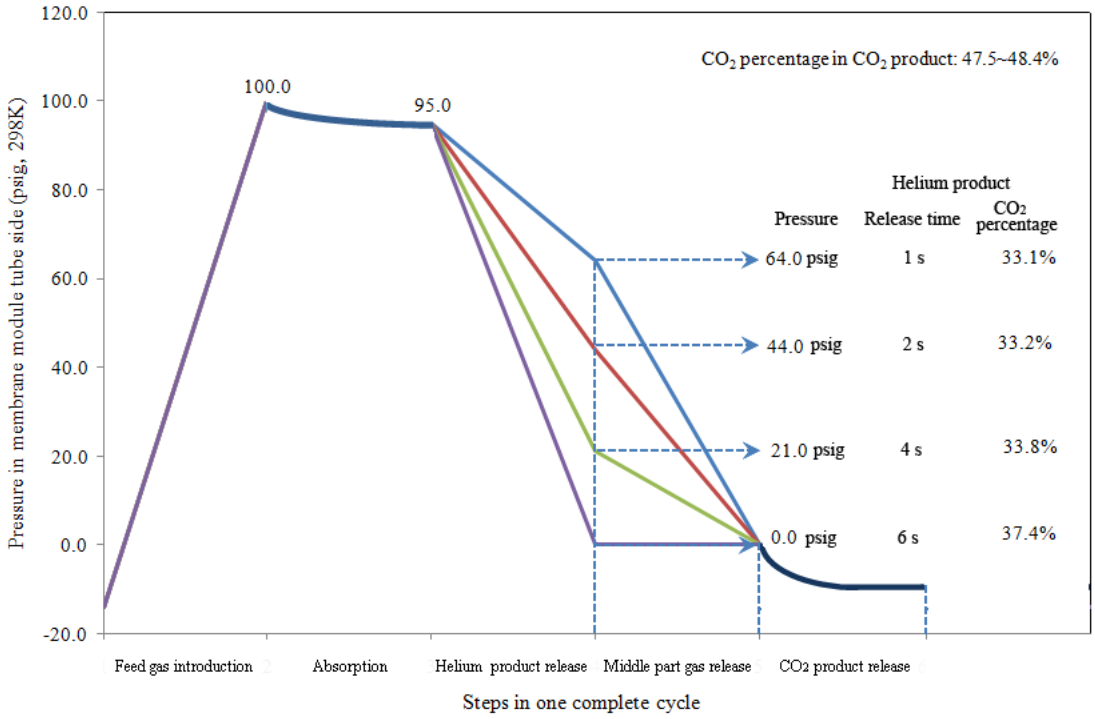

Figure 6b. Pressure in tube side and product changes with different helium product release quantity for three ceramic modules in series.

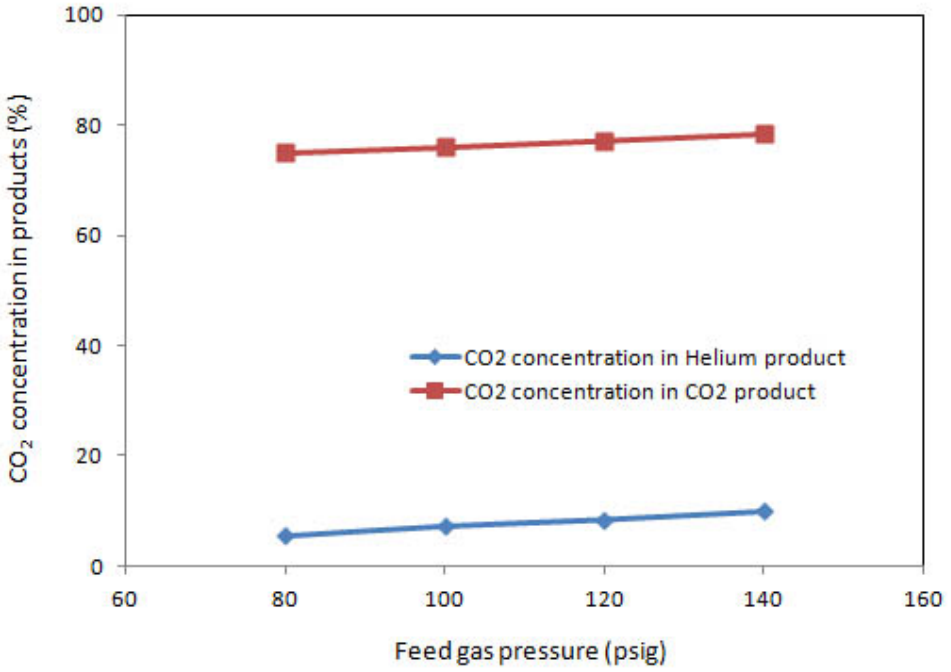

Figure 7a. Influence of feed gas pressure on the product quality with two PEEK-S modules in series.

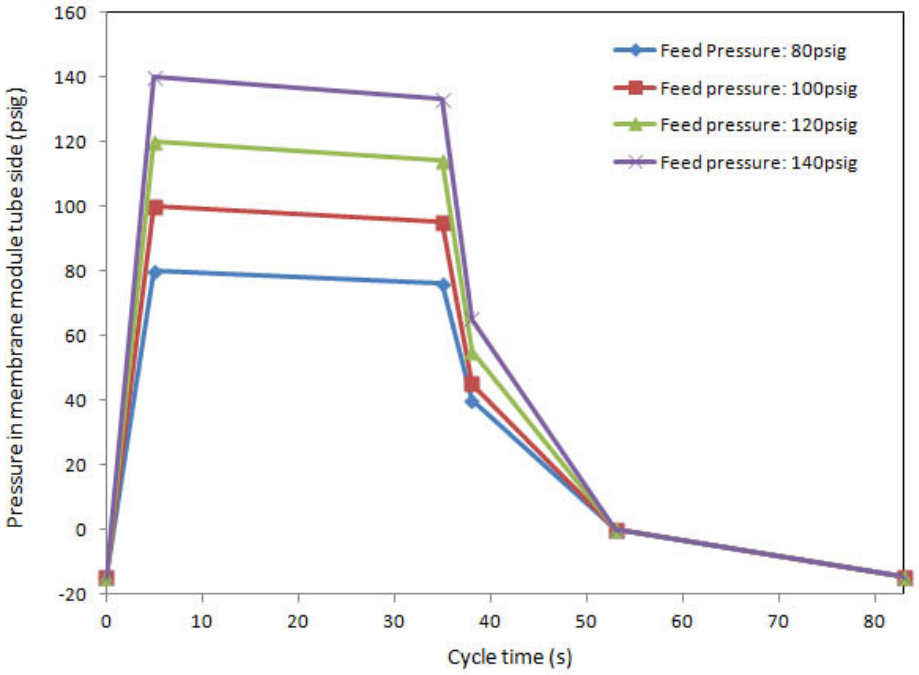

Figure 7b. Pressure changes in tube side with different feed gas pressure for two PEEK-S modules in series.

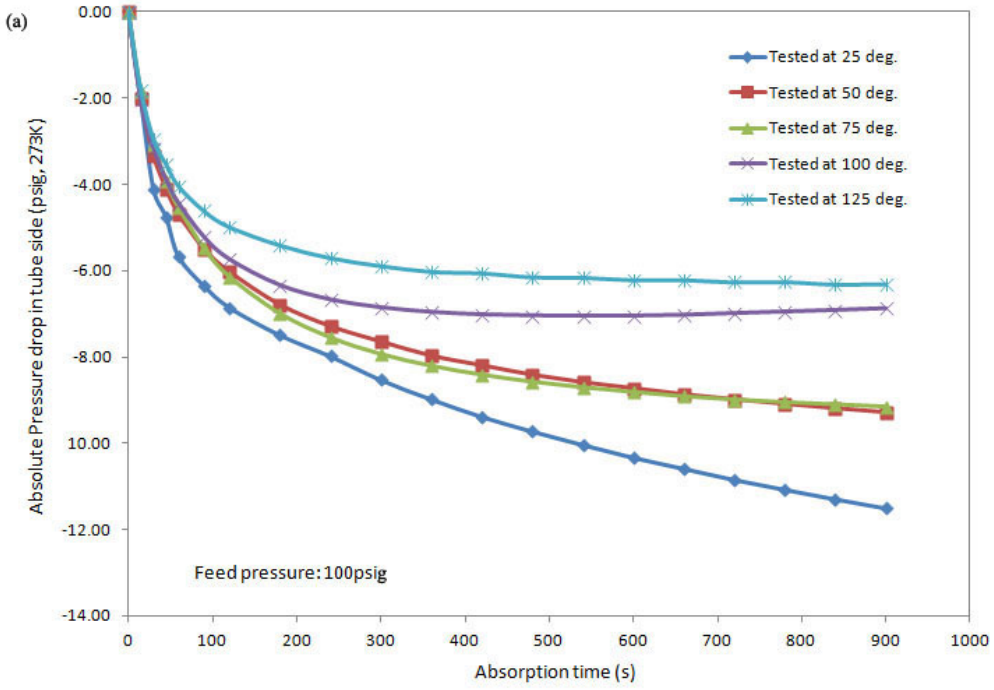
(a)
Absolute Pressure drop in tube side (psig, 273K)
0.00
-2.00
-4.00
-6.00
-8.00
10.00
-12.00
-14.00
0
100
200
300
400
500
600
700
800
900
1000
Absorption time (s)
Tested at 25 deg.
Tested at 50 deg.
Tested at 75 deg.
Tested at 100 deg.
Tested at 125 deg.
Feed pressure: 100psig

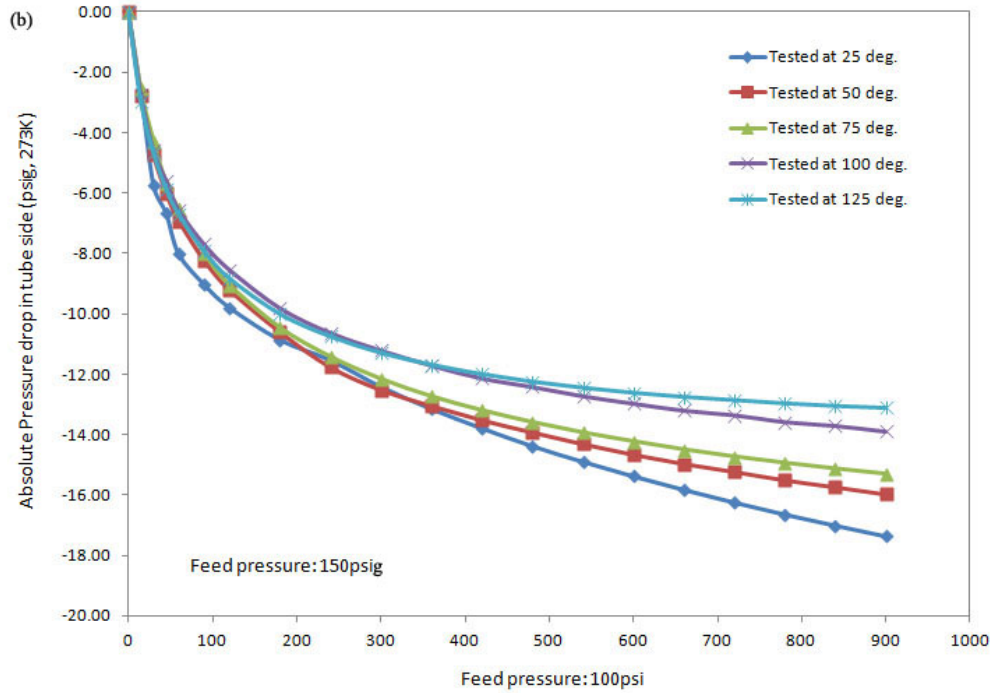
(b)
Absolute Pressure drop in tube side (psig, 273K)
0.00
-2.00
-4.00
-6.00
-8.00
-10.00
-12.00
-14.00
-16.00
-18.00
-20.00
0
100
200
300
400
500
600
700
800
900
1000
Feed pressure: 100psi
Tested at 25 deg.
Tested at 50 deg.
Tested at 75 deg.
Tested at 100 deg.
Tested at 125 deg.
Feed pressure: 150psig

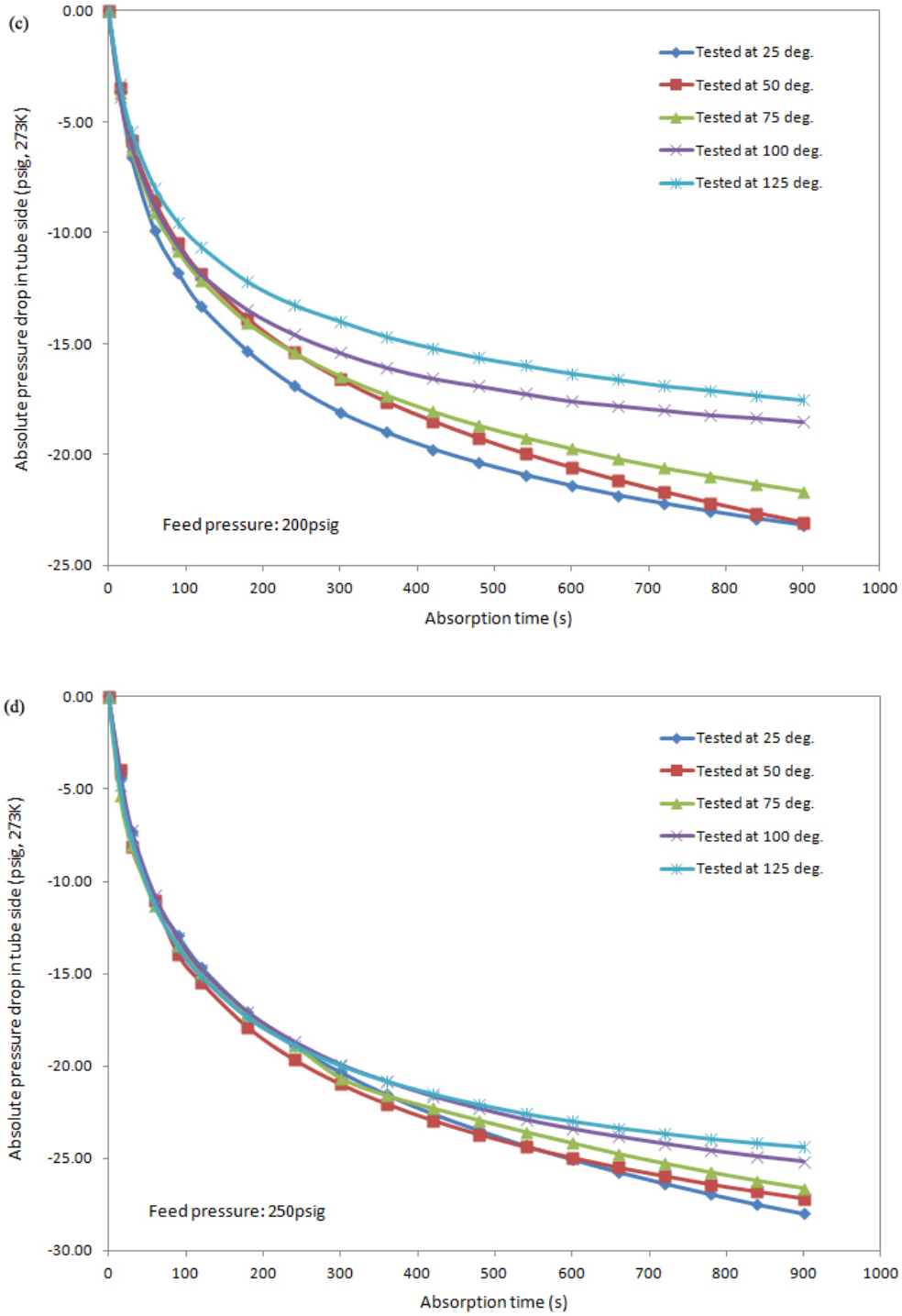

Figure 8. Influence of temperature and feed pressure on absorption behavior in four ceramic modules in series: (a) 100 psig; (b) 150 psig; (c) 200 psig; (d) 250 psig.

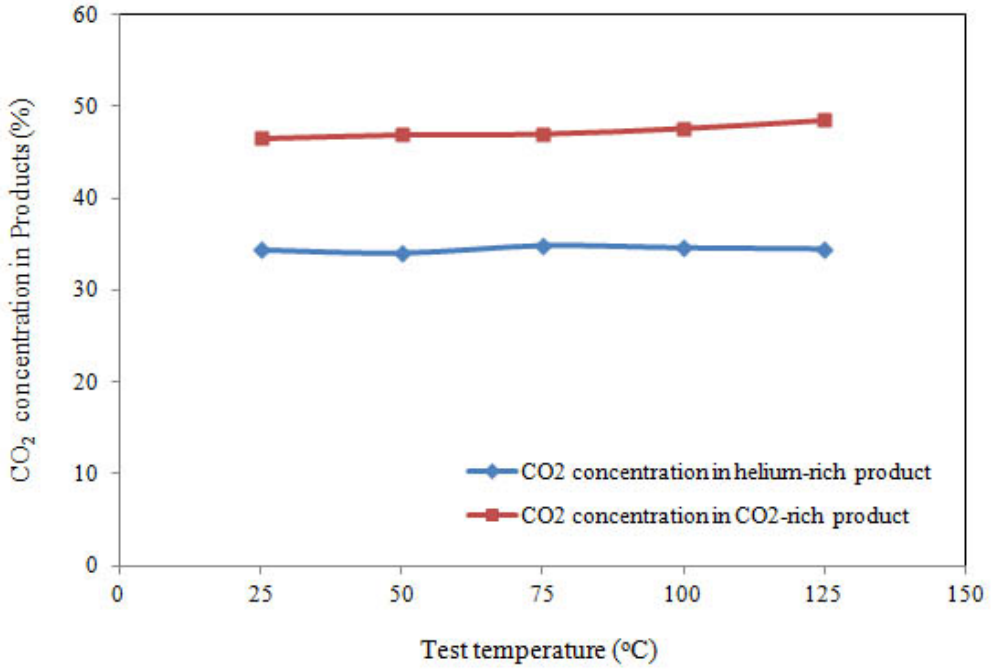

Figure 9. Influence of test temperature on the product quality with four ceramic modules at 250 psig.

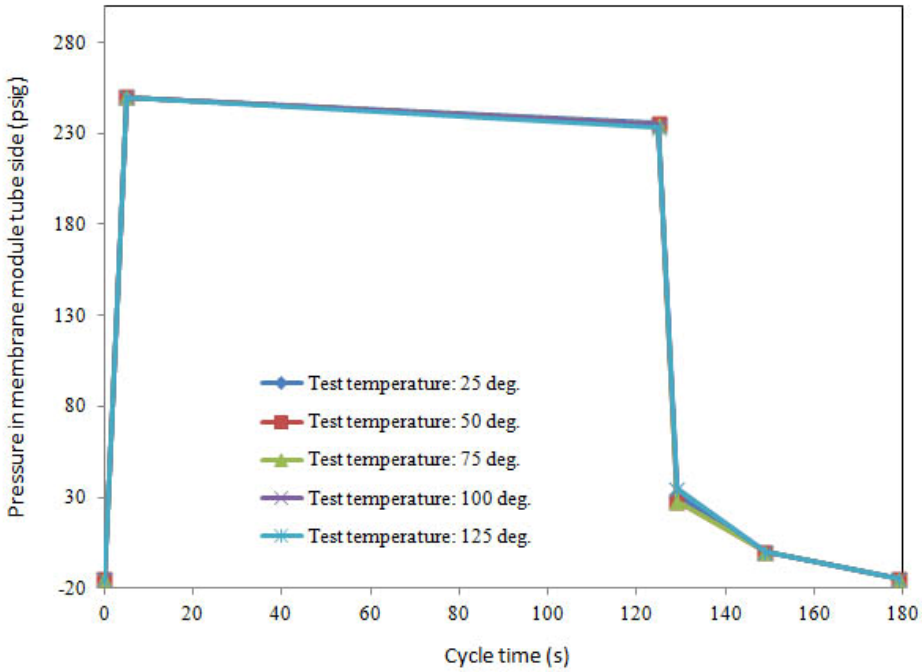

Figure 10. Pressure changes in tube side with different test temperature with ceramic membrane modules at 1723 kPag (250 psig).

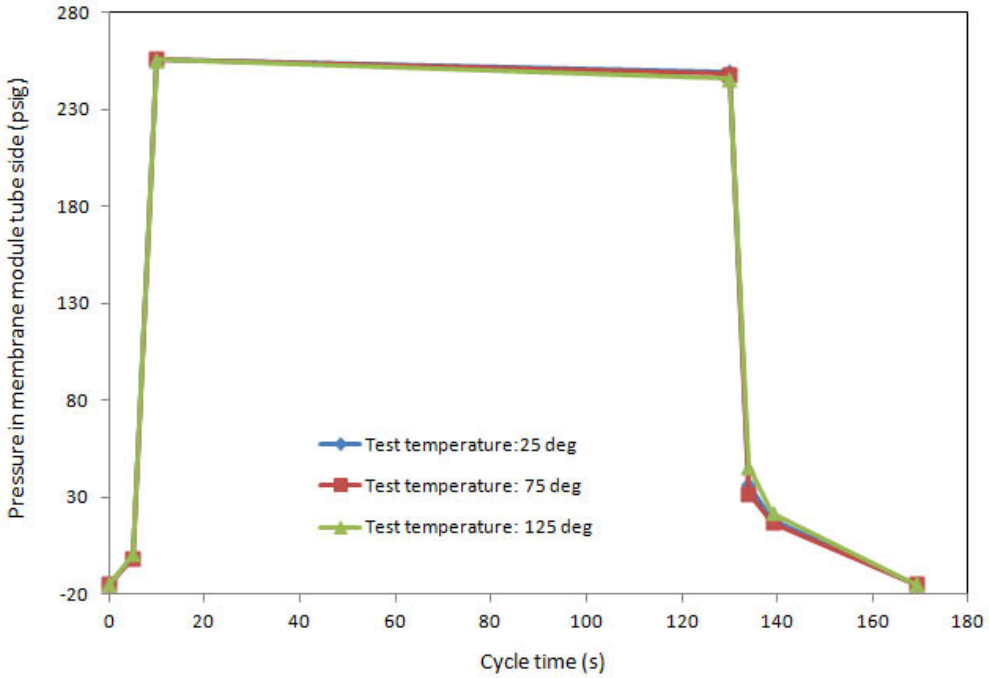

Figure 11a. Pressure changes in tube side with different test temperature with ceramic membrane modules when middle part gas was recycled.

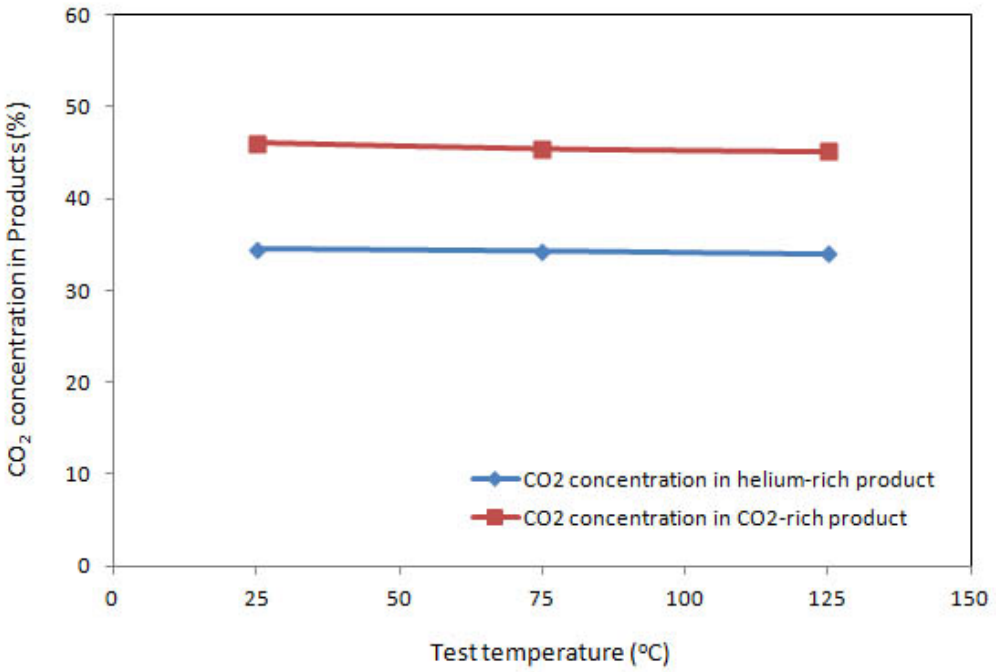

Figure 11b. Influence of test temperature on the product quality with ceramic modules when middle part gas was recycled.

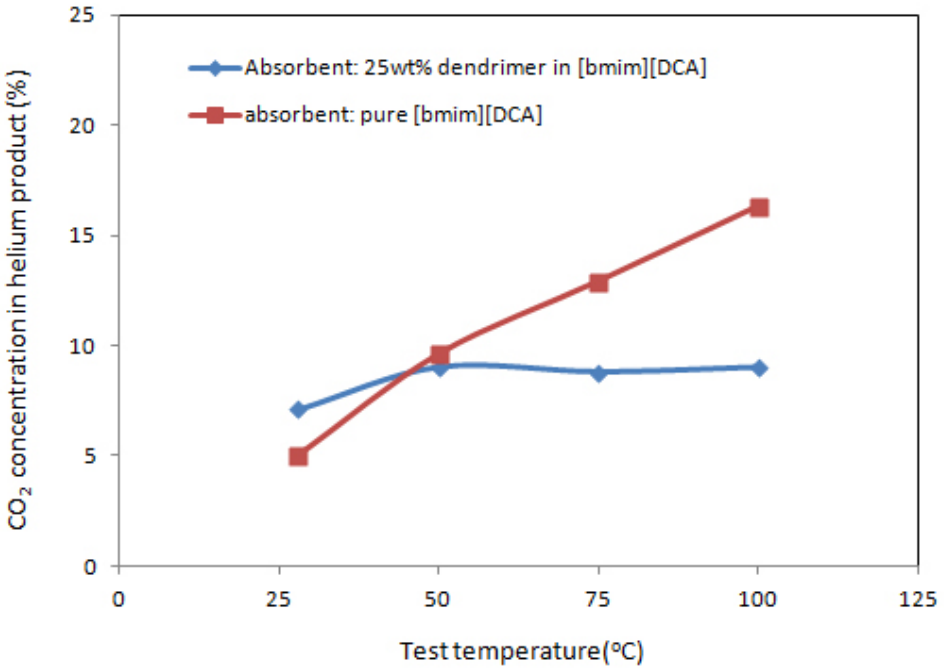

Figure 12. Influence of test temperature on the helium quality using module PEEK-L and ionic liquid with or without dendrimer as absorbent liquid.

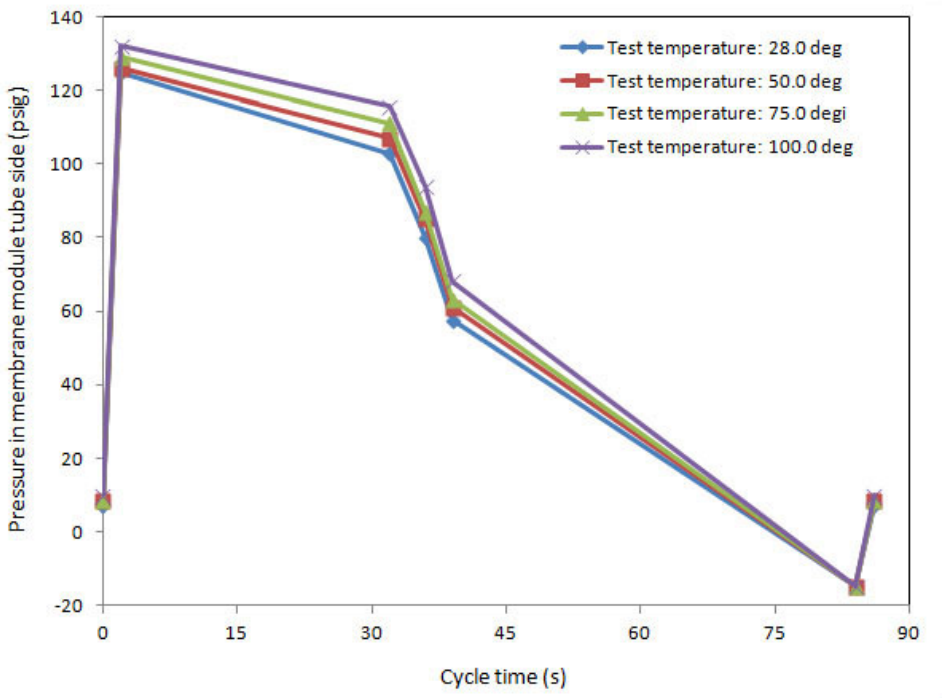

Figure 13a. Pressure changes in tube side for different test temperatures with PEEK-L membrane module using pure [bmim][DCA] as absorbent.

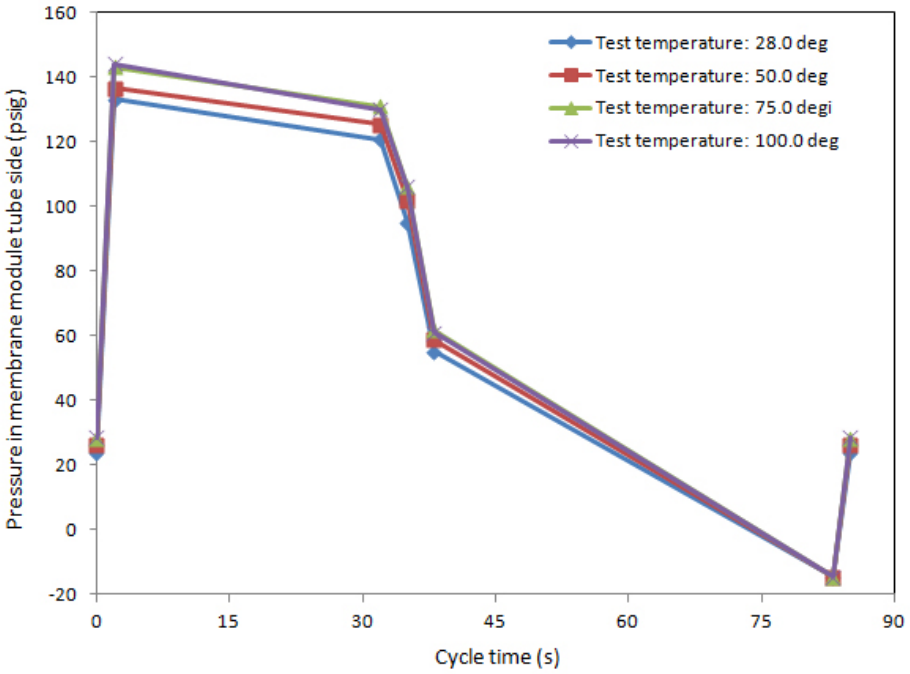

Figure 13b. Pressure changes in tube side for different test temperatures with PEEK-L membrane module using 25wt% dendrimer in [bmim][DCA] as absorbent.

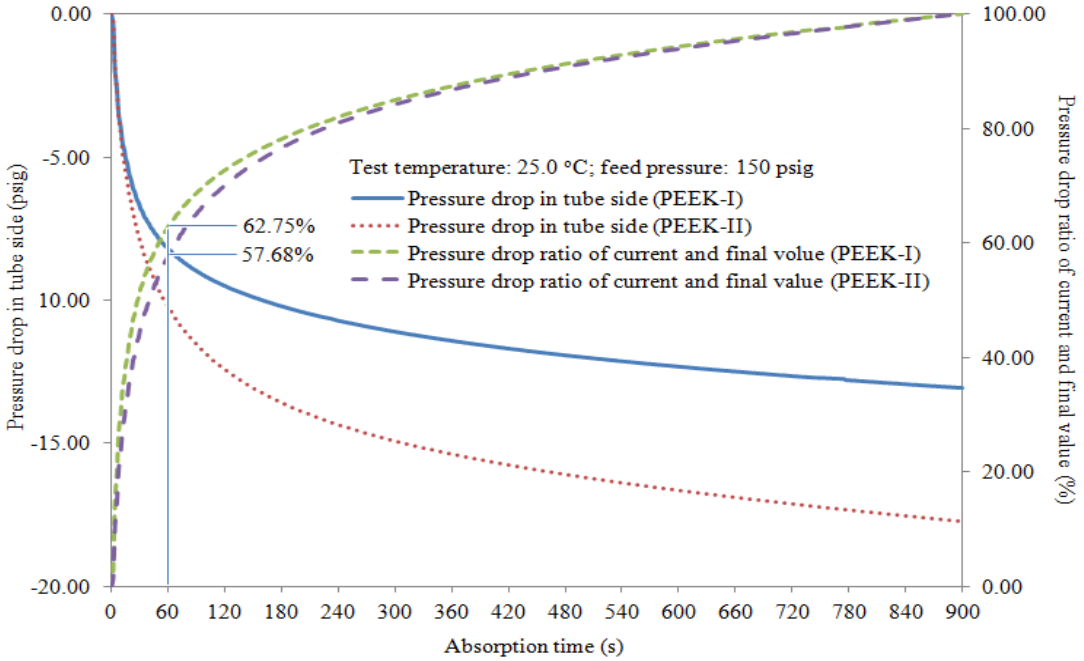

Figure 14. Pressure drop and percentage completed to total pressure drop during 900 s absorption for PEEK-I and PEEK-II at 25°C with a feed pressure of 1034 kPag (150 psig).

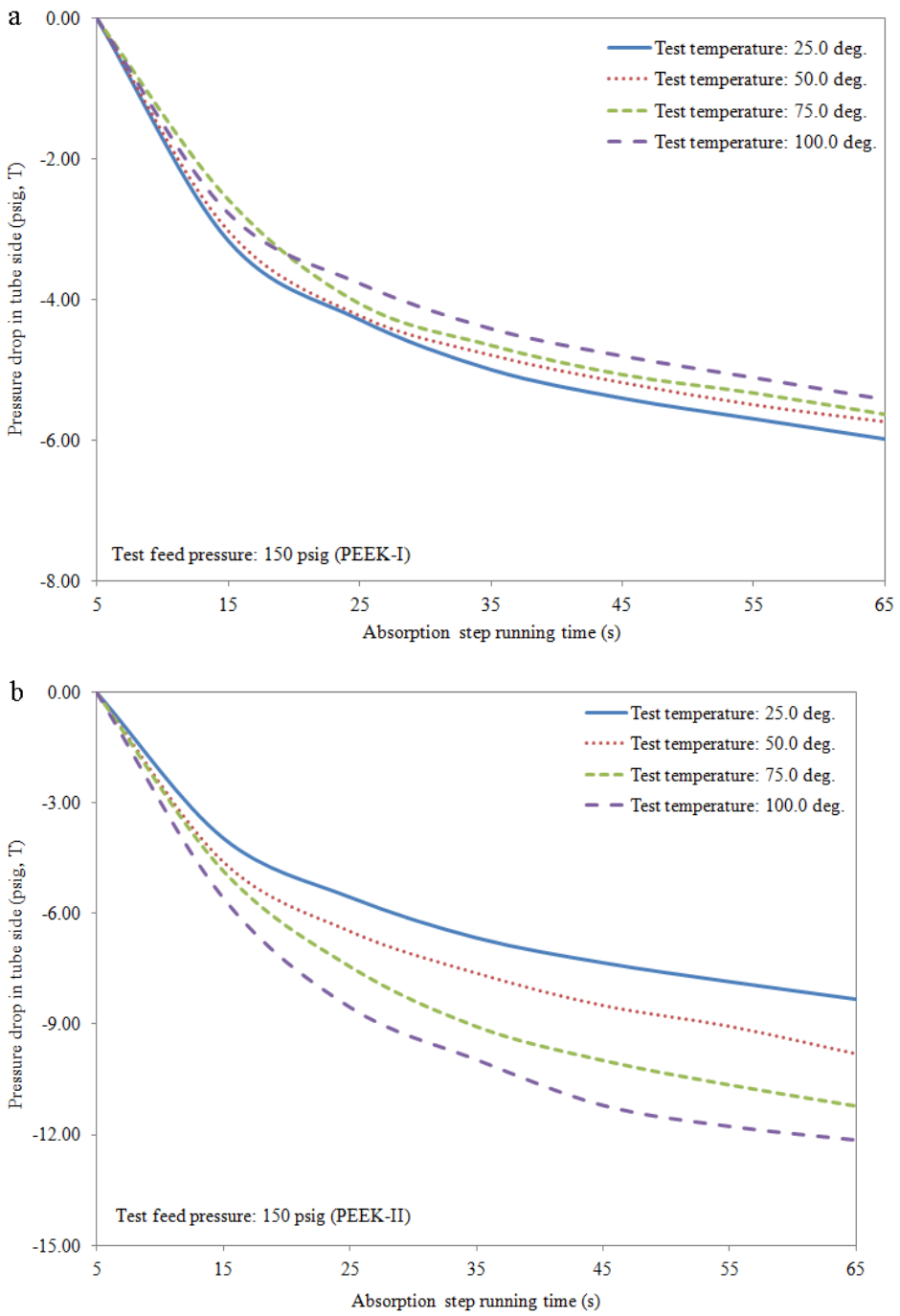

Figure 15. Pressure drop in membrane module tube side during absorption step at different temperatures with feed gas pressure of 1034 kPag (150 psig): (a) PEEK-I; (b) PEEK-II.

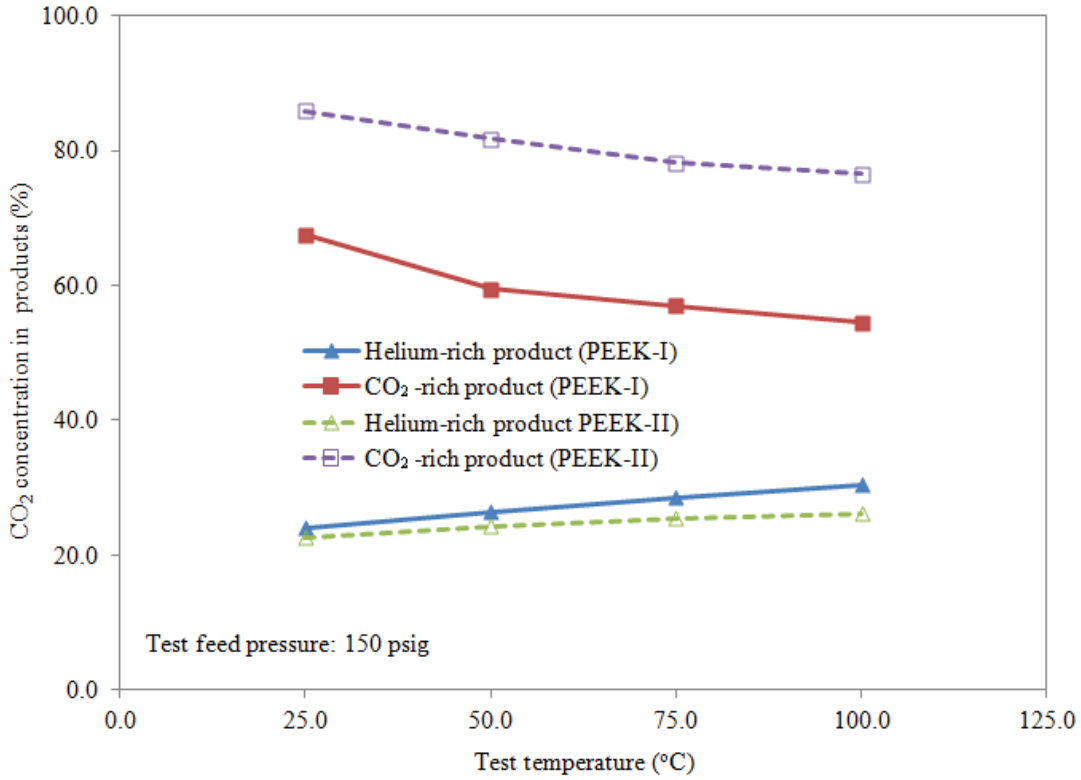

Figure 16. Comparison of product qualities between PEEK-I and PEEK-II modules at different running temperatures for a feed gas pressure of 1034 kPag (150 psig) for pure [bmim] [DCA].

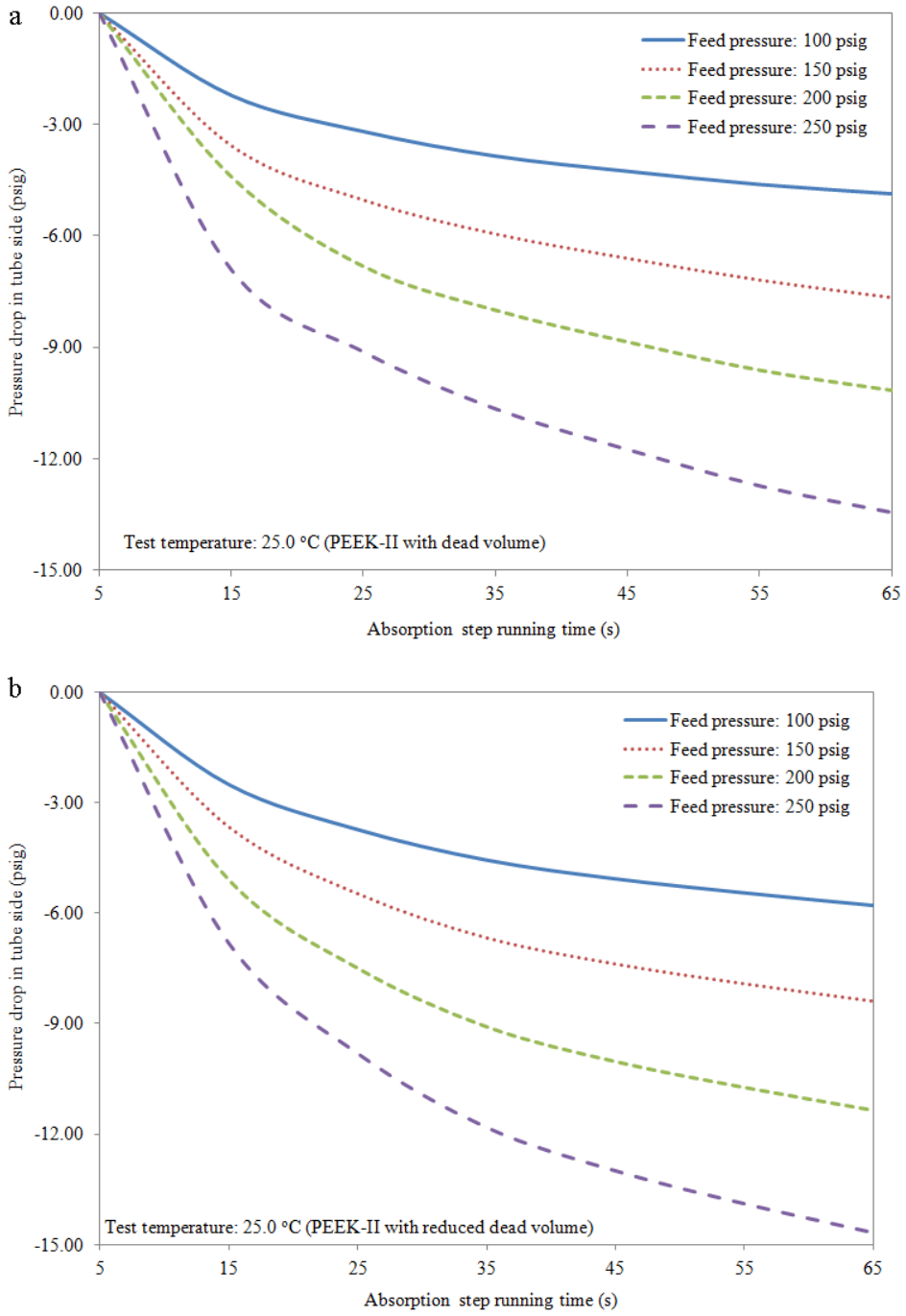

Figure 17. Pressure drop in PEEK-II module tube side during absorption step at 25 ^{o}C for different feed gas pressures: (a) with full dead volume; (b) reduced dead volume.

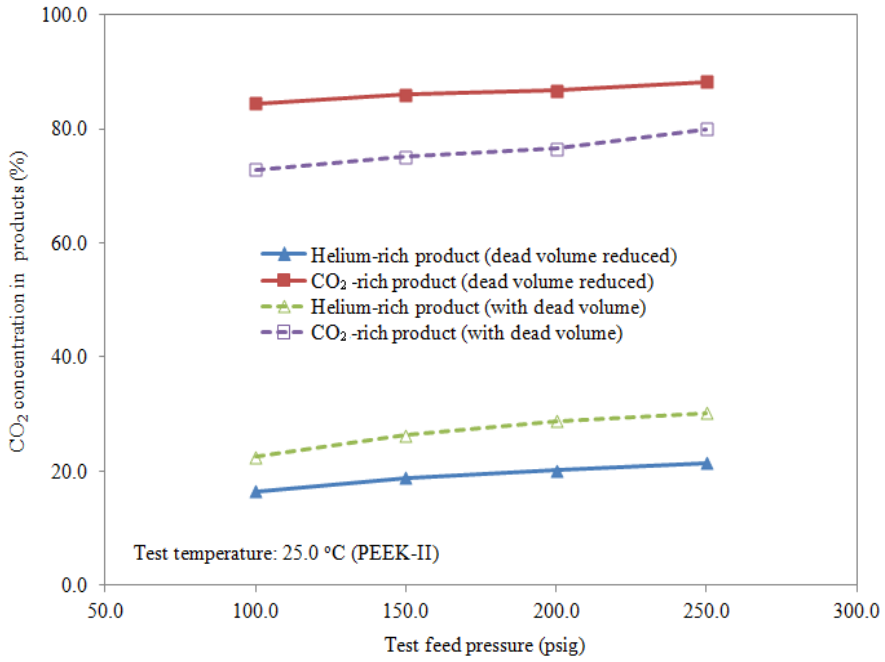

Figure 18. Comparison of product qualities of PEEK-II module between full and reduced dead volume at 25°C for different feed gas pressures.

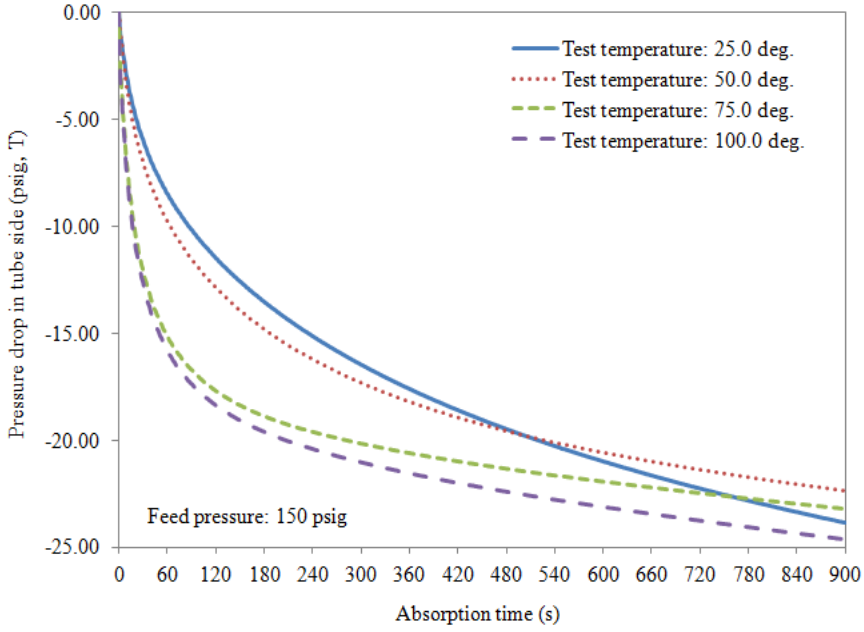

Figure 19. Influence of test temperature on pressure drop in module tube side during 900 s absorption for PEEK-II with a feed pressure of 1034 kPag (150 psig) when a 10 wt% dendrimer in [bmim][DCA] mixture was used as absorbent.

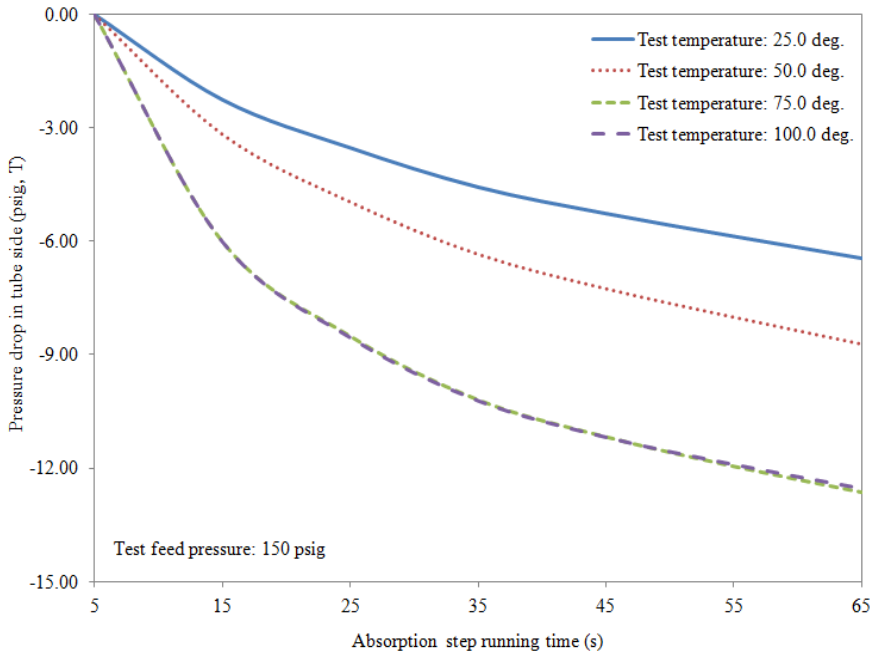

Figure 20. Pressure drop in membrane module tube side during the initial absorption step at different temperatures with feed gas pressure of 1034 kPag (150 psig) when a 10 wt% dendrimer in [bmim][DCA] mixture as absorbent.

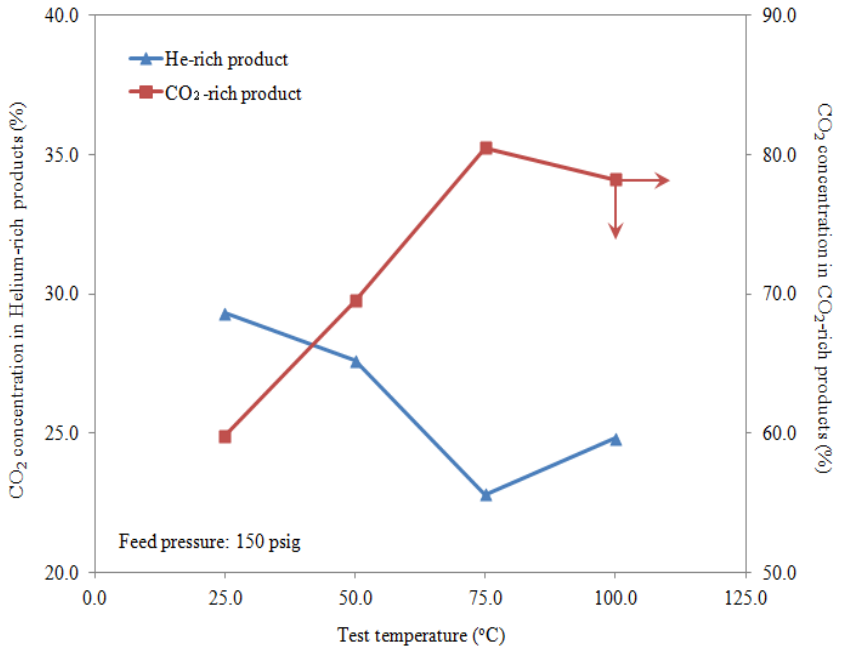

Figure 21. Influence of running temperature on product qualities with a feed gas pressure of 1034 kPag (150 psig) when a 10 wt% dendrimer in [bmim][DCA] mixture as absorbent.

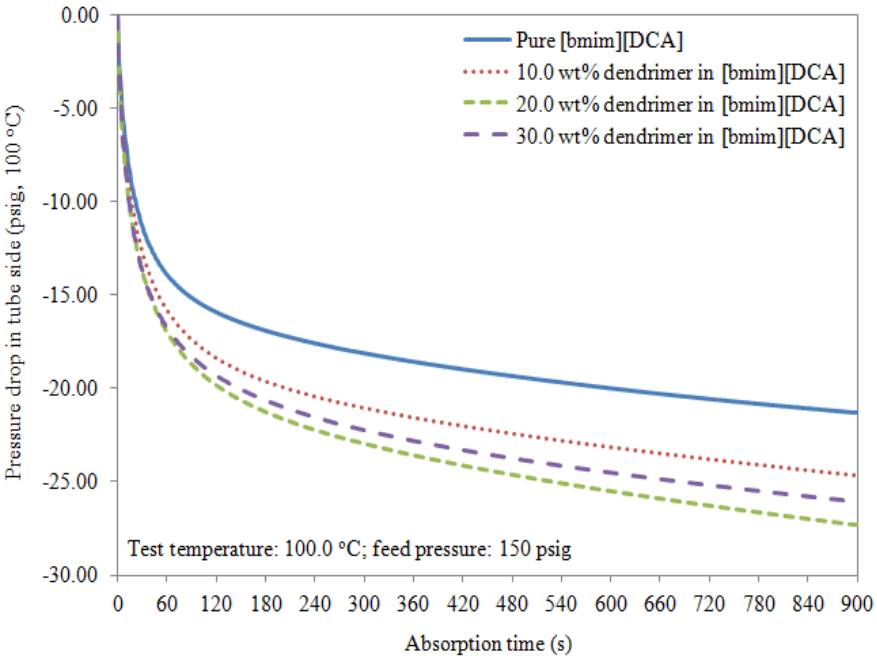

Figure 22a. Pressure drops in module tube side during 900 s absorption from different dendrimer-[bmim][DCA] mixtures at 1034 kPag (150 psig) and 100 °C.

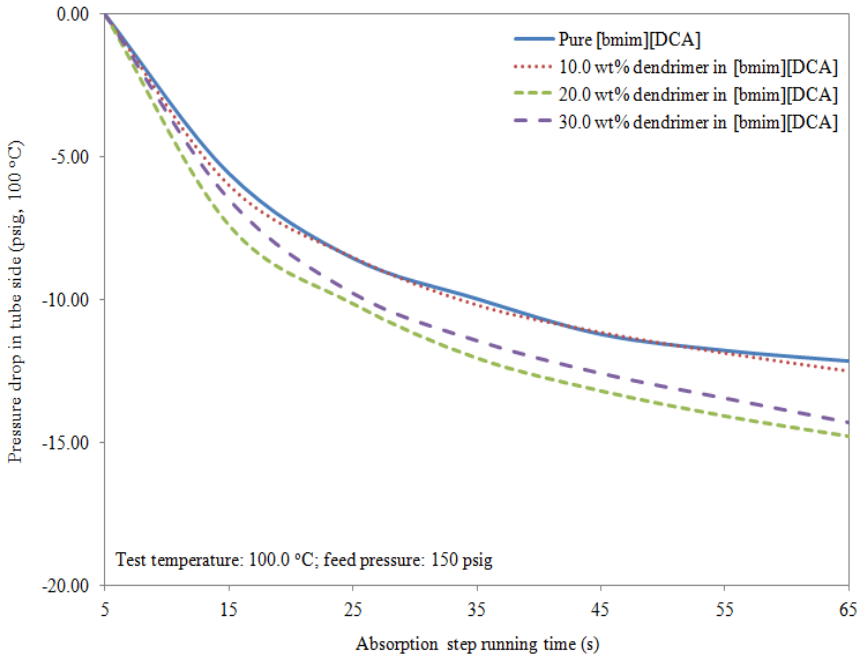

Figure 22b. Pressure drop in membrane module tube side during absorption step from different absorbents at 100 °C with feed gas pressure of 1034 kPag (150 psig).

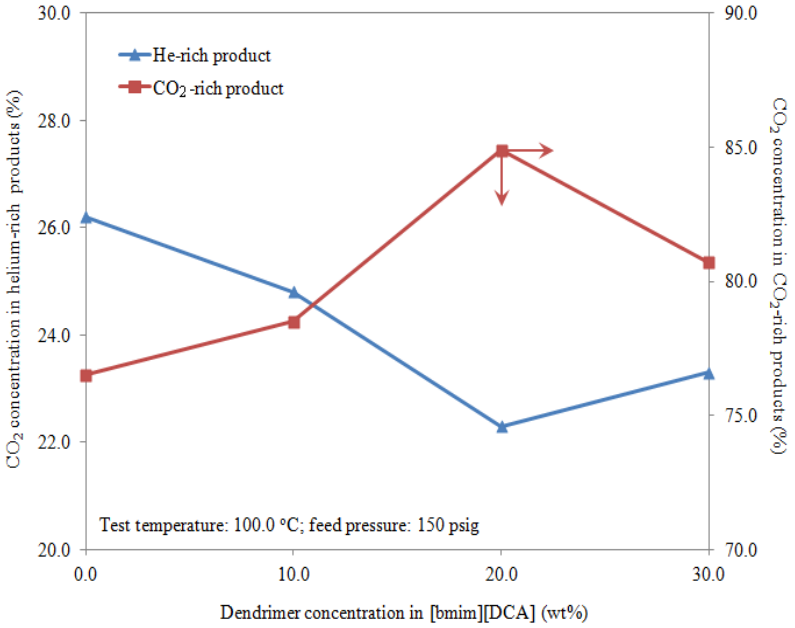

Figure 23. Influence of dendrimer concentration on product qualities when tested at 100 °C with a feed gas pressure of 1034 kPag (150 psig).

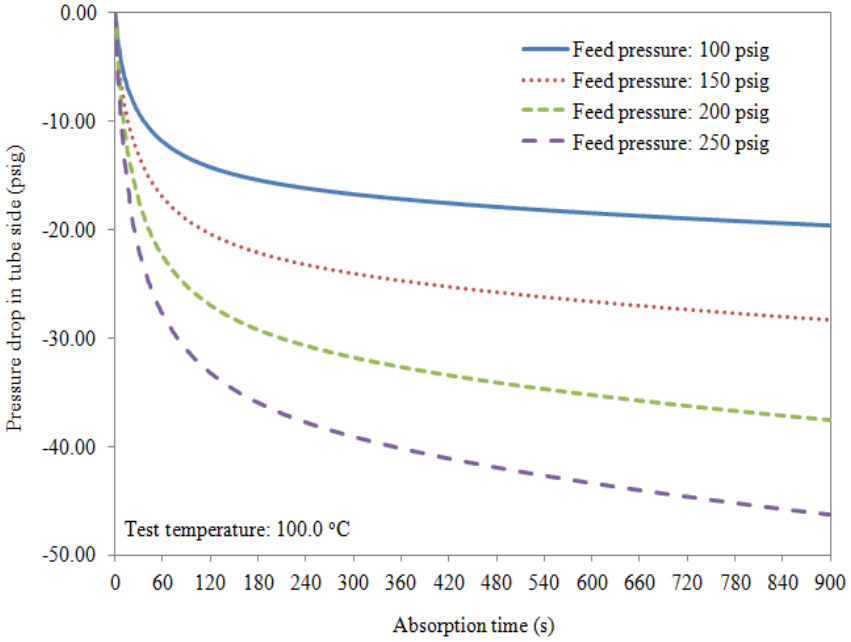

Figure 24. Pressure drops in PEEK-II module tube side (dead volume reduced) during 900 s absorption from 20.0 wt% dendrimer-[bmim][DCA] mixture at 100°C with different feed gas pressures.

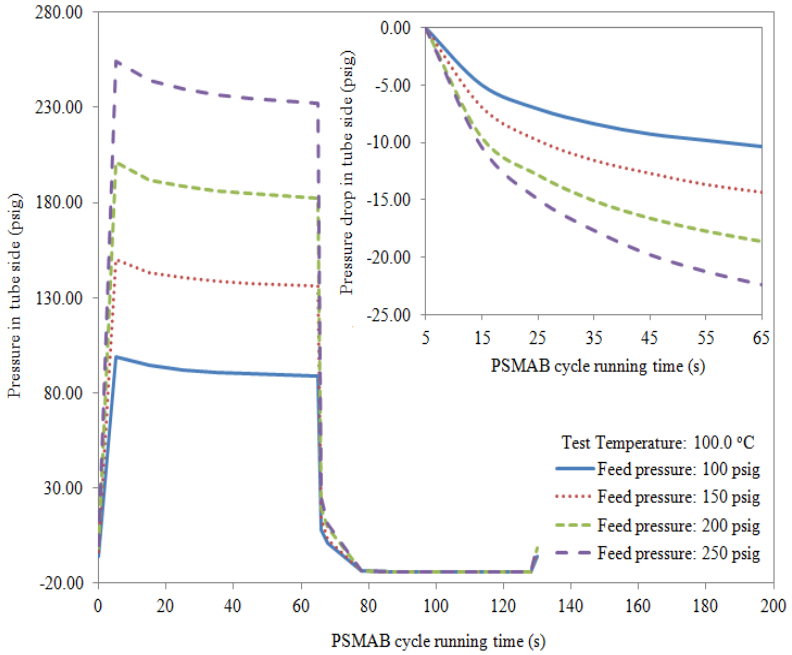

Figure 25a. Pressure drop in PEEK-II membrane module tube side (dead volume reduced) during one complete PSMAB cycle and absorption step from 20.0 wt% dendrimer-[bmim][DCA] mixture at 100°C with different feed gas pressures.

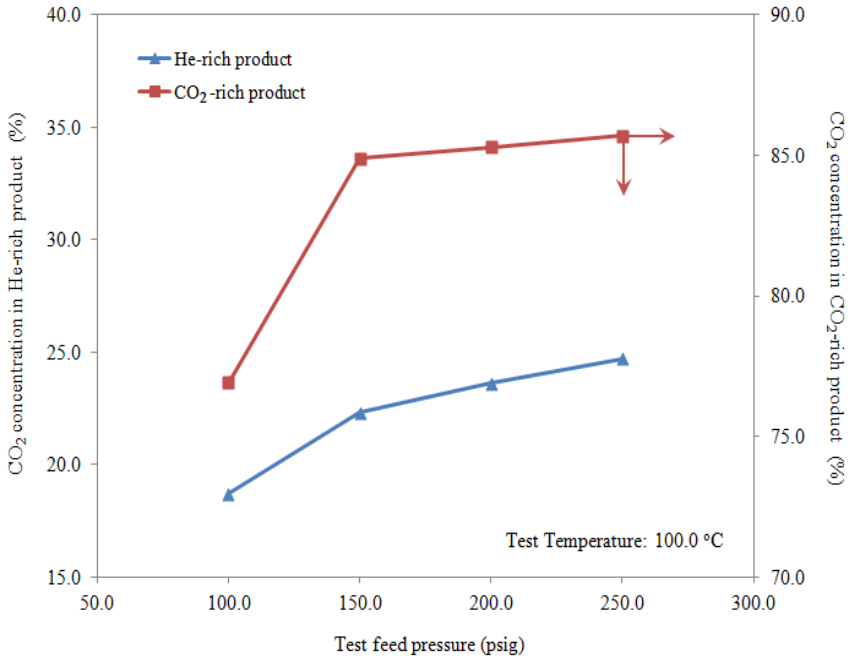

Figure 25b. Influence of feed gas pressure on product qualities with 20.0 wt% dendrimer-IL mixture as absorbent and tested at 100°C; PEEK-II module with dead volume reduced.

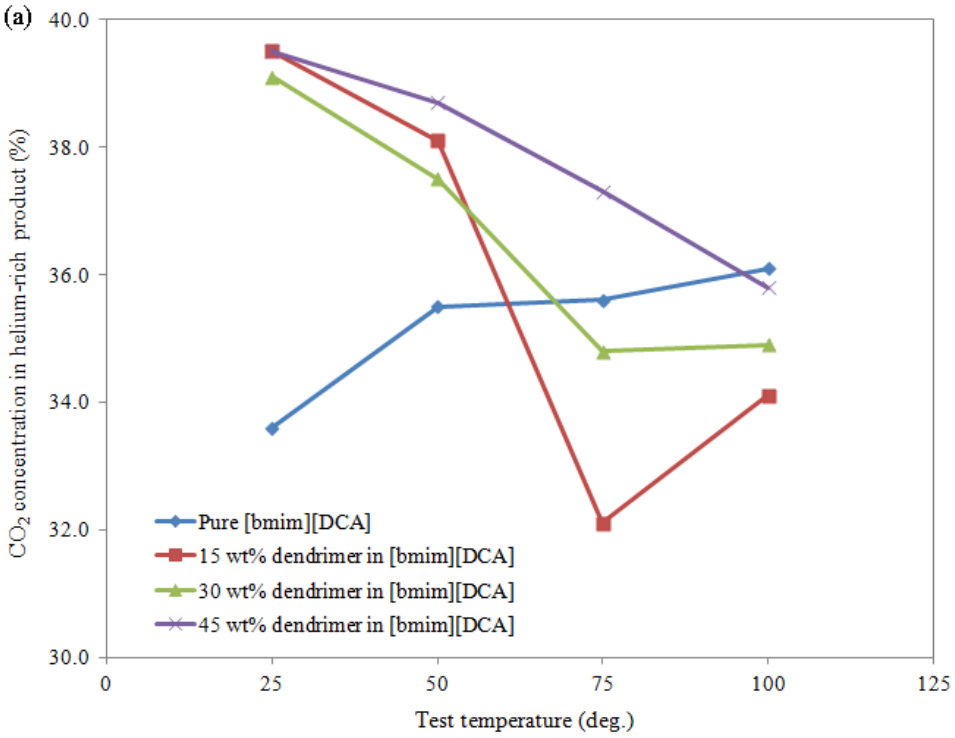

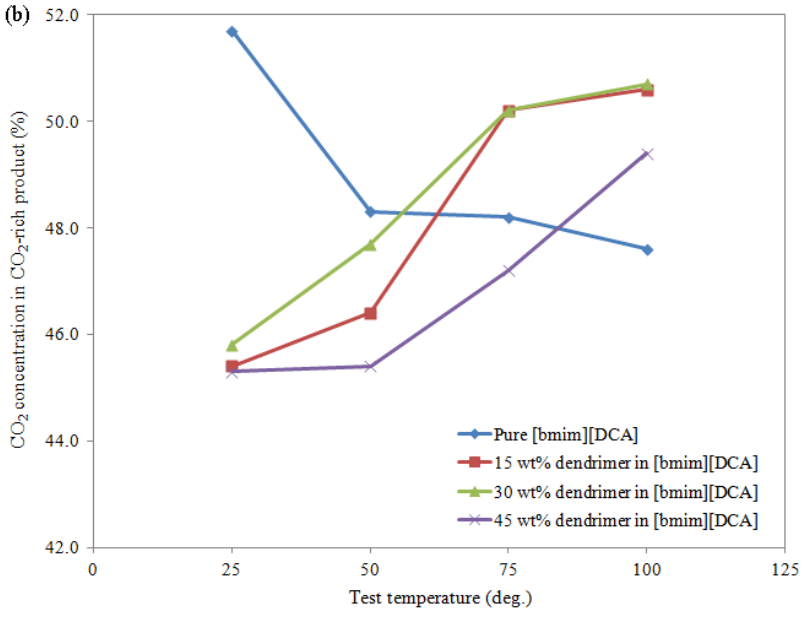

Figure 26 a,b. Product changes from different absorbents at different test temperatures for three ceramic modules in series for various dendrimer containing ionic liquid as absorbent: (a) He-rich products; (b) CO_2-rich products.

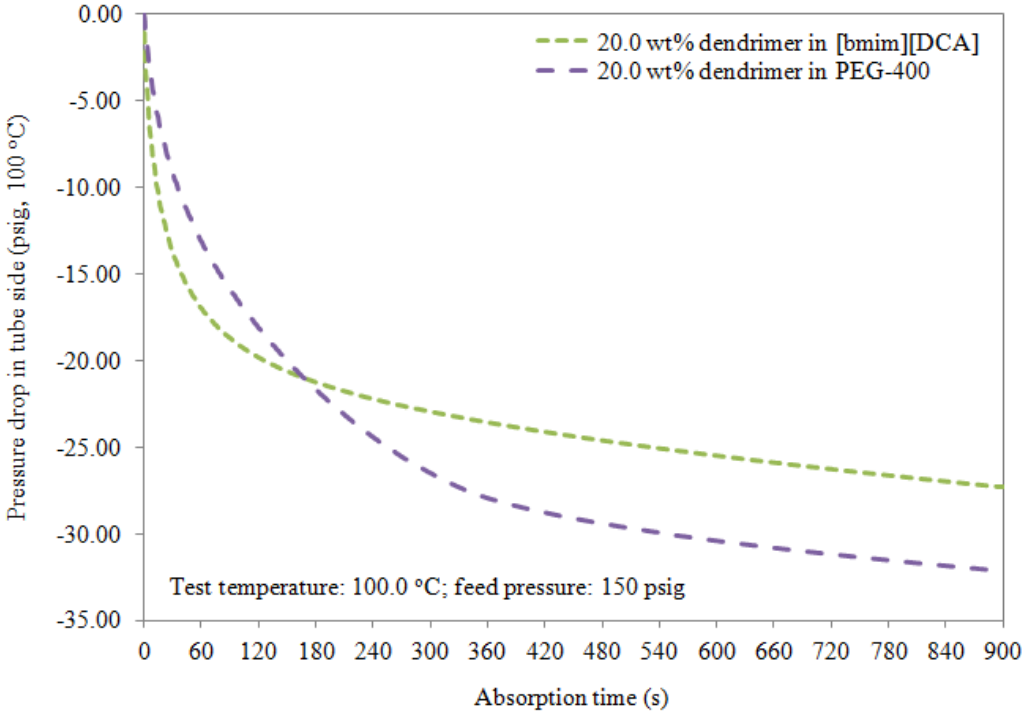

Figure 26c. 900 s absorption duration tests and pressure drop in tube side of PEEK-L II with dead volume reduced: comparison between dendrimer in PEG 400 and [bmim][DCA] solutions.

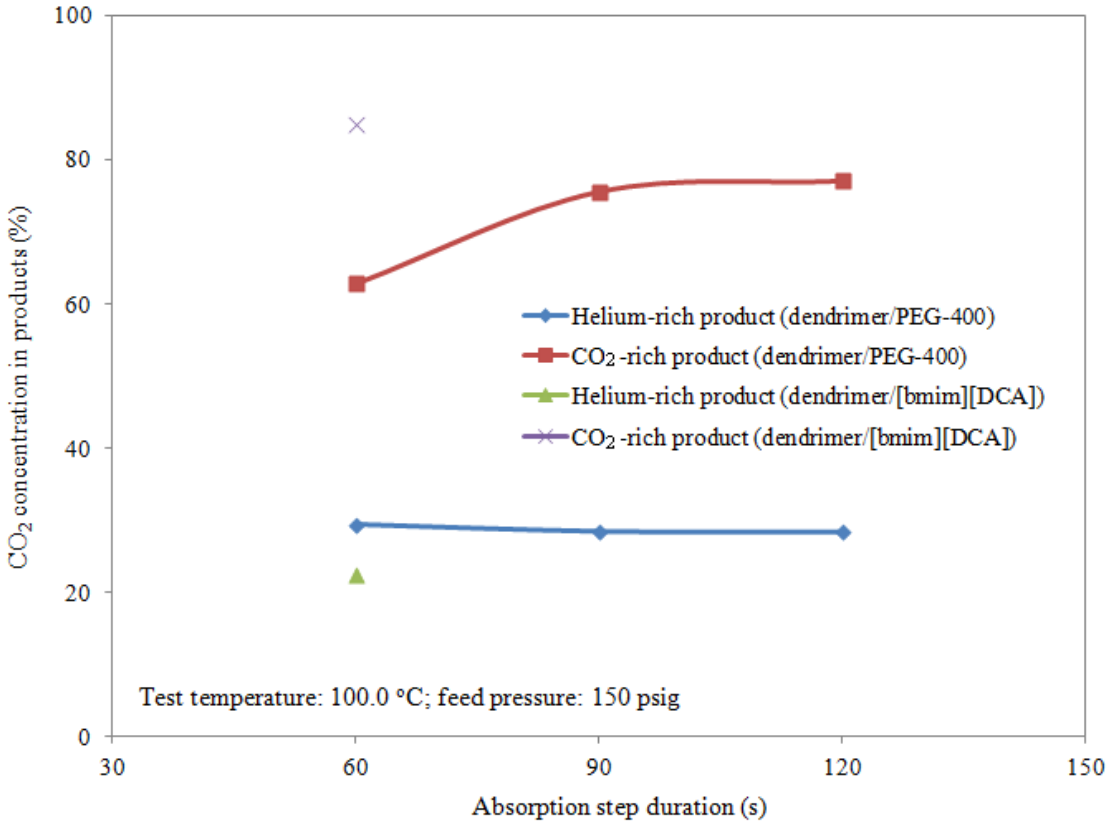

Figure 26d. Influence of absorption step duration on product qualities when dendrimer-PEG 400 solution was used as absorbent in PEEK-L II with dead volume reduced.

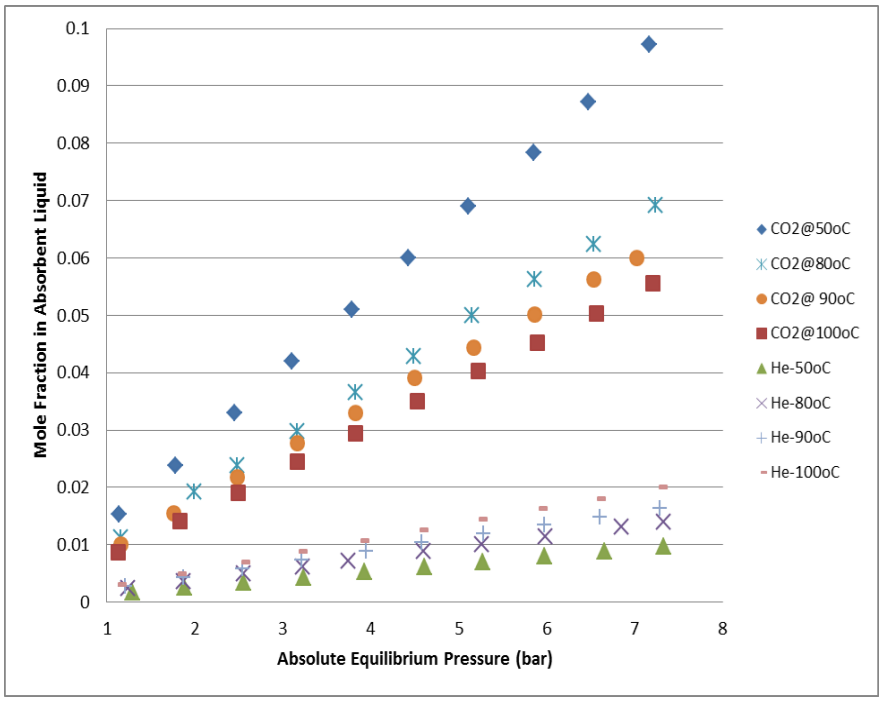

Figure 27. Influence of temperature on solubilities of pure CO_2 and He in [bmim][DCA].

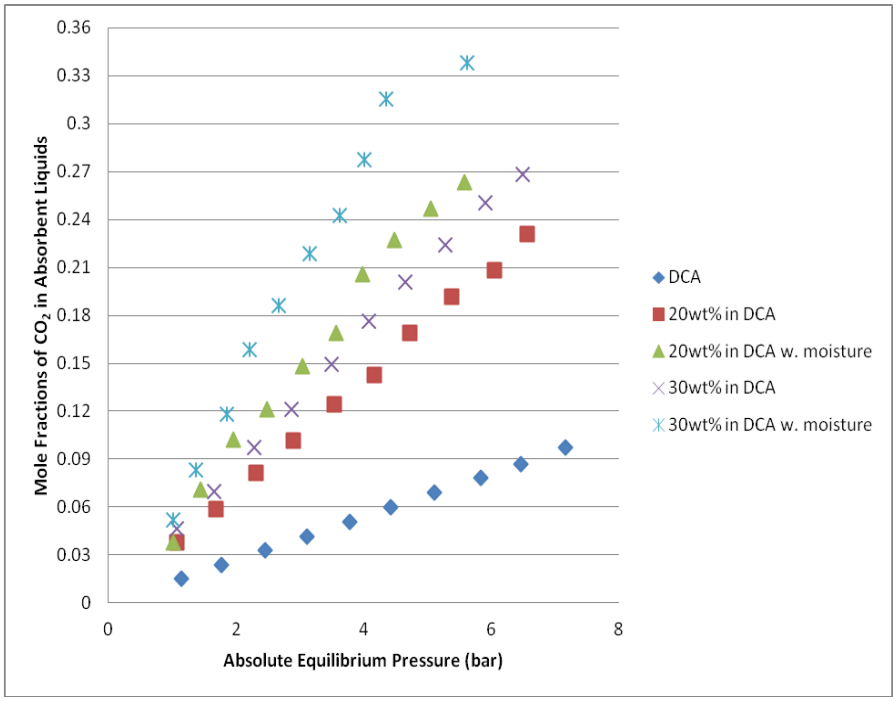

Figure 28. Solubility of pure CO_2 in different absorbent liquids at 50°C.

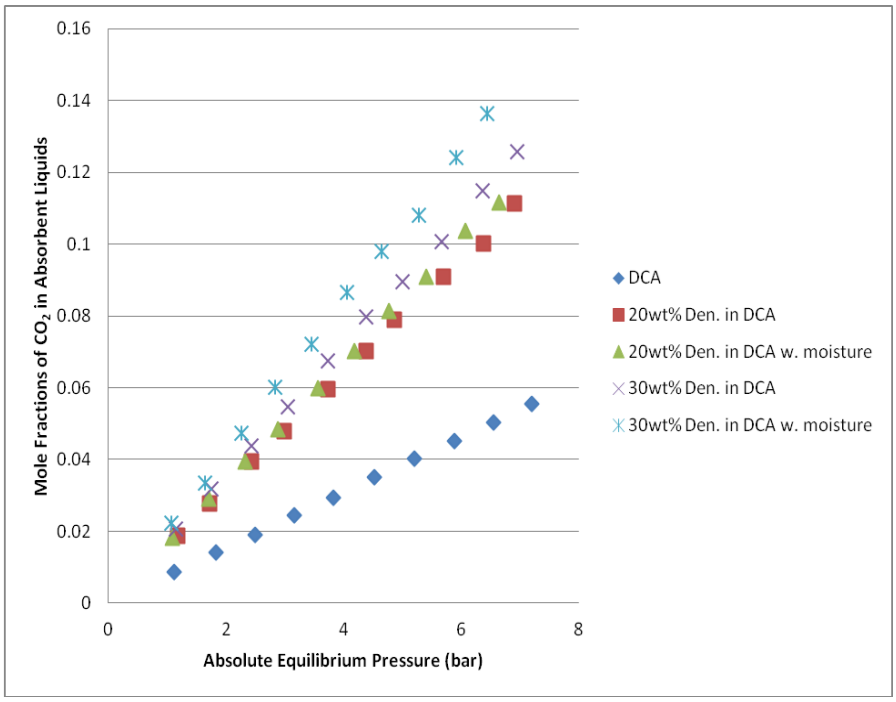

Figure 29. Solubilities of pure CO_2 in different absorbent liquids at 100°C.

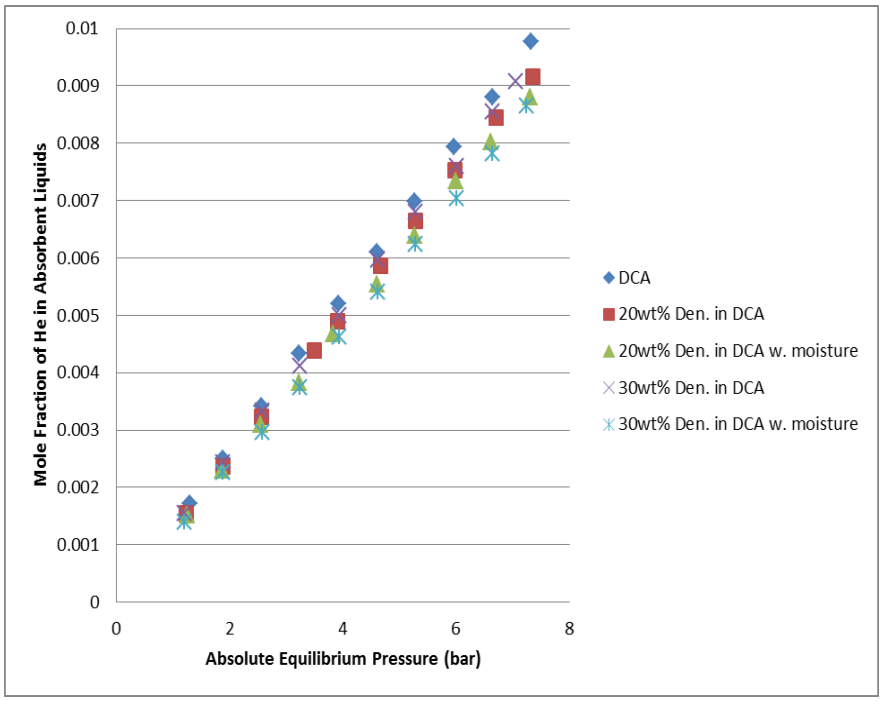

Figure 30. Solubilities of pure He in different absorbent liquids at 50°C.

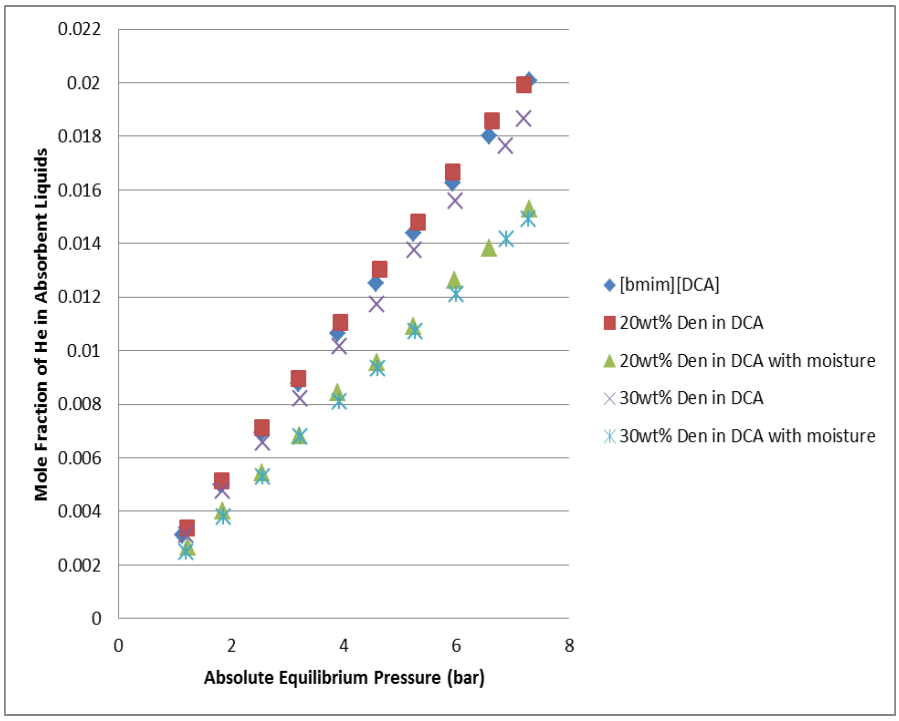

Figure 31. Solubilities of pure He in different absorbent liquids at 100°C.

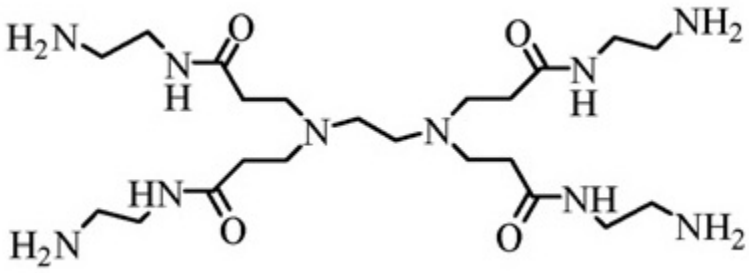

Figure 32. PAMAM dendrimer of generation 0 (Kovvali et al., 2001).

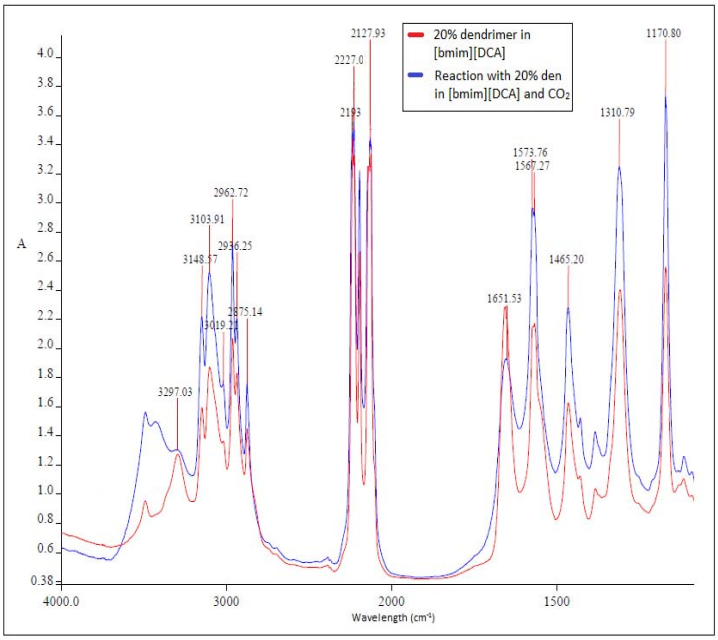

Figure 33. IR spectra of 20 wt% dendrimer in [bmim][DCA] and other species in the solution exposed to CO_2.

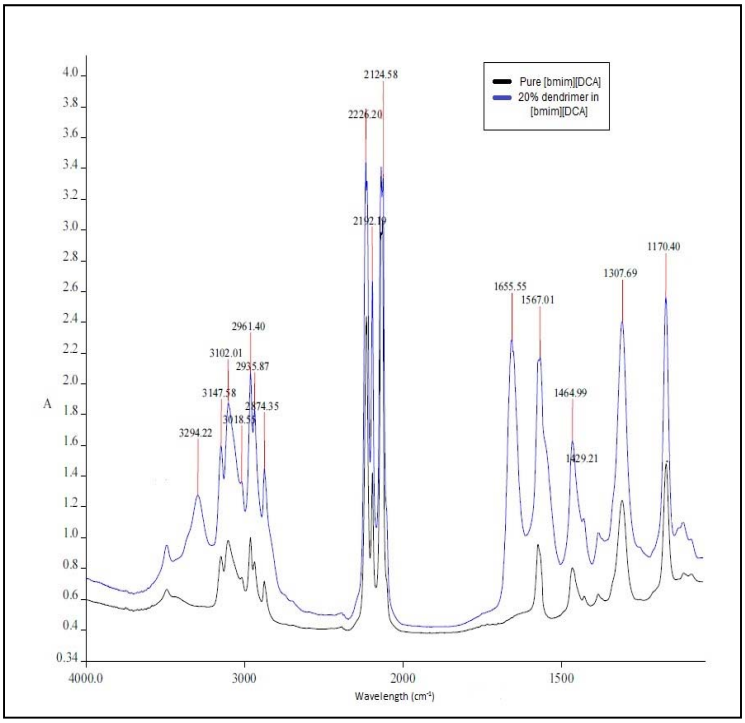

Figure 34. IR spectra of pure [bmim][DCA] and 20wt% of dendrimer Gen 0 in [bmim][DCA] not exposed to CO_2.

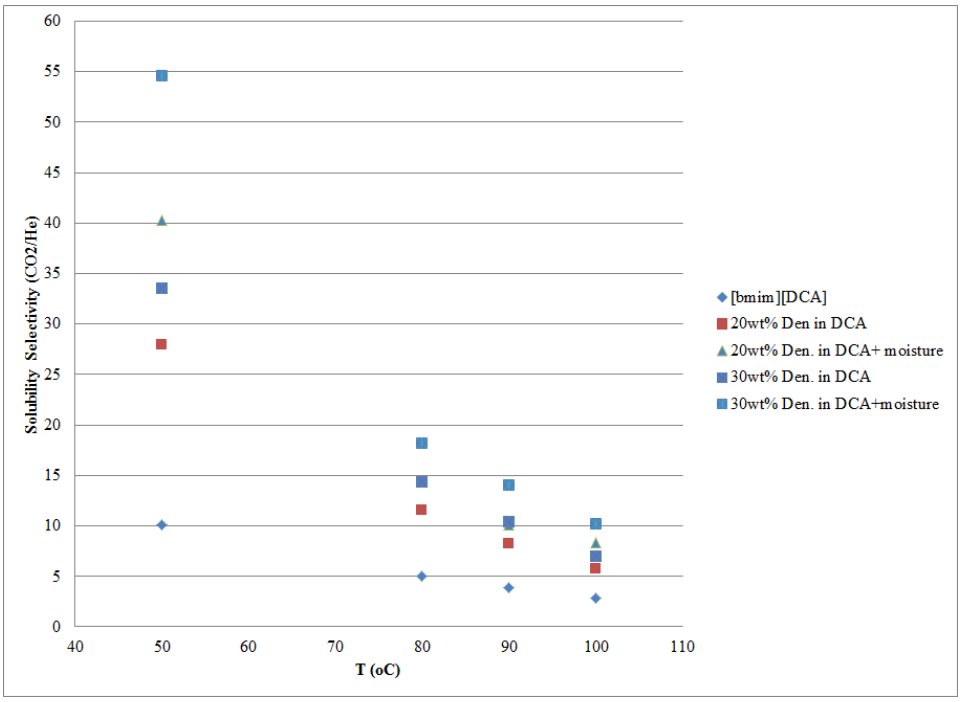

Figure 35. Solubility selectivity of CO_2/He in IL-based absorbent liquids at different temperatures.

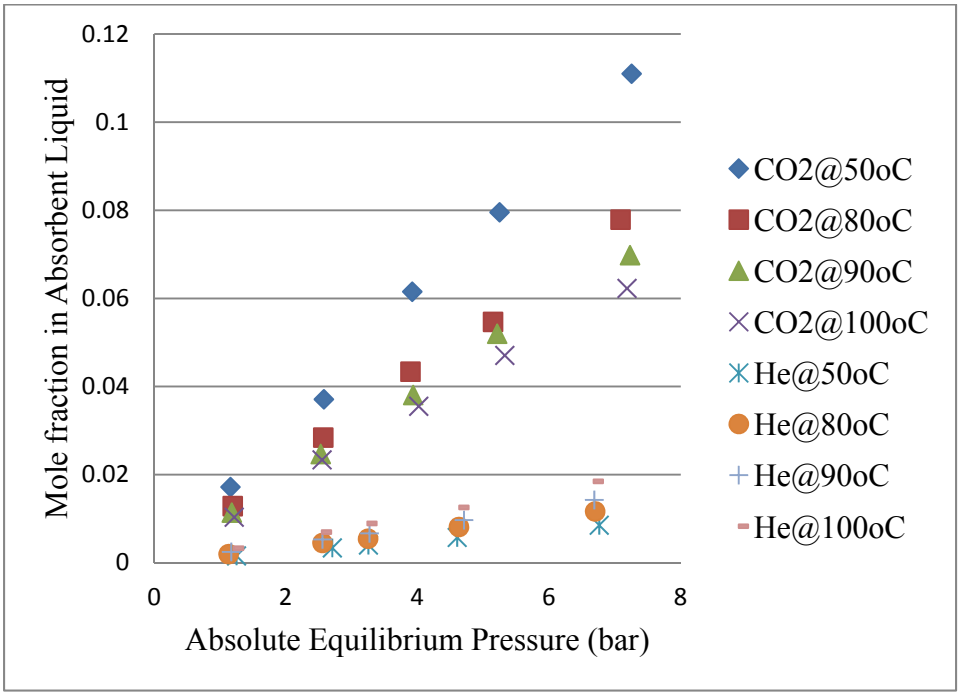

Figure 36a. Solubilities of CO_2 and He in PEG 400 at different temperatures.

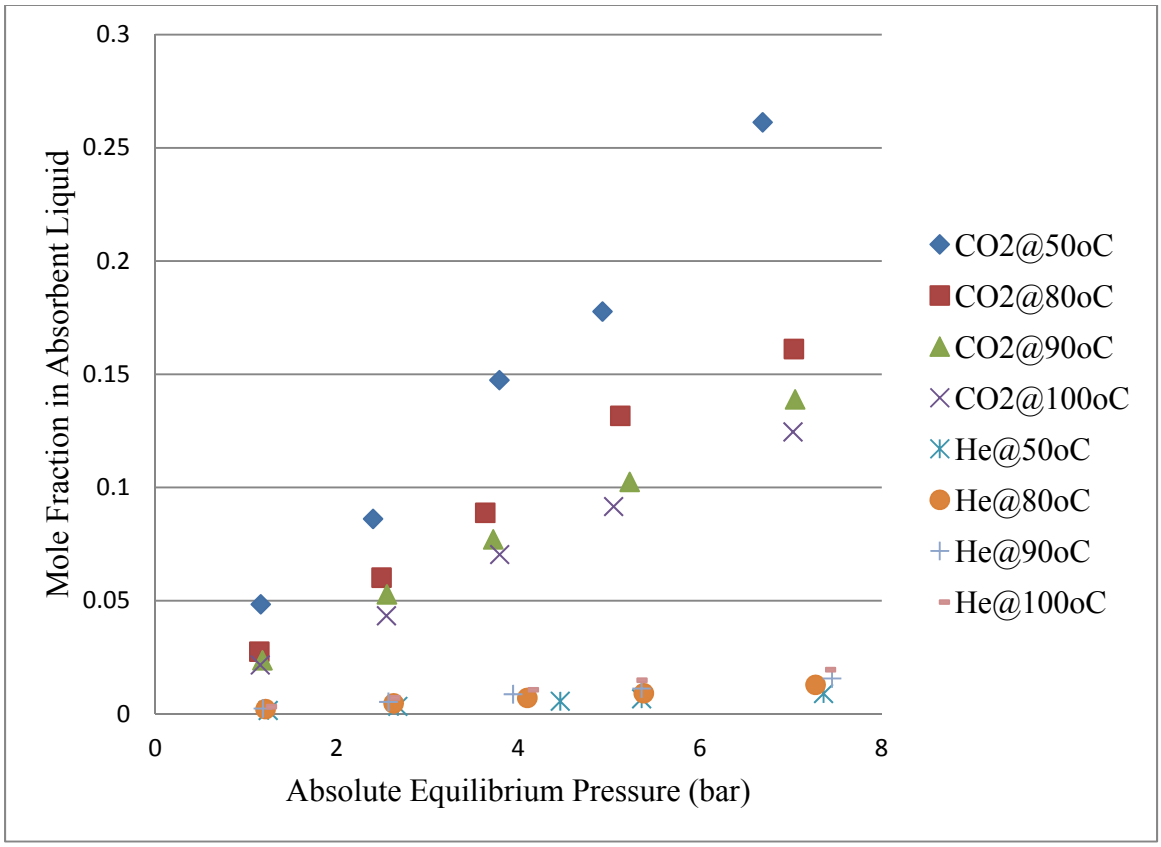

Figure 36b. Solubilities of CO_2 and He in 20wt% dendrimer in PEG 400 at different temperatures.

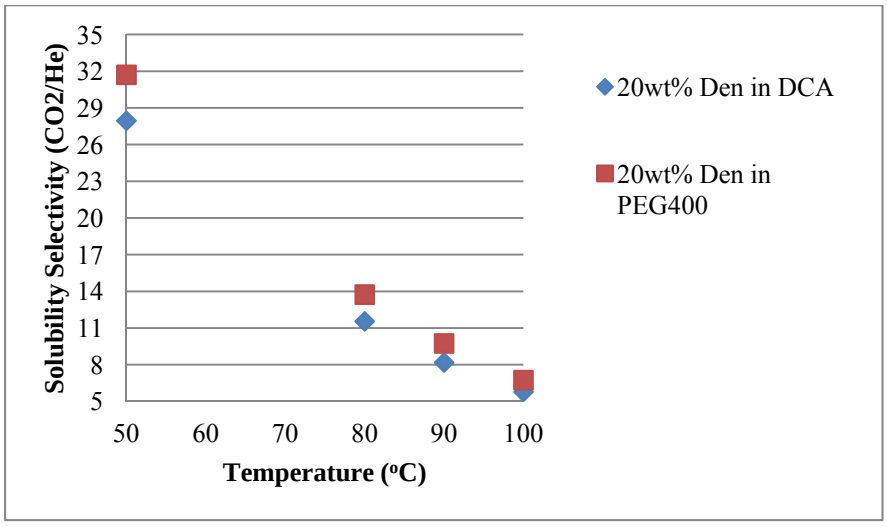

Figure 36c. Solubility selectivity of CO_2/He in different absorbent liquids: 20wt% dendrimer in [bmim][DCA] and PEG 400.

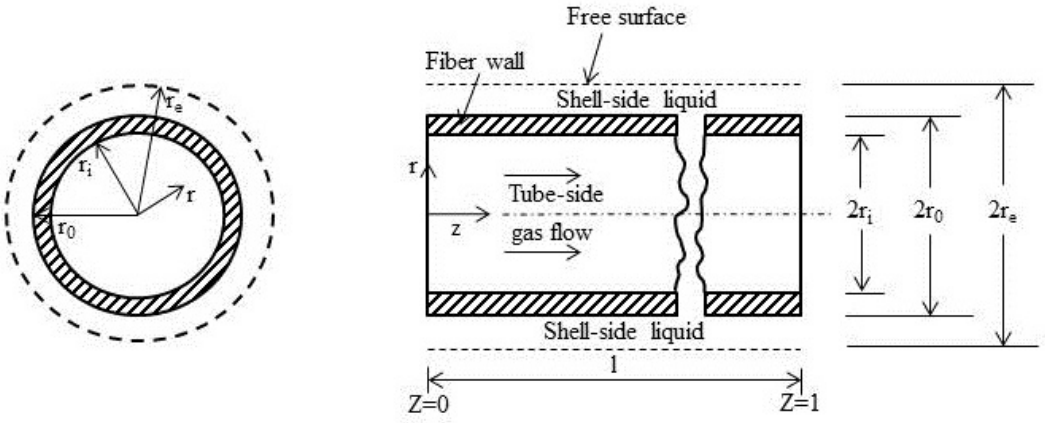

Figure 37. Schematic representation of Happel's free surface model (Karoor and Sirkar, 1993).

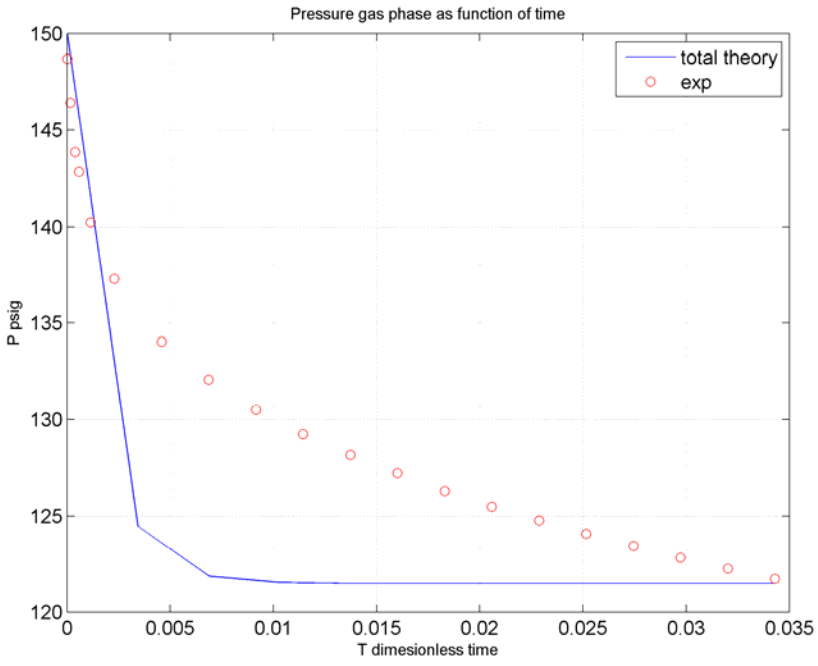

Figure 38. Pressure of gas phase as a function of time during the absorption step in 3 ceramic modules in series at 25°C and 1034 kPag (150 psig) (r_e= 0.00368 m).

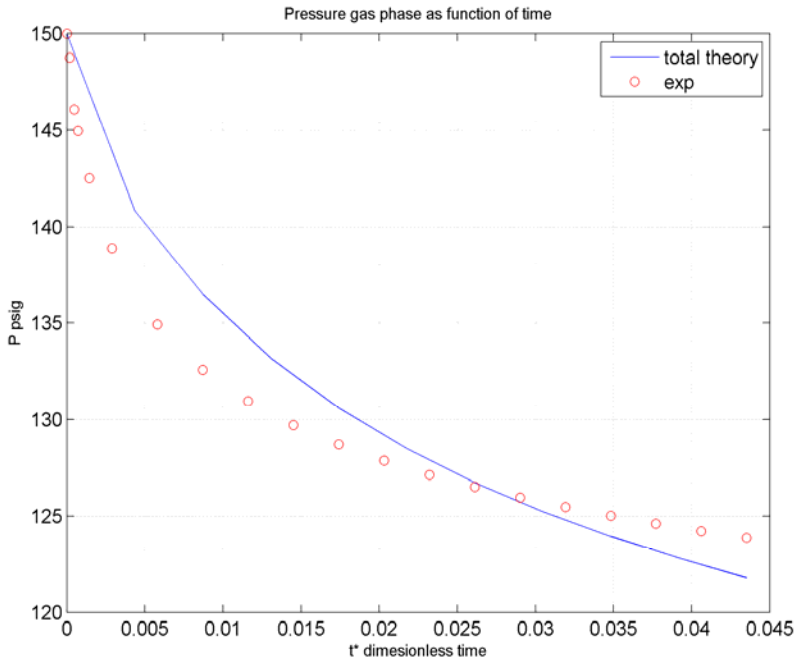

Figure 39. Pressure of gas phase as a function of time during the absorption step in 3 ceramic modules in series at 50°C and 1034 kPag (150 psig) (r_e= 0.00368 m).

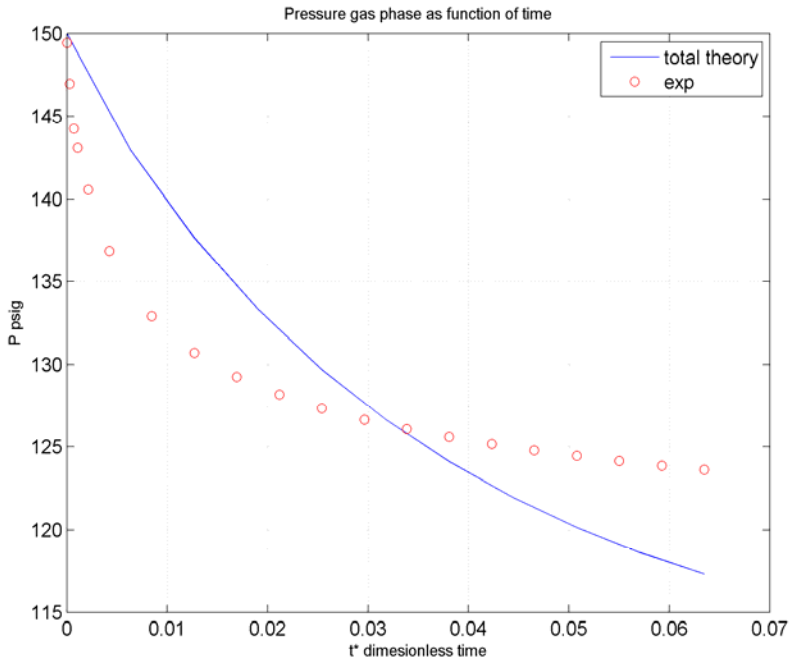

Figure 40. Pressure of gas phase as a function of time during the absorption step in 3 ceramic modules in series at 100°C and 1034 kPag (150 psig) (r_e= 0.00368 m).

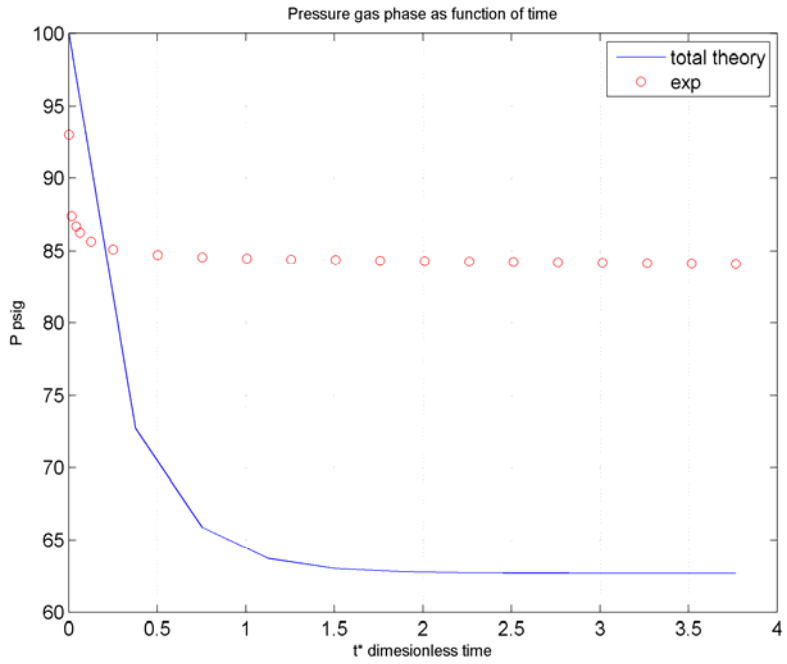

Figure 41. Pressure of gas phase as a function of time during the absorption step in a PEEK-L module at room temperature, 100 psig, and r_e= 0.000291 m.

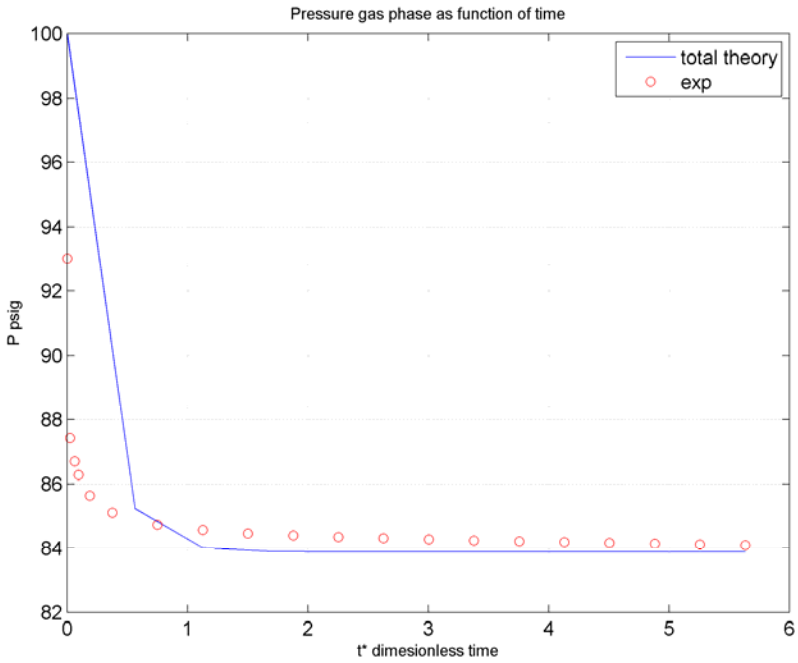

Figure 42. Pressure of gas phase as a function of time during the absorption step in a PEEK-L module at room temperature, 689 kPag (100 psig), and r_e= 0.000238 m.

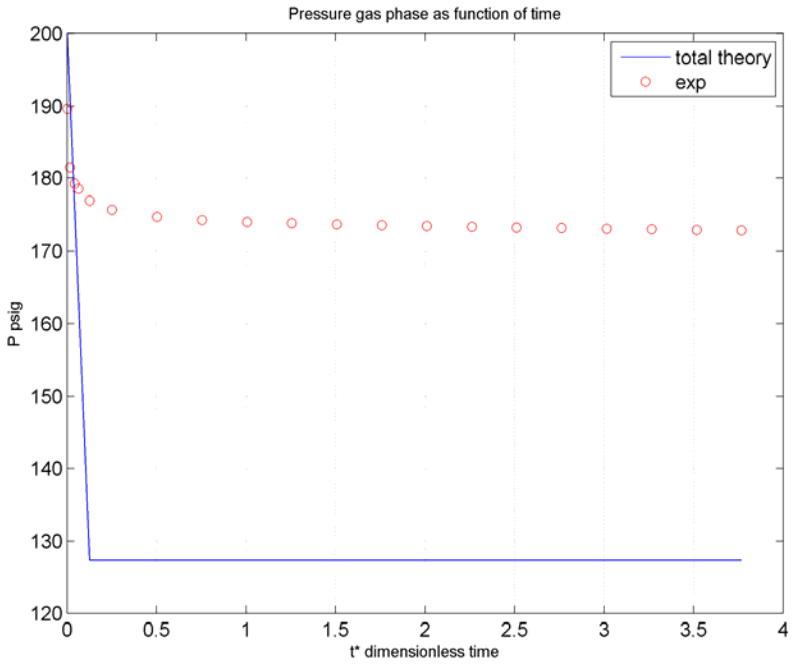

Figure 43. Pressure of gas phase as a function of time during the absorption step in a PEEK-L module at room temperature, 1379 kPag (200 psig), and r_e= 0.000291 m.

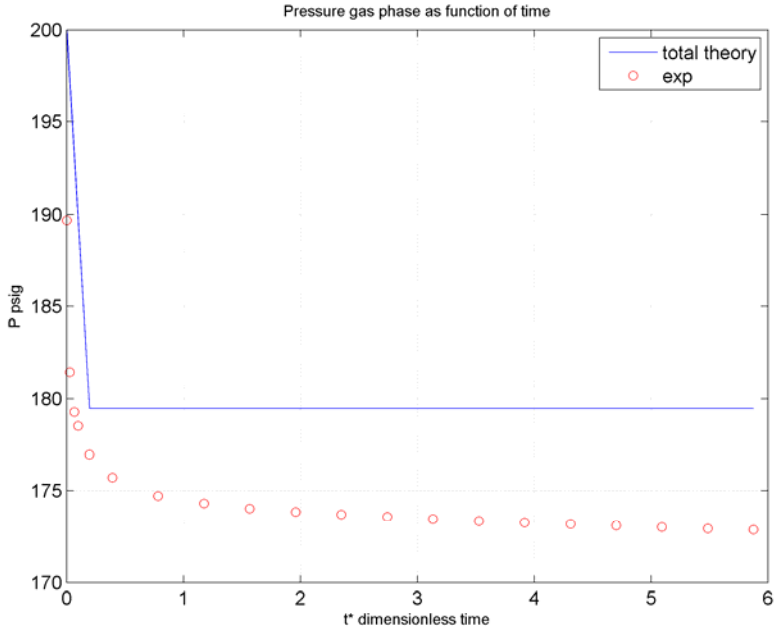

Figure 44. Pressure of gas phase as a function of time during the absorption step in a PEEK-L module at room temperature for feed gas pressure, 1379 kPag (200 psig) and r_e= 0.000233 m.

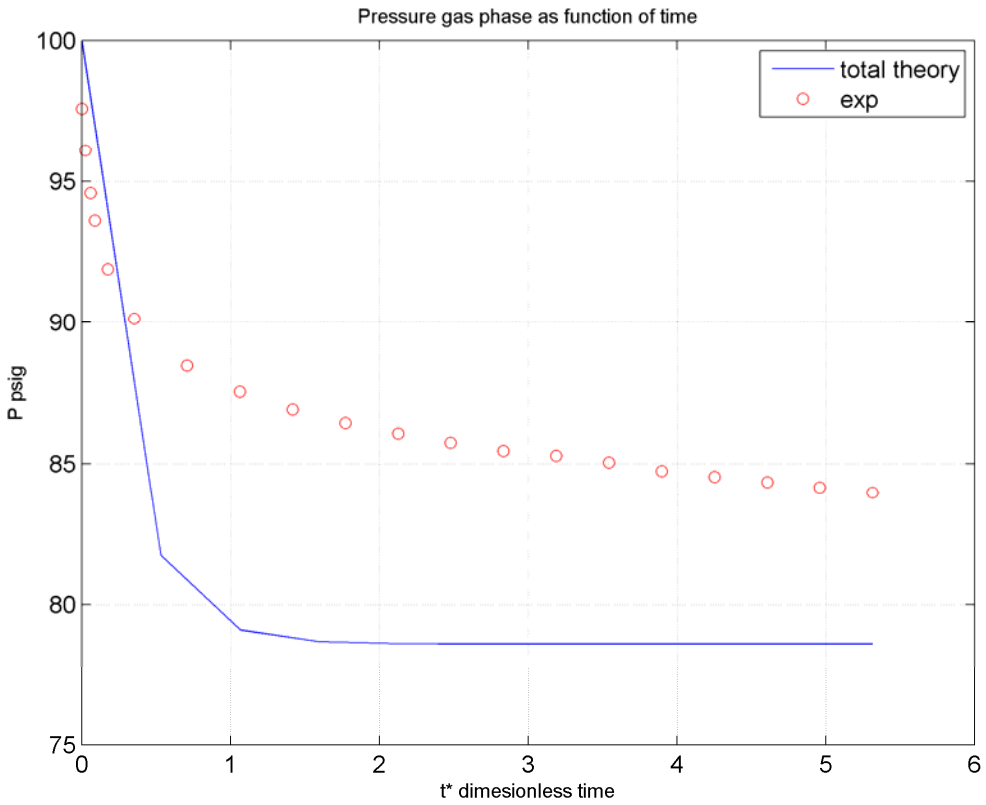

Figure 45. Pressure of gas phase as a function of time during the absorption step in a PEEK-L module with PTFE balls in the module tube-side headers at room temperature and 689 kPag (100 psig) (r_e= 0.00243 m).

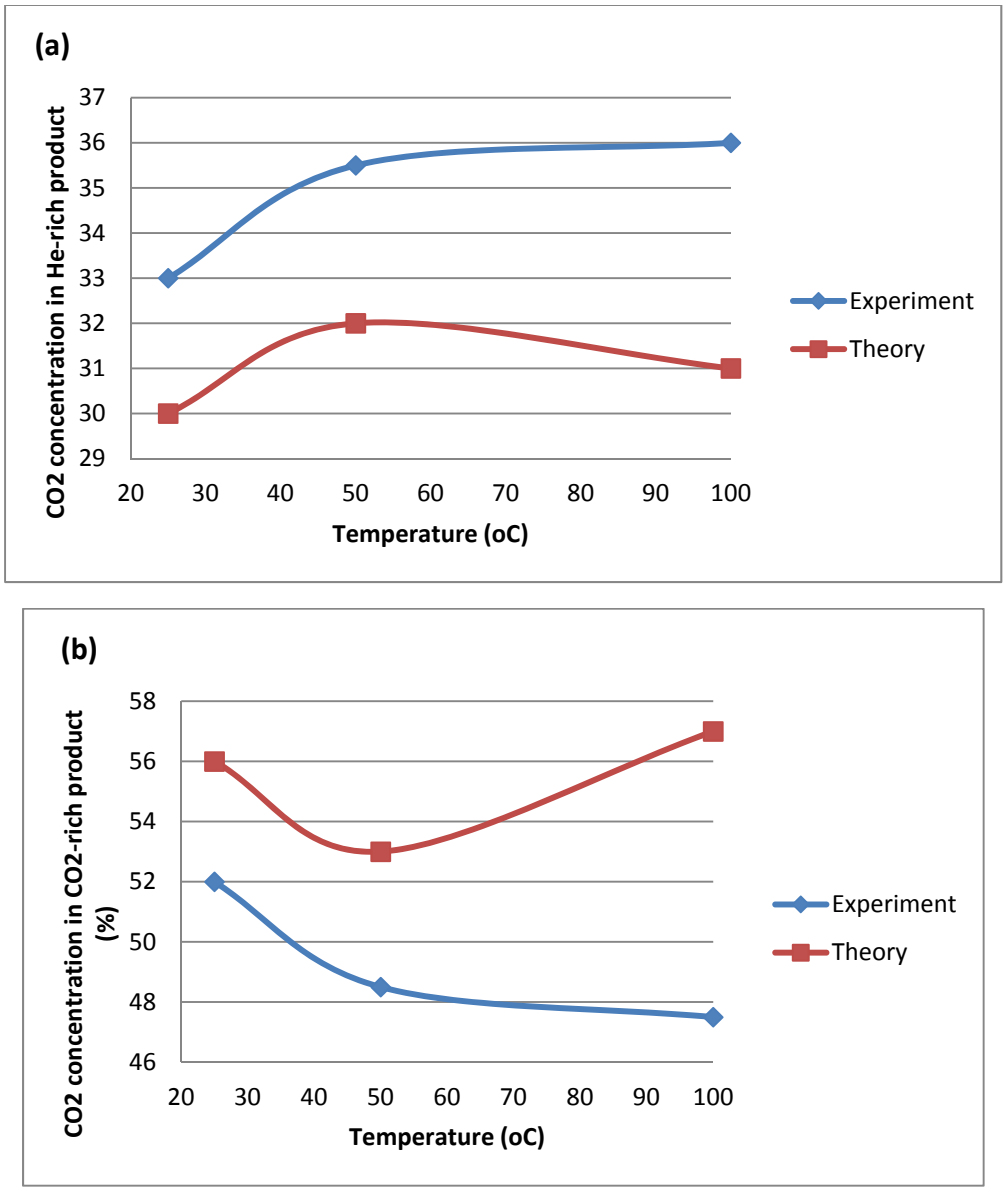

Figure 46. Product composition changes at three different temperatures for 3 ceramic modules in series at 1034 kPag (150 psig) (r_e= 0.00368 m).

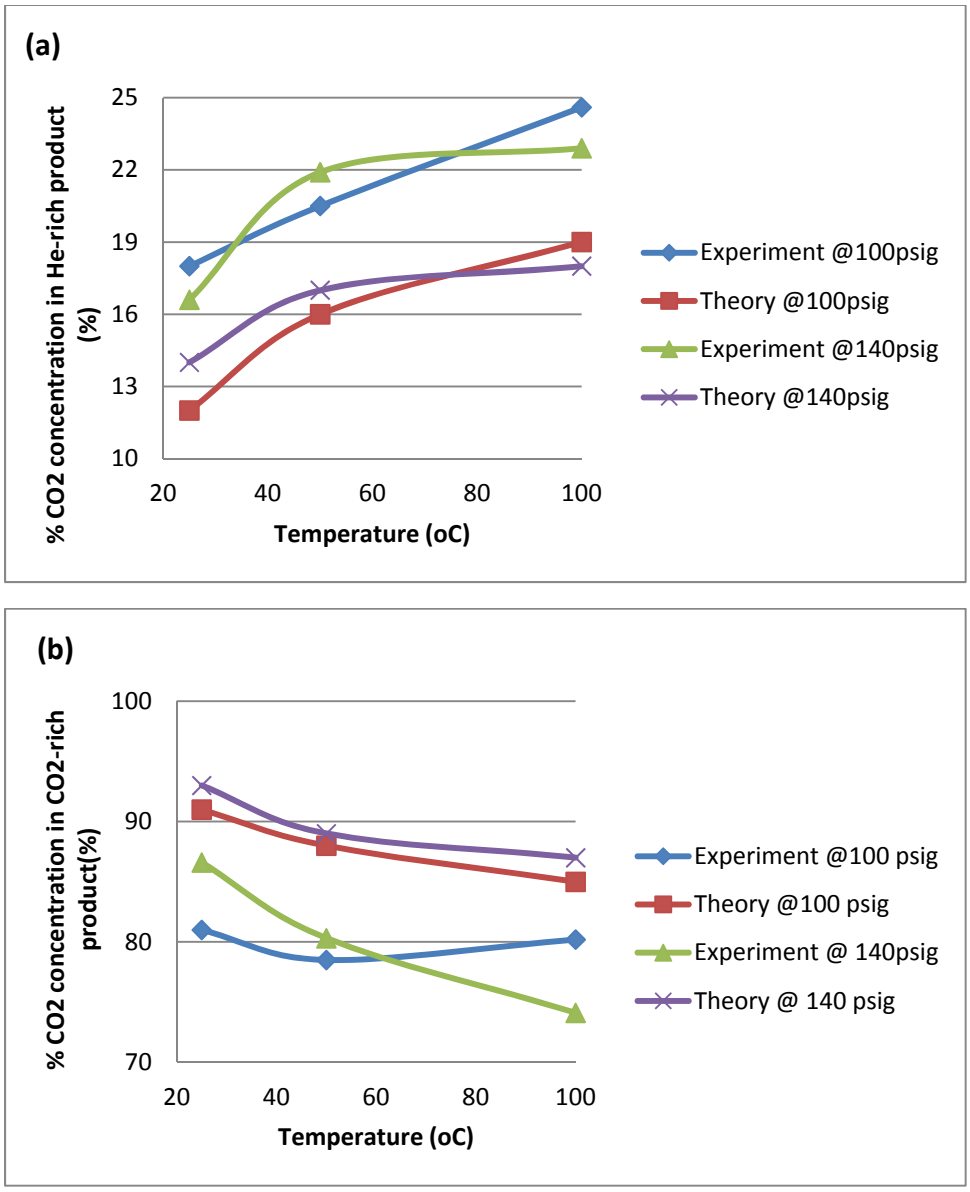

Figure 47. Product composition changes for PEEK-L system at different feed pressures and temperatures (r_e= 0.00243 m).

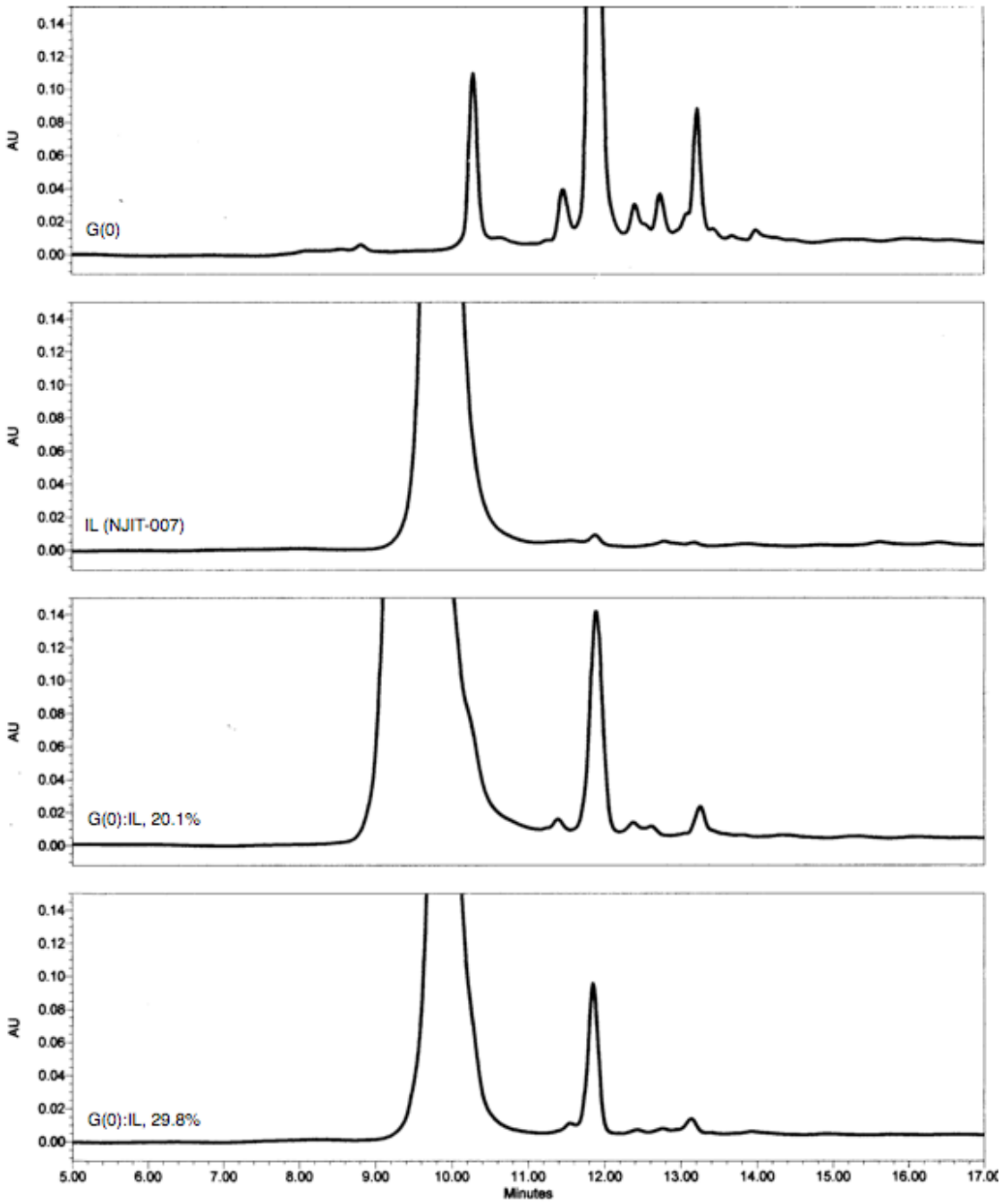

Figure 48. Freshly prepared samples of dendrimer (represented as G(0)), IL and IL containing two levels of dendrimer G(0).

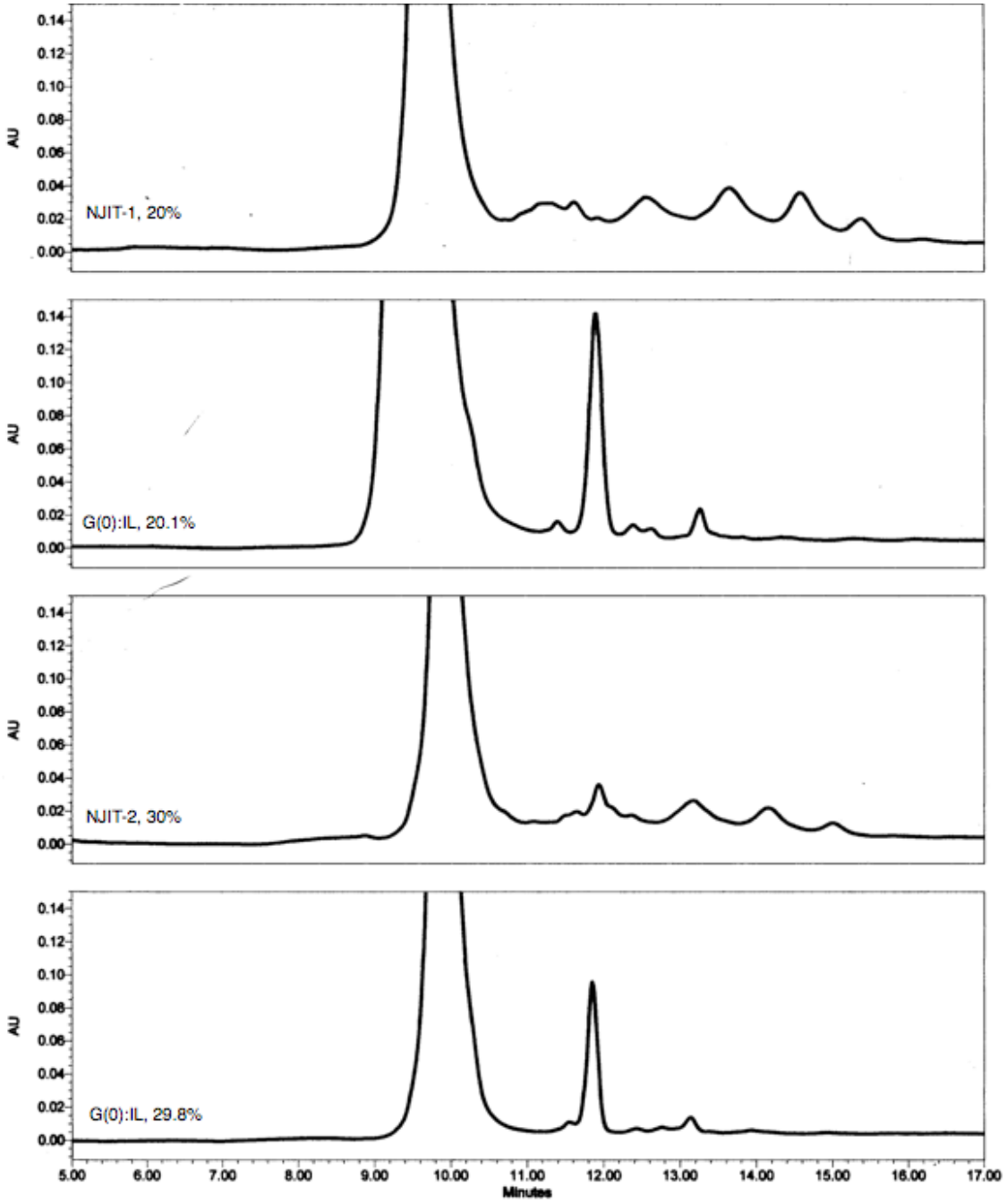

Figure 49. Expanded chromatograms of used absorbent samples (NJIT-1 and NJIT-2) compared with those of freshly prepared samples.

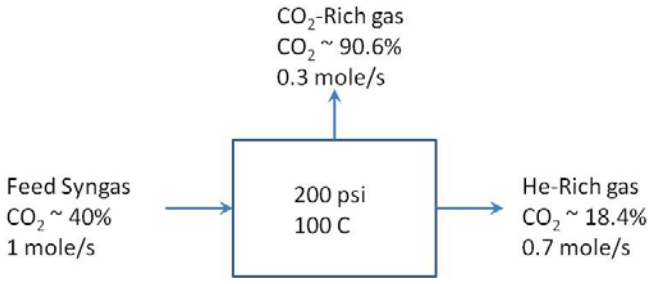

Figure 50. Single stage PSMAB process – CO_2 recovery 67.71%.

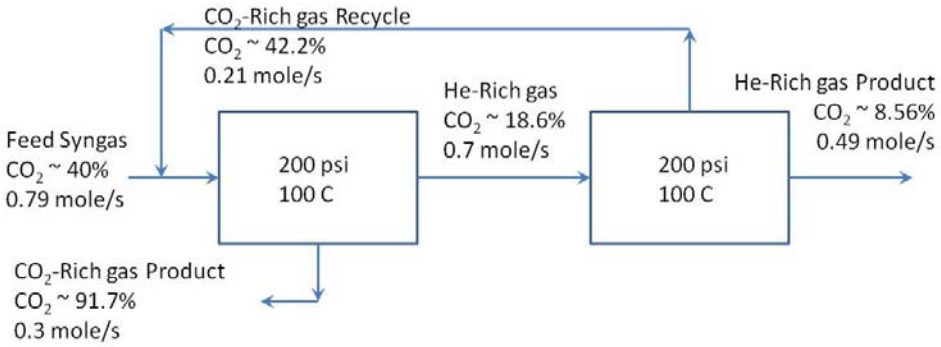

Figure 51. Two stage PSMAB process – CO_2 recovery 86.6%.

6. REFERENCES

Angus, S., Armstrong, B., and deReuck, K.M., eds., "Carbon dioxide international thermodynamic tables of the fluid state-3", IUPAC Project Center, Imperial College, London, **1976**.

Angus, S. and deReuck, K.M., eds. "International thermodynamic tables of the fluid state-4", IUPAC Project Center, Imperial College, London, on the basis of tables and equations published by R.D. McCarthy. National Bureau of Standards, Cryogenics Research Division, Boulder, USA, **1977**.

Anthony, J.L., Maginn, E.J., and Brennecke, J.F., "Solubilities and thermodynamic properties of gases in the ionic liquid 1-n-butyl-3-methylimidazolium hexafluorophosphate", *J. Phys. Chem. B,* **2002**, 106, 7315.

Azar, C., Lindgren, K., Larson, E., Mollersten, K., "Carbon capture and storage from fossil fuels and biomass – costs and potential role in stabilizing the atmosphere", *Climatic Change*, **2006**, 74, 47.

Baltus, R.E., Culbertson, B.H., Dai, S., Luo, H.M., DePaoli, D.W., "Low-pressure solubility of carbon dioxide in room-temperature ionic liquids measured with a quartz crystal microbalance", *J. Phys. Chem. B,* **2004**, 108, 721.

Baltus, R.E., Moganty, S.S., "Diffusivity of Carbon Dioxide in Room-Temperature Ionic Liquids", *Ind. Eng. Chem. Res.,* **2010**, 49, 9370.

Bhaumik, S.; Majumdar, S.; Sirkar, K. K., "Rapid Pressure Swing Absorption Cleanup of Post-Shift Reactor Synthesis Gases," Final Report to DOE PETC, Pittsburgh, DOE Grant No. DE-FG22-90 PC 90300, **1994**.

Bhaumik S., Majumdar, S., Sirkar, K.K., "Hollow-fiber membrane-based rapid pressure swing absorption", *AIChE Journal*, **1996**, 42, 409.

Blanchard, L.A., Gu, Z. Y., Brennecke, J.F., "High pressure phase behavior of ionic liquid/CO_2 systems*", J. Phys. Chem. B,* **2001**, 105, 2437.

Blauwhoff, P.M.M., Versteeg, G.F., Van Swaaij, W.P.M., "A study on the reaction between CO_2 and alkanolamines in aqueous solutions", *Chem. Eng. Sci.,* **1983**, 38, 1411.

Brian III, B.F., Zwiebel, I.,Artigue, R. S., "Numerical Simulation of Fixed-bed Adsorption Dynamics by the Method of Lines", *AIChE Symp. Ser.,* **1988**, 84, 57.

Camper, D., Becker, C., Koval, C., and Noble, R., "Diffusion and Solubility Measurements in Room Temperature Ionic Liquids", *Ind. Eng. Chem. Res.,* **2006**, 45, 445.

Danckwerts, P.V., "The reaction of CO_2 with ethanolamines", *Chem. Eng. Sci.*, **1979**, 34, 479.

Dendritech Inc., Mark Kaiser, Personal Communication, January 20, **2012**.

Duan, S., Kouketsu, T., Kazama, S., Yamada, K., "Development of PMAM dendrimer composite membranes for CO_2 separation", *J. Membrane Sci.*, **2006**, 283, 2.

Duan, S., Kouketsu, T., Kai, T., Kazama, S., Yamada, K., "PAMAM dendrimer composite membrane for CO_2 separation: Formation of a chitosan gutter layer", *J. Membrane Sci.*, **2007**, 287, 51.

Finotello, A., Bara, J.E., Camper, D., and Noble, R.D., "Room-Temperature Ionic Liquids: Temperature Dependence of Gas Solubility Selectivity", *Ind. Eng. Chem. Res.*, **2008**, 47, 3453.

Han, S., Kim, C., and Kwon, D., "Thermal degradation of poly(ethyleneglycol)", *Polymer Degradation and Stability*, **1995**, 47, 203.

Happel, J., "Viscous Flow Relative to Arrays of Cylinders", *AIChE Journal*, **1959**, 5, 174.

Harrison, Douglas P. "Sorption-enhanced hydrogen production: a review", *Ind. Eng. Chem. Res.*, **2008**, 47, 6486.

Hou, Y., "Experimental Measurement of Solubility and Diffusivity of CO_2 in Room Temperature Ionic Liquids", M.S. Thesis; Clarkson University, Potsdam, NY, **2006**.

Hou, Y., and Baltus, R.E., "Experimental measurement of the solubility and diffusivity of CO_2 in room-temperature ionic liquids using a transient thin-liquid-film method", *Ind. Eng. Chem. Res.*, **2007**, 46, 8166.

Husson-Borg, P., Majer, V., Gomes, M.F.C., "Solubilities of oxygen and carbon dioxide in butyl methyl imidazolium tetraluoroborate as a function of temperature and at pressures close to atmospheric pressure", *J. Chem. Eng. Data*, **2003**, 48, 480.

Jalili A.H., Rostami, M.R., Ghotbi, C., Jenab, M.H., Ahmadi, A.N., "Solubility of H_2S in Ionic Liquids [bmim][PF_6], [bmim][BF_4], and [bmim][Tf_2N]", *J. Chem. Eng. Data*, **2009**, 54, 1844.

Kamps, A.P.S., Tuma, D., Xia, J.Z., Maurer, G., "Solubility of CO_2 in the ionic Liquid [bmim][PF6].", *J. Chem. Eng. Data*, **2003**, 48, 746.

Kanniche, M., Gros-Bonnivard, R., Jaud, P., Valle-Marcos, J., Amann, J.-M., Bouallou, C., "Pre-combustion, post-combustion and oxy-combustion in thermal power plant for CO_2 capture", *Applied Thermal Engineering*, **2010**, 30, 53.

Karoor, S., and Sirkar, K.K., "Gas Absorption Studies in Microporous Hollow Fiber Membrane Modules", *I&EC Res*., **1993**, 32, 674.

Kosaraju P., Kovvali, A.S., Korikov A., and Sirkar, K.K., "Hollow Fiber Membrane Contactor Based CO2 Absorption-Stripping Using Novel Solvents and Membranes", *Ind. Eng. Chem. Res.*, **2005**, 44, 1250.

Kovvali A.S., Chen H., Sirkar K.K., "Dendrimer Membranes: A CO_2-Selective Molecular Gate", *JACS*, **2000**, 122, 7594.

Kovvali A.S., and Sirkar K.K., "Dendrimer Liquid Membranes: CO_2 Separation from Gas Mixtures", *Ind. Eng. Chem. Res*., **2001**, 40, 2502.

Krevelen, V., Hoftijzer, P.J., Huntjens, F.J., "Composition and vapour pressures of aqueous solutions of ammonia, carbon dioxide and hydrogen sulphide", *Re. Trav. Chim., Pays-bas,* **1949**, 68, 191.

Lashof, D.A., Dilip, R.A., "Relative contributions of greenhouse gas emissions to global warming", *Nature*, **1990**, 334, 529.

Lee, S.C., Ho, J.C., Soo J.L., et al., "Development of regenerable MgO-Based sorbent promoted with K_2CO_3 for CO_2 capture at low temperatures", *Environ. Sci. Technol.*, **2008**, 42, 2736.

Meindersma, W.G., Sanchez, L.M.G., Hansmeier, A.R., de. Haan, A.B., "Application of task-specific ionic liquids for intensified separations", *Monatshefte fur Chemie*, **2007**, 138, 1125.

Merkel T.C., Lin, H., Wei, X., Baker, R., "Power plant post-combustion carbon dioxide capture: An opportunity for membranes", *Journal of Membrane Science*, **2010**, 359, 126.

Moganty, S.S., "Thermodynamic, Transport and Electrochemical Properties of Room Temperature Ionic Liquids", Ph.D. Thesis, Clarkson University, Potsdam, NY, **2009**.

Mohamed, K., Gros-Bonnivard, R., Jaud, P., Valle-Marcos, J., Amann, J.-M., Bouallou, C., "Pre-combustion, post-combustion and oxy-combustion in thermal power plant for CO_2 capture", *Applied Thermal Engineering*, **2010**, 30, 53.

Muldoon, M. J., Aki, S.N.V.K., Anderson, J.L., Dixon, J.K., Brennecke, J.F. Improving carbon dioxide solubility in ionic liquids. *J. Phys. Chem. B,* **2007**, 111, 9001.

Myers, C., Pennline, H., Luebke, D., Ilconich, J., Dixon, J.K., Maginn, E.J., Brennecke, J.F., "High temperature separation of carbon dioxide/hydrogen mixtures using facilitated supported ionic liquid membrane", *J. Membrane Sci.,* **2008**, 322, 28.

Obuskovic G., Poddar, T.K., Sirkar, K.K., "Flow swing membrane absorption-permeation", *Ind. Eng. Chem. Res*., **1998**, 37, 212.

Park, H.S., Jung, Y. M., You, J. K., Hong, W. H., Kim, JN., "Analysis of the CO_2 and NH_3 Reaction in an Aqueous Solution by 2D IR COS: Formation of Bicarbonate and Carbamate", *J. Phys. Chem. A,* **2008**, 112, 6558.

Pachauri, R.K. and Reisinger, A., Intergovernmental Panel on Climate Change's Fourth Assessment Report, **2007**, Chapter 2, "Changes in atmospheric constituents and radiative forcing," pp 135.

Pomelli C. S., Chiappe, C., Vidis, A., Laurenczy, G., Dyson, P.J., "Influence of the Interaction between Hydrogen Sulfide and Ionic Liquids on Solubility: Experimental and Theoretical Investigation", *J. Phys. Chem. B*, **2007**, 111, 13014.

Raeissi S., Peters, C.J., "A potential ionic liquid for CO_2-separaiting gas membranes: selection and gas solubility studies", *Green Chem*., **2009**, 11, 185.

Rolker, J.,Seiler, M., Mokrushina, L., Arlt, W., "Potential of branched polymers in the field of gas absorption: experimental gas solubilities and modeling", *Ind. Eng. Chem. Res.,* **2007**, 46, 6572.

Rubin, E.S., Chen, C., Rao, A.B., "Cost and performance of fossil fuel power plants with CO_2 capture and storage", Energy Policy, **2007**, 35, 4444.

Sanchez, L.M.G., "Functionalized Ionic Liquids Absorption Solvents for Carbon Dioxide and Olefin Separation", Ph.D. Thesis, Eindhoven University of Technology, Enschede, The Netherlands, **2008**.

Shiflett M. B., Yokozeki, A. "Solubilities and diffusivities of carbon dioxide in ionic liquids: [bmim][PF_6] and [bmim][BF_4]", *Ind. Eng. Chem. Res*., **2005**, 44, 4453.

Shiflett, M.B., Harmer, M.A., Junk, C.R., Yokozeki, A., "Solubility and diffusivity of 1,1,1,2-tetrafluoroethane in room-temperature ionic liquids", *Fluid Phase Equilib*, **2006**, 242, 220.

Shiflett, M.B., Yokozeki, A., "Solubility of CO_2 in room temperature ionic liquid [hmim][Tf_2N]", *J. Phys. Chem. B,* **2007**, 111.

Shiflett M. B., Niehaus, A. M. S., Yokozeki, A., "Separation of CO_2 and H_2S Using Room-Temperature Ionic Liquid [bmim][$MeSO_4$]", *J. Chem. Eng. Data*, **2010**, 55, 4785.

Sudhir, Aki N.V.K., Mellein, B.R., Saurer, E.M., Brennecke, J.F., "High–pressure phase behavior of carbon dioxide with imidazolium-based ionic liquids", *J. Phys. Chem. B*, **2004**, 108, 20355.

Tan Y., Douglas, M.A., Thambimuthu K.V., "CO_2 capture using oxygen enhanced combustion strategies for natural gas power plants", Fuel, **2002**, 81, 1007.

Taniguchi, I., Duan, S., Kazama, S., Fujioka, Y., "Facile fabrication of a novel high performance CO_2 separation membrane: Immobilization of poly (amidoamine) dendrimers in poly(ethylene glycol) networks", *J. Membrane Sci.,* **2008**, 322, 277.

Versteeg, G.F., Van Dijck, L.A.J., Van Swaaij, W.P.M., "On the kinetics between CO_2 and alkanolamies both in aqueous and non-aqueous solutions: An overview", *Chem. Eng. Commun.,* **1996**, 144, 113.

Yang R.H, Xu, Z., Fan, M., Gupta, R., Slimane, R.B., Bland, A.E., Wright, I.,"Progress in carbon dioxide separation and capture: A review", *Journal of Environmental Sciences*, **2008**, 10, 14.

Yegani R., Hirozawa, H., Teramoto, M., Himei, H., Okada, O., Takigawa, T., Ohmura, N., Matsumiya, N., Matsuyama, H., "Selective separation of CO_2 by suing novel facilitated transport membrane at elevated temperatures and pressures", *Journal of Membrane Science*, **2007**, 291, 157.

Yuan Xiaoliang, Suojiang Zhang, Jun Liu, Xingmei Lu, "Solubilities of CO_2 in hydroxyl ammonium ionic liquids at elevated pressures", *Fluid Phase Equilibria*, **2007**, 257, 195.

Yokozeki A., Shiflett, M.B., "Hydrogen purification using room-temperature ionic liquids", *Applied Energy*, **2007**, 84, 351.

Yuan Xiaoliang, Suojiang Zhang, Yuhuan Chen, Xingmei Lu, Wenbin Dai, Ryohei Mori, "Solubilities of gases in 1,1,3,3-Tetramethylguanidium Lactate at Elevated Pressures", *J. Chem. Eng. Data*, **2006**, 51, 645.

Zou J., and Ho, W.S. Winston, "CO_2-selective polymeric membranes containing amines in crosslinked poly(vinyl alcohol)", *Journal of Membrane Science*, **2006**, 286, 310.

7. LIST OF ACRONYMS AND ABBREVIATIONS

[bmim] [DCA]	1-butyl-3-methylimidazolium dicyanamide
CCS	Carbon Capture and Storage
FSLM	Facilitated Supported Liquid Membrane
Gen	Generation
IGCC	Integrated Gasification Combined Cycle
IL	Ionic Liquid
IR	Infrared
MATLAB	Matrix Laboratory Programming Language
ODE	Ordinary Differential Equation

PDE	Partial Differential Equation
PAMAM	Polyamidoamine
PEEK	Poly ether ether ketone
PSA	Pressure Swing Adsorption
PSAB	Pressure Swing Absorption
PSMAB	Pressure Swing Membrane Absorption
PTFE	Polytetrafluoroethylene
RTIL	Room Temperature Ionic Liquid
TSIL	Task Specific Ionic Liquid

8. ACKNOWLEDGMENTS

Dr. Ashok Damle of Techverse Inc., Cary, NC was a consultant to the project for a limited period and provided a perspective on the two-stage process using the PSMAB process. Mark Kaiser of Dendritech Inc., Midland, MI provided the HPLC analysis of IL-dendrimer samples. Ms.Tripura Mulukutla of Chemical Engg. at NJIT provided the spectra shown in Figures 33 and 34. Norman Popkie and Steven R. Markovich served as the successive Program Officers for this project.